

2006

Synthesis of Some Pyridinone Nucleoside Analogues as Antitumor Agents

Shaikha Saif Saeed Alneyadi

Follow this and additional works at: https://scholarworks.uaeu.ac.ae/all_theses

Part of the [Environmental Sciences Commons](#)

Recommended Citation

Saeed Alneyadi, Shaikha Saif, "Synthesis of Some Pyridinone Nucleoside Analogues as Antitumor Agents" (2006). *Theses*. 410.
https://scholarworks.uaeu.ac.ae/all_theses/410

This Thesis is brought to you for free and open access by the Electronic Theses and Dissertations at Scholarworks@UAEU. It has been accepted for inclusion in Theses by an authorized administrator of Scholarworks@UAEU. For more information, please contact fadl.musa@uaeu.ac.ae.



United Arab Emirates University
Deanship of Graduate Studies
M.Sc. Program in Environment Sciences

“Synthesis of Some Pyridinone Nucleoside Analogues as Antitumor Agents”

By

Shaikha Saif Saeed Alneyadi

A thesis
Submitted to
United Arab Emirates University
In partial fulfillment of the requirements
For the Degree of M.Sc. in Environment Sciences

Supervisors

Ibrahim M. Abdou
Assistant Professor
Department of Chemistry
Faculty of Science
UAEU

Ahmed Al-Marzouqi
Assistant Professor
Department of Biochemistry
Faculty of Medicine & Health Science
UAEU

2006



United Arab Emirates University
Deanship of Graduate Studies
M.Sc. Program in Environment Sciences

CERTIFICATE OF APPROVAL

M.Sc. THESIS

This is to certify that the M.Sc. thesis of

Shaikha Saif Alneyadi

Has been approved by the Examining Committee for the thesis requirement for the

Degree of M.Sc. in Environment Sciences

At the 2006 graduation.

Thesis Committee:

Date

Signature

1-

2-

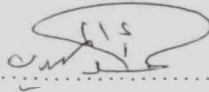
3-

Dean of Graduate Studies

The Thesis of Sheikha Saif Al-Neyadi for the Degree of Master of Science in Environmental is approved.



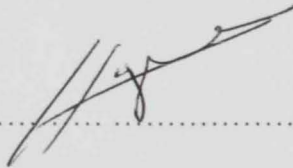
Examining Committee Member, Dr. Ibrahim Abdou



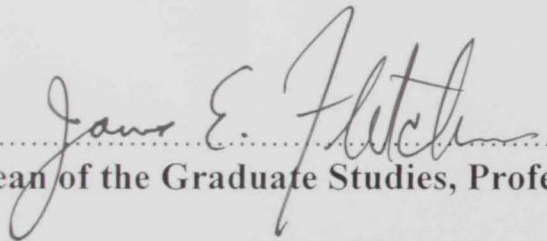
Examining Committee Member, Dr. Ahmed M. Almdhdi



Examining Committee Member, Prof. Philip W. LeQuesne



Director of the Program, Dr. Hazem A. H. Kataya

 2/11/06
Dean of the Graduate Studies, Professor James E. Fletcher



United Arab Emirates University
2005/2006

UAEU Library



1000442477



مكتبة زايد المركزية
ZAYED CENTRAL LIB.

Dedication

With all my love to

My husband, saif

My daughter, fatima

My son, saeed

You keep my spirit alive!

Also, to my parents and family,

For their guidance, support, love and enthusiasm. Without these things this thesis
could not have been possible

Finally,

This thesis is dedicated to all those who believe in the richness of learning.

Acknowledgments

In the race against the clock in which one almost inevitably becomes enmeshed when preparing a thesis, it is a true relief to be surrounded by people who show sympathy and who continue to believe in what you are doing. First I want to thank God, who has sustained me through these, the best and toughest years of my life

The main credit for such support should undoubtedly go to my long-suffering supervisors Dr. Ibrahim M. Abdou for his excellent supervision of the work which led to this thesis, for his enormous support and encouragement during my research. I am also thankful for his steady stream of advice and guidance he gave me in spite of his busy schedule, for helping me organize the thesis draft and refine its contents, Thank you for making constructive comments, criticisms and suggestions for improving the various drafts of this thesis. And for being patient with me through all the times I have been frustrated. This thesis would not exist at all without him, His knowledge, guidance, energy, companionship and inspiration will always serve to me as an example of the perfect supervisor. Thanks for teaching me how to be a (successful?) researcher.

I would like to thank my secondary supervisor, Dr. Ahmed Al-Marzooqi, for his encouragement, advice and support. I would also like to extend my gratitude to Prof. Abdullfatah Haikal, Dr. Adel Amer, Dr. Mohamed Alazab, for their continuous support, encouragement and guidance I received from them. I would like to express my gratitude to all staff members at the Chemistry department, for all their support and guidance. I want to reserve a special word of gratitude to Dr. Ihsan Shahada for his support and for his valuable guidance in the QM calculations. My deep thanks to the United Arab Emirates University, Deanship of Graduate Studies and Dr. Ahmed

Al-Shamsi the Chairman of the Chemistry Department. In addition, I offer my deep gratitude to Mr. Esam at the Central Laboratories Unit. I am extremely grateful to Mr. Bassam for his stimulating support during the whole project. Since part of this research project was carried out in faculty of Medicine & Health Science, I am grateful to my friend salma for her generous help, support and infinite patience. I would like to express my appreciation for the valuable comments and suggestions from thesis examiners, However, to those who hindered me, those who were the very antithesis of helpfulness, you know who you are and so do I, I would just like to say this; thank you, you only made me more determined. Many special thanks to all my family members. I am indebted to my parents for the sacrifices they have made for me. For they have given me much support throughout the years of my thesis research. They, not only gave me life, but also fill it with all the love and affection one can wish for. My father for pushing me to be the best, and giving me a shoulder to lean on when times were hard. My mother has been an inspiration throughout my life. She has always supported my dreams and aspirations; I'd like to thank her for all she is, and all she has done for me. Writing a thesis is not only a personal academic mission but also a family affair. I know that the research work has often required my time and the time I was supposed to spend with my family. Special thanks from my heart to my husband who all have understood my provisional dedication to my research work and supported me greatly to achieve my goal. My brothers and sister, I thank them for always being at my side, listening to me and giving me their love and support. My most sincere appreciation goes to all my friends, without whom these four years would have been insufferable. I would also like to thank all of my friends for the encouragement given, for the reducing some of the pressure when things were stressful.

Last but not least, I would like to thank all the people who made this work possible. Who have acted as catalysts in my transformation? Who helped me to develop the project by giving time, insight, ideas and criticism? I apologize to all I have forgotten, I assure them that their help was valued as much as that of the people mentioned above.

Shaikha alneyadi

Abstract

3-Deazapyrimidine nucleosides have been shown to exhibit great potential as pro drug for use in medicine especially as antagonists to cancer tumors and the HIV-virus. Recent research has focused on the design, synthesis and characterization of novel nucleoside analogues.

Fluoropyridinone and their corresponding nucleoside derivatives have been synthesized and characterized to induce the activity against tumors. 4,6-diaryl-3-cyano-2(1*H*)-pyridinones (**82a-i**) and their nucleosides were prepared. A trifluoromethyl group was introduced into the pyridinone ring system to study its effect on different tumor cells. The glycoside analogues (**83a-e**, **85a-e**, **87a-e** and **88a-d**) have been synthesized in good yield *via* the reaction between pyridinone derivatives and an activated hexapyranosyl sugar to give *N*-nucleosides (**83a-e**, **85a-e**, **87a-e** and **88a-d**) as the sole product. In our biological screening, it was found that the fluorine and trifluoromethyl derivatives of the pyridine ring enhance the biological activity. Moreover, the novel non-nucleoside derivatives (**89a-d**) are found to be more active than the corresponding *N*-nucleosides. This enhancement in biological properties is due to the presence of the fluorine groups on the pyridine ring.

Computer aided Quantum Mechanics (QM) calculations using density functional theory (DFT) were used to study the reactivity of 3-deazapyrimidines with activated sugar molecules. Gaussian 98 was employed for the calculation of geometries and energies. Charge density gas phase calculations were performed at the B3LYP level with the 6-31G basis set. The data obtained from QM calculations supports our experimental results by showing higher charge density on the pyridine *N*-atom than on the oxygen atom at C-2. *HOMO-LUMO* charge density studies of the isolated compounds are fully consistent with the spectroscopic results.

Structure-Activity Relationships (SAR) of nucleosides (**83a-e**, **85a-e**, **87a-e** and **88a-d**) and other non-nucleosides (**89a-d**) showed an interesting biological activity. Structure-activity relationships studies of 3-deazapyrimidine derivatives were used to determine the parts of the structure that are responsible for its biological activity and its side effects according to the nature of the substituents. The results have shown that 2-thiophene at the 4-position has the highest activity among all analogues. In addition, the aryl group at the 6-position has shown similar activities. For example, 4-(thiophen-2-yl)-6-phenyl-3-cyano-2(1*H*)-pyridinones (**82d**) and 4-(thiophen-2-yl)-6-(*p*-chlorophenyl)-3-cyano-2(1*H*)-pyridinones (**82e**) have shown the same activity at lower and higher concentrations. This result indicates that aryl groups at the 6-position have the same effects, based on the results obtained from biological screening. Meanwhile, nucleosides containing the glucopyranosyl ring system showed higher activity than the galactose isomer. For example, compounds (**83a-e**) have shown better activity than the corresponding galactoside analogues (**87a-e**). All free nucleosides showed higher activity due to the solubility factor, where the low soluble acetylated derivatives showed good activities.

2-Thiophene present at the 4-position showed promising biological activity in both nucleosides and non-nucleosides. Meanwhile, more interesting results were obtained from the non-nucleoside analogues (**89a-d**). SAR has explained these results as follows:

The solubility factor might not be the dominant factor because even the low soluble non-nucleoside (**89a**) was found to have the highest potential activity.

TABLE OF CONTENTS

Part One

Chemical synthesis

1. Introduction	1
1.1 Synthesis of Nucleosides	3
1.1.2 Condensation Methods Using Protected Sugar Derivatives	3
1.1.2.1 Metal Salts Methods	4
1.1.2.2 The Hilbert-Johnson Method	6
1.1.2.3 Fusion Method	7
1.1.2.4 The Silyl Method	9
1.1.3 Construction of the Pyrimidine and Purine Ring System	11
1.1.3.1 Construction of Pyrimidine Ring System	11
1.1.3.2 Construction of Purine Ring System	12
1.1.4 Effects of Catalyst and Solvent	13
1.1.5 Transglycosylation	17
1.1.6 Synthesis of Deazanucleosides	19
1.2 Aims and Objectives	23
2. Materials and Methods	25
2.1 General Procedure for the Synthesis of 2(<i>IH</i>)-Pyridinones	25
2.2 General Procedure for Nucleoside Synthesis	29
2.2.1 Method A (The Potassium Salt Method)	29
2.2.2 Method B (The Silyl Method)	29
2.3 General Procedure for Free Nucleoside Synthesis	36
2.3.1 Method A (Transesterification-Saponification Using Saturated Methanolic Ammonia)	36
2.3.2 Method B (Transesterification-Saponification Using Triethylamine)	36
2.4 General Procedure for Synthesis of 4,6-Diaryl-1-(<i>p</i> -fluorobenzoyl)-3-cyano-2-pyridinone (89a-d)	41
3. Results and Discussion	44
3.1 Synthesis of 3-Deazapyrimidine Derivatives	44
3.2 Nucleosides Derived from 3- Deazapyrimidines	51
3.2.1 Prydinone Glucosides (83a-e)	51
3.2.1.1 Potassium Salt Method	51
3.2.1.2 The Silyl Method	52
3.2.2 Ammonolysis of Nucleosides (83a-e)	58
3.2.3 Pyridinone Galactosides	62
3.2.4 Ammonolysis of Nucleosides (87a-d)	68
3.3 Synthesis of Non-Nucleoside Derivatives (89a-d)	68
Summary	69

Part Two

4. Biological activity

4.1	Introduction	75
4.1.1	Biochemistry of Nucleosides	78
4.1.1.1	Purine and Pyrimidine Nucleoside Analogues	78
4.1.1.2	Pyrimidine Nucleoside Analogues and Nucleobases	80
4.1.1.2.1	Biological Properties of Pyrimidine Nucleoside	80
4.1.1.2.2	Biological Properties of Deazapyrimidines	81
4.1.2	Fluoropyrimidines Nucleosides	82
4.1.2	Nucleosides and Cancer	82
4.1.2.1	Apoptosis	83
4.1.2.2	Nucleosides and Apoptosis	85
4.2	Materials and Methods	87
4.2.1	Reagents	87
4.2.2	Tissue Culture	87
4.2.3	MTT Cell Proliferation Assay	87
4.3	Results and Discussion	88
4.3.1	Effects on HL-60 Proliferation and Integrity by Nucleosides	88
4.3.2	Discussion	93
4.4	Conclusion	94
4.5	Recommendation and Future Work	95
	References	96
	Appendixes	98

LIST OF FIGURES

- Figure 1** Structures of nucleic acid bases
- Figure 2** Structures of β -form of Cytidine and Deoxadenosine
- Figure 3** Structures of an β - and α -isomers of Deoxycytosine.
- Figure 4** Hexapyranosyl conformers 4C_1 and 1C_4
- Figure 5** General structures of 3-deazapyrimidinone (82a-i) and related 1-(*p*-fluorobenzoyl) derivatives (89a-d)
- Figure 6** Molecular Orbital Calculations for compound (82e): Wire structures show the total charge density. Solid colors (red and blue) show *HOMO* and *LUMO* electron density
- Figure 7** Optimizing structure for compound (82e) using DFT at B3YLP level using the 6-31G basis set
- Figure 8** COSY spectrum of compound (83b)
- Figure 9** COSY spectrum of compound (83c)
- Figure 10** COSY spectrums of compound (83d)
- Figure 11** Optimizing structure for compounds (85a,e) using DFT at B3YLP level using 6-31G basis
- Figure 12** NOESY spectrum of compound (85a)
- Figure 13** COSY spectrum of compound (88a)
- Figure 14** COSY spectrum of compound (88d)
- Figure 15** Some FDA-approved nucleoside drugs
- Figure 16** Some potent nucleoside-based inhibitors of HIV-1 RT
- Figure 17** Pyrimidine and purine analogues used in chemotherapy Gemcitabine, (ara-C, cytarabine) are pyrimidine analogues, whereas fludarabine and (2-CdA, cladribine) are purine analogues. 5-fluorouracil and capecitabine are example for Fluoropyrimidine
- Figure 18** Hallmarks of the apoptotic and necrotic cell death process. Apoptosis includes cellularshrinking, chromatin condensation and margination at the nuclear periphery with the eventual formation of membrane-bound apoptotic bodies that contain organelles, cytosol and nuclear fragments and are phagocytosed without triggering inflammatory processes. The necrotic cell swells, becomes leaky and finally is disrupted and releases its contents into the surrounding tissue resulting in inflammation
- Figure 19** % Viability in HL-60 Cell Line treated with 3-Deazapyrimidine Derivative from MTT cell proliferation assay
- Figure 20** % Viability in HL-60 Cell Line treated with Prydinone glucosides (83a-e) from MTT cell prolieration assay
- Figure 21** % Viability in HL-60 Cell Line treated with Pyridinone Galactosides (87a-d) from MTT cell proliferation assay
- Figure 22** % Viability in HL-60 Cell Line treated non-nucleoside derivatives (89a-d) from MTT cell proliferation assay
- Figure 23** Infrared spectra for (82a), (83a) and (85a)
- Figure 24** Infrared spectra for (82e), (87e) and (88e)
- Figure 25** Infrared spectra for (89a), (89b) and (89c)
- Figure 26** ${}^1\text{H}$ NMR spectrum of compound (82a)
- Figure 27** ${}^{13}\text{C}$ NMR spectrum of compound (82a)
- Figure 28** ${}^1\text{H}$ NMR spectrum of compound (82b)

Figure 29	^{13}C NMR spectrum of compound (82b)
Figure 30	^1H NMR spectrum of compound (82c)
Figure 31	^{13}C NMR spectrum of compound (82c)
Figure 32	^1H NMR spectrum of compound (82d)
Figure 33	^{13}C NMR spectrum of compound (82d)
Figure 34	^1H NMR spectrum of compound (82e)
Figure 35	^{13}C NMR spectrum of compound (82e)
Figure 36	^1H NMR spectrum of compound (82f)
Figure 37	^{13}C NMR spectrum of compound (82f)
Figure 38	^1H NMR spectrum of compound (82g)
Figure 39	^{13}C NMR spectrum of compound (82g)
Figure 40	^1H NMR spectrum of compound (82h)
Figure 41	^{13}C NMR spectrum of compound (82h)
Figure 42	^1H NMR spectrum of compound (82i)
Figure 43	^{13}C NMR spectrum of compound (82i)
Figure 44	^1H NMR spectrum of compound (83a)
Figure 45	^{13}C NMR spectrum of compound (83a)
Figure 46	^1H NMR spectrum of compound (83b)
Figure 47	^{13}C NMR spectrum of compound (83b)
Figure 48	^1H NMR spectrum of compound (83c)
Figure 49	^{13}C NMR spectrum of compound (83c)
Figure 50	^1H NMR spectrum of compound (83d)
Figure 51	^{13}C NMR spectrum of compound (83d)
Figure 52	^1H NMR spectrum of compound (83e)
Figure 53	^{13}C NMR spectrum of compound (83e)
Figure 54	^1H NMR spectrum of compound (85a) DMSO- d_6 & D_2O
Figure 55	^{13}C NMR spectrum of compound (85a)
Figure 56	^1H NMR spectrum of compound (85b)
Figure 57	^{13}C NMR spectrum of compound (85b)
Figure 58	^1H NMR spectrum of compound (85c)
Figure 59	^{13}C NMR spectrum of compound (85c)
Figure 60	^1H NMR spectrum of compound (85d)
Figure 61	^{13}C NMR spectrum of compound (85d)
Figure 62	^1H NMR spectrum of compound (85e)
Figure 63	^{13}C NMR spectrum of compound (85e)
Figure 64	COSY spectrum of compound (85e)
Figure 65	^1H NMR spectrum of compound (87a)
Figure 66	^{13}C NMR spectrum of compound (87a)
Figure 67	^1H NMR spectrum of compound (87b)
Figure 68	^{13}C NMR spectrum of compound (87b)
Figure 69	^1H NMR spectrum of compound (87c)
Figure 70	^{13}C NMR spectrum of compound (87c)
Figure 71	^1H NMR spectrum of compound (87d)
Figure 72	^{13}C NMR spectrum of compound (87d)
Figure 73	^1H NMR spectrum of compound (87e)
Figure 74	^{13}C NMR spectrum of compound (87e)
Figure 75	^1H NMR spectrum of compound (88a)
Figure 76	^{13}C NMR spectrum of compound (88a)
Figure 77	^1H NMR spectrum of compound (88b)
Figure 78	^{13}C NMR spectrum of compound (88b)

Figure 79	COSY spectrum of compound (88b)
Figure 80	¹ HNMR spectrum of compound (88c)
Figure 81	¹³ CNMR spectrum of compound (88c)
Figure 82	¹ HNMR spectrum of compound (88d)
Figure 83	¹ HNMR spectrum of compound (88d) in D ₂ O
Figure 84	¹³ CNMR spectrum of compound (88d)
Figure 85	¹ HNMR spectrum of compound (89a)
Figure 86	¹³ CNMR spectrum of compound (89a)
Figure 87	¹ HNMR spectrum of compound (89b)
Figure 88	¹³ CNMR spectrum of compound (89b)
Figure 89	¹ HNMR spectrum of compound (89c)
Figure 90	¹³ CNMR spectrum of compound (89c)
Figure 91	¹ HNMR spectrum of compound (89d)
Figure 92	¹³ CNMR spectrum of compound (89d)

LIST OF SCHEMES

- Scheme 1** Synthesis of mono- and bis *N*-glucoside using silver salt
Scheme 2 Formation of mono- and bis *N*-glucoside as well as the bis *O*-glucosides
- Scheme 3** Synthesis of cytosine and uracil from the same intermediate
Scheme 4 One-step synthesis of α - and β -isomers of deoxyadenosine derivatives
- Scheme 5** Synthesis of substituted adenosine *via* fusion
Scheme 6 Synthesis of uracil by two different methods
Scheme 7 Synthesis of *N*⁷ and *N*⁹ nucleosides using HgBr₂
Scheme 8 Synthesis of pyrimidine nucleoside using ring closure
Scheme 9 Purine nucleosides using ring construction
Scheme 10 Schematic mechanism of tribenzoyluracil formation
- Scheme 11** Synthesis of 6-methylpyrimidine-2,4-dione nucleosides
Scheme 12 Synthesis of 6-methylpyrimidine-2,4-dione nucleosides
Scheme 13 Pyrimidine-purine transglycosylation
Scheme 14 Synthesis of an α - and β - isomers *via* *O*→*N* transglycosidation.
Scheme 15 Synthesis of 4-hydroxy-2-pyridinone nucleoside
Scheme 16 Synthesis of 2-pyridinone nucleoside
Scheme 17 Synthesis of 3-cyano-4,6-disubstituted pyridine-2(*1H*)-ones (**82a-i**)
- Scheme 18** Suggested mechanism of 3-cyano-4,6-disubstituted pyridine-2(*1H*)-ones (**82a-i**)
- Scheme 19** Two way synthesis of pyridinone glucosides (**83a-e**)
Scheme 20 Schematic Mechanism of the Silyl Method
Scheme 21 Ammonolysis step of the Pyridinone glucosides
Scheme 22 Synthesis of Pyridinone Galactoside (**87a-e**) in aqueous KOH
Scheme 23 Ammonolysis step of the Pyridinone galactosides
Scheme 24 Synthesis of 1-(*p*-Fluorobenzoyl)-3-cyano-4,6-diaryl-2-pyridinone (**89a-d**)
- Scheme 25** General synthetic scheme for nucleosides and non-nucleosides derivatives

LIST OF ABBREVIATIONS

2-CdA	2-chlorodeoxyadenosine or Cladribine
3TC	Lamivudine
5-FdUMP	5-fluorodeoxyuridine 5'-monophosphate
5-FdUTP	5-fluorodeoxyuridine triphosphate
5-FU	5-Fluorouracil
5-FUTP	5-fluorouridine triphosphate
A	Adenine
AIDS	Acquired Immunodeficiency Syndrome
Ara-A	Arabinosyladenosine
Ara-C	Arabinosylcytidine
AZT	3'-azido-3'-deoxythymidine
Bz	Benzoyl
Bcl-2	B-cell lymphoma 2
C	Cytosine
Calcd	Calculated
d4T	Stavudine
ddC	Zalcitabine
ddI	didanosine
DFT	Density Function Theory
DMA	<i>N,N</i> -Dimethylaniline
DNA	Deoxyribonucleic acid
RNA	Ribonucleic acids
DMSO	Dimethyl sulfoxide
dUTP	Deoxyuridine triphosphate
FUDR	5-Fluoro-2'-deoxyuridine
G	Guanine
HIV	Human Immunodeficiency Virus
HIV-RT	HIV-reverse transcriptase
HL-60	Human promyeloblastic leukemia cell line
HMDS	1,1,1,3,3,3 hexamethyldisilazane
NA	Nucleoside analogues
NMR	Nuclear magnetic resonance
NOESY	Two dimensional nuclear Overhauser spectroscopy
QM	Quantum mechanics
SAR	Structure Activity Relationships
T	Thymine
TMSCl	Trimethylsilyl chloride
TMSOTf	Trimethylsilyl triflate
TMSClO ₄	Trimethylsilyl perchlorate
(TMS) ₂ SO ₄	Trimethylsilylsulfate
TMSI	Trimethylsilyl iodide
TLC	Thin layer chromatography
TS	Thymidylate synthase
U	Uracil

PART ONE

CHEMICAL SYNTHESIS

INTRODUCTION

1. Introduction

The word "nucleoside" originally coined by Levene and Jacobs at 1909⁽¹⁾, for some time referred to compounds isolated from nucleic acids, contained a carbohydrate attached through a nitrogen to either a purine or pyrimidine base. Currently, a nucleoside is defined as a compound of natural or synthetic origin that has a carbohydrate attached to a nitrogen heterocycle through either a carbon-nitrogen bond, as is commonly found, or a carbon-carbon bond, as found in C-nucleosides.

There are two major bases found in natural nucleosides. Purines (Adenine A, and Guanine G) consist of a six-membered and a five-membered nitrogen-containing ring, fused together and Pyrimidines (Cytosine C, Thymine T and Uracil U) which have only a six-membered nitrogen-containing ring (Figure 1).

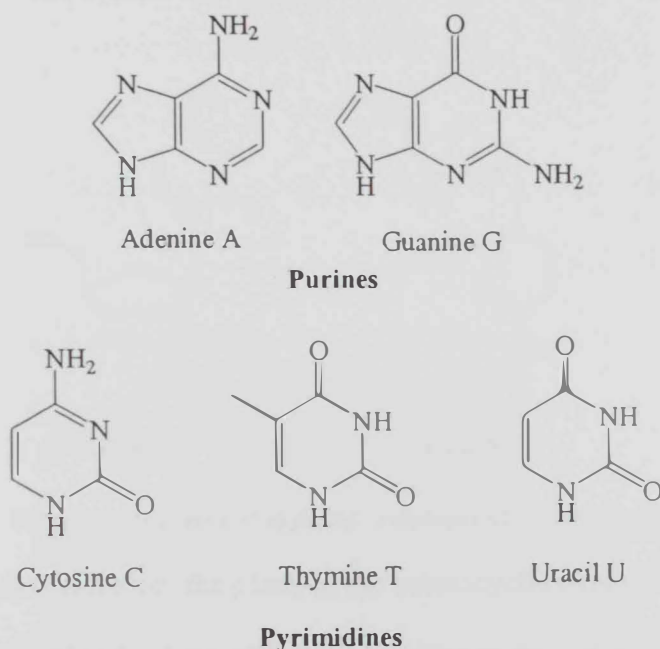


Figure 1: Structures of nucleic acid bases

The bases may be attached to different sugar residues such as hexapyranoside. The glycosidic bond is formed between the anomeric carbon atom of the carbohydrate moiety (C-1

of the sugar) and a ring of the heterocyclic base. The bases are attached to C-1 of the sugar unit, through *N-9* of a purine or *N-1* of a pyrimidine (Figure 2).

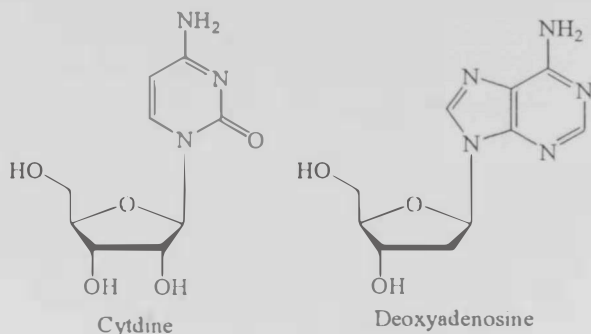


Figure 2: Structures of β -form of Cytidine and Deoxyadenosine

The nucleosides may have two different configurations, the α - or β - configuration. In the α - form, the glycosidic bond and 2'-OH adopt an axial-equatorial correlation, while in the β -form the glycosidic bond and 2'-OH are in the equatorial-equatorial relationship (Figure 3).

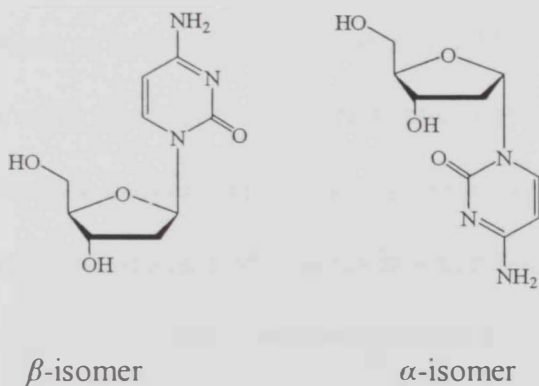


Figure 3: Structures of an β - and α -isomers of Deoxycytosine

In the first approximation, the plane of the heterocyclic base in a nucleoside is almost perpendicular to the "folded" plane of the sugar. The sugar moiety itself in a nucleoside usually exists in one major thermodynamically stable conformation. The 4C_1 is thermodynamically a more stable isomer than the 1C_4 conformations of the hexapyranosides

sugar (Figure 4). Similarly, the pentapyranoside and pentafuranoside ring structures exist in one preferred conformation.

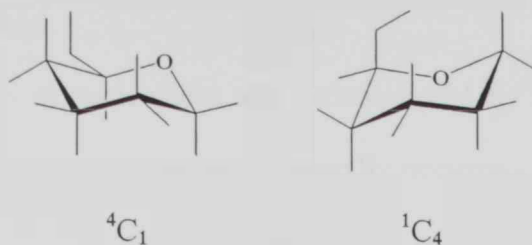


Figure 4: Hexapyranosyl conformers 4C_1 and 1C_4

1.1 Synthesis of Nucleosides

The chemistry of nucleosides is rapidly becoming a very attractive area of research. This is due to the fact that the study of structures and biological applications require a large number of new synthetic nucleosides. It is reasonably expected that the nucleoside analogues will exhibit different activities through the interaction at many enzymatic pathways of synthesis and metabolism of nucleosides, nucleotides, DNA and RNA respectively.

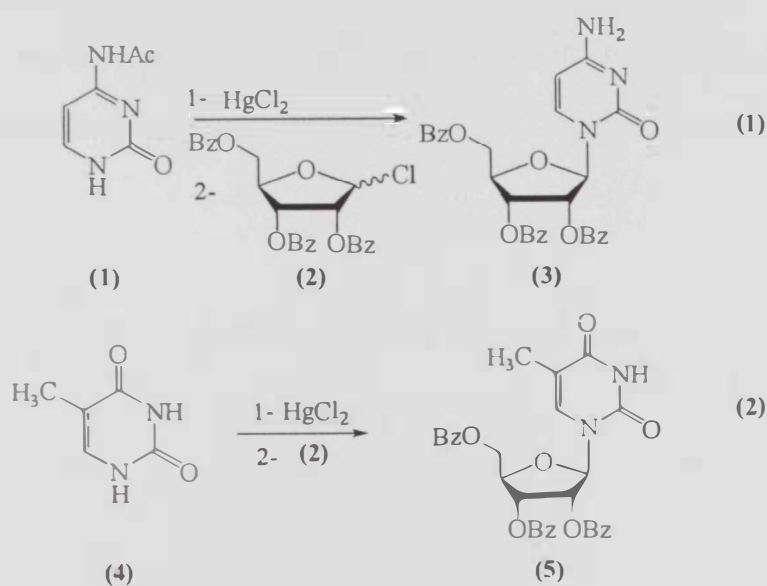
There are two main approaches to the synthesis of pyrimidine nucleosides. The first one is based on the reaction between an activated pyridinone substrate or its derivatives and 1-halo-or 1-acetoxy-substituted sugar derivatives in which the hydroxyl groups are protected with acetyl or benzoyl groups. A less common approach involves construction of a pyridine ring system.^(2,3)

1.1.2 Condensation Methods Using Protected Sugar Derivatives

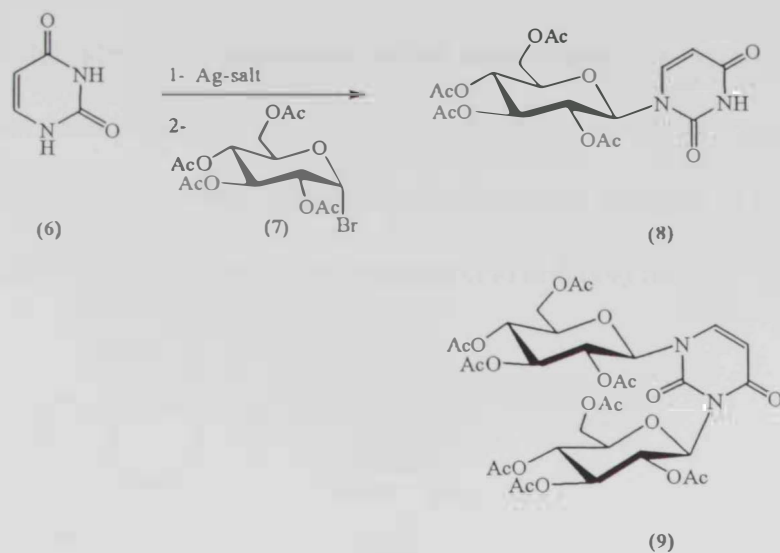
The following examples illustrate the application of this method:

1.1.2.1 Metal Salts Method

The first synthesis of nucleosides was accomplished by Fischer and Helferich⁽⁴⁾ in 1914 by the reaction of silver derivatives of naturally occurring pyrimidine with glycosyl halides. It was shown that, the monomeric derivatives of *N'*-acetylcytosine (**1**) condensed with 2,3,4-tri-*O*-acetyl-D-ribofuranosyl chloride (**2**) gave the cytosine nucleoside (**3**). In a similar way, the treatment of the mercury salt of thymine (**4**) with (**2**) afforded a thymine nucleoside (**5**) (Equations 1 and 2).

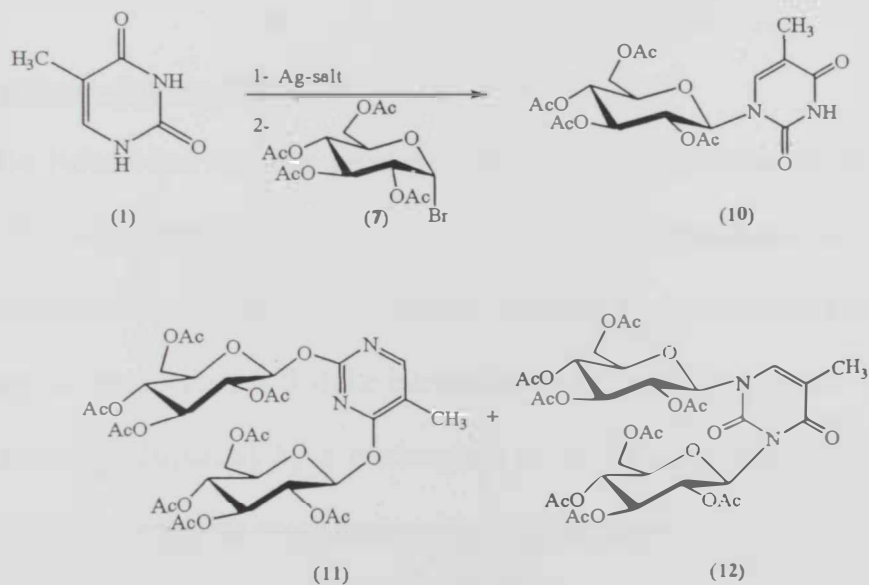


On the other hand, treatment of the silver salt of uracil (**6**) with tetra-*O*-acetyl- α -D-glucopyranosyl bromide (**7**) gave a mixture of nucleosides 1-(2',3',4',6'-tetra-*O*-acetyl- β -D-glucopyranosyl) uracil (**8**) and 2,4-bis (2',3',4',6'-tetra-*O*-acetyl- β -D-glucopyranosyloxy) uracil⁽⁵⁾ (**9**) in yield 28 % and 52 % respectively (Scheme 1).



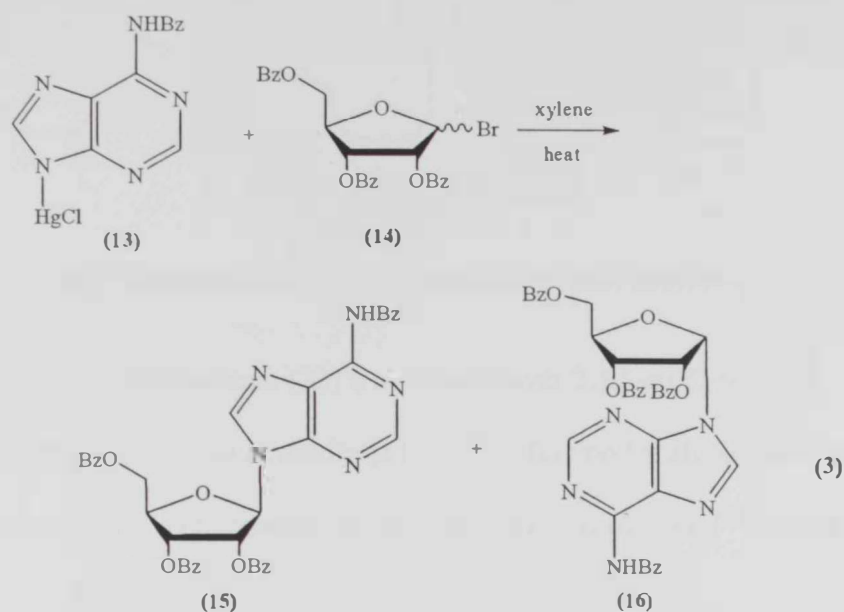
Scheme 1: Synthesis of mono- and bis-*N*-glucoside using silver salt

When the reaction was repeated with the silver salt of thymine (1) under similar conditions the products were *N*¹-glucoside (10), 2,4-bis-*O*-glucoside (11) and *N*¹,*N*³-isomer (12) (Scheme 2).



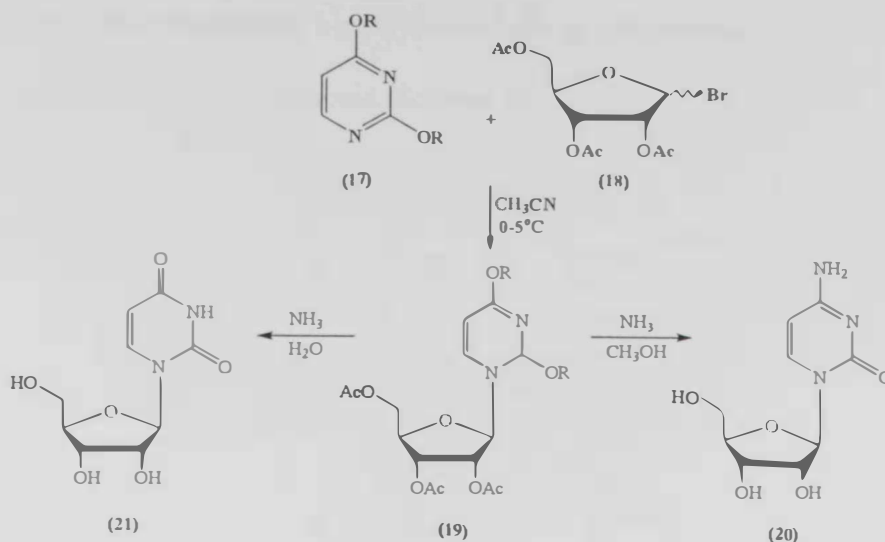
Scheme 2: Formation of mono- and bis-*N*-glucoside as well as the bis-*O*-glucosides

A successful attempt to synthesize purine nucleosides was reported by Davoll and Lowy.⁽⁶⁾ They obtained purine nucleosides by condensation of the mercury derivative of 6-benzoyl-purine (**13**) with 2,3,5-tri-*O*-benzoyl-D-ribofuranosyl bromide (**14**). The product of this reaction was a mixture of α - and β -nucleosides (**15**) and (**16**) respectively (Equation 3).



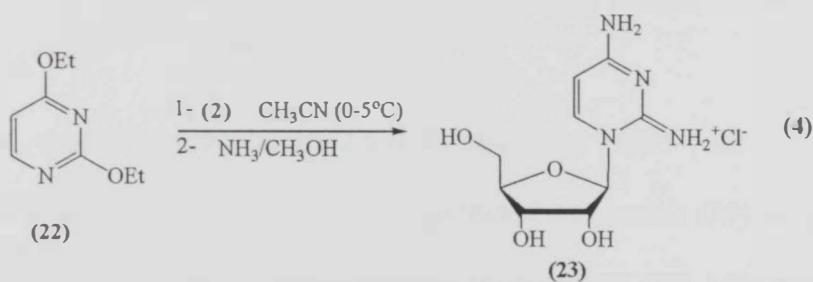
1.1.2.2 The Hilbert–Johnson Method

In 1930 Hilbert and Johnson developed the first general method for the synthesis of nucleosides.⁽⁷⁾ 2,4-Dialkoxy pyrimidine (**17**) reacted with 2,3,5-tri-*O*-acetyl-D-ribofuranosyl bromide (**18**) to produce *via* ammonolysis the non isolated intermediate (**19**) cytidine⁽⁸⁾ (**20**). The advantage of this method is that the intermediate (**19**) contains a reactive group at C-4 which can be easily displaced by a nucleophile as in the synthesis of (**20**), or can be converted to the corresponding uracil nucleosides (**21**) (Scheme 3).



Scheme 3: Synthesis of cytosine and uracil from the same intermediate

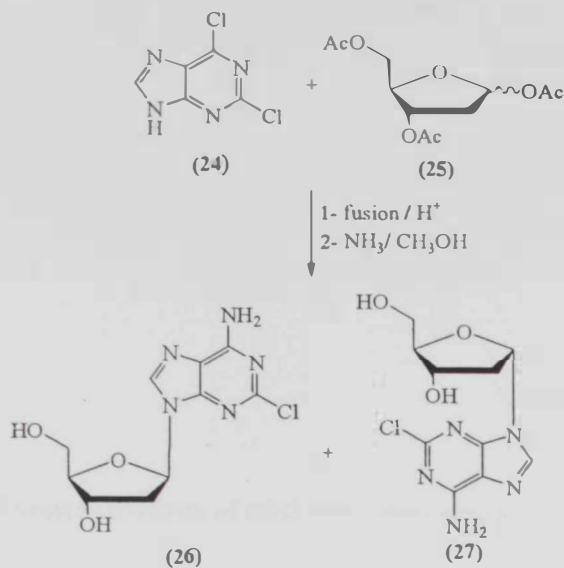
When 2,4-diethoxypyrimidine (22) was treated with 2,3,5-tri-*O*-benzoyl- β -D-ribofuranosylchloride (2) in acetonitrile at 0-5 °C followed by alcoholic ammonia, 2,4-diamino-1-(β -D-ribofuranosyl) pyrimidinium chloride (23) was obtained⁽⁹⁾ (Equation 4).



1.1.2.3 Fusion Method

One of the major advances in nucleoside synthesis was the introduction of the fusion method by Shimadate and co-workers.⁽¹⁰⁻¹²⁾ In its original form the method consisted of heating the aglycon under vacuum with polyacetylated sugar in an acidic medium. Sato and co-workers⁽¹³⁾ used this method to prepare 2-methylthioadenine nucleosides. Two isomeric nucleosides (26) and (27) were obtained by the fusion of 2,6-dichloropurine (24) with sugar

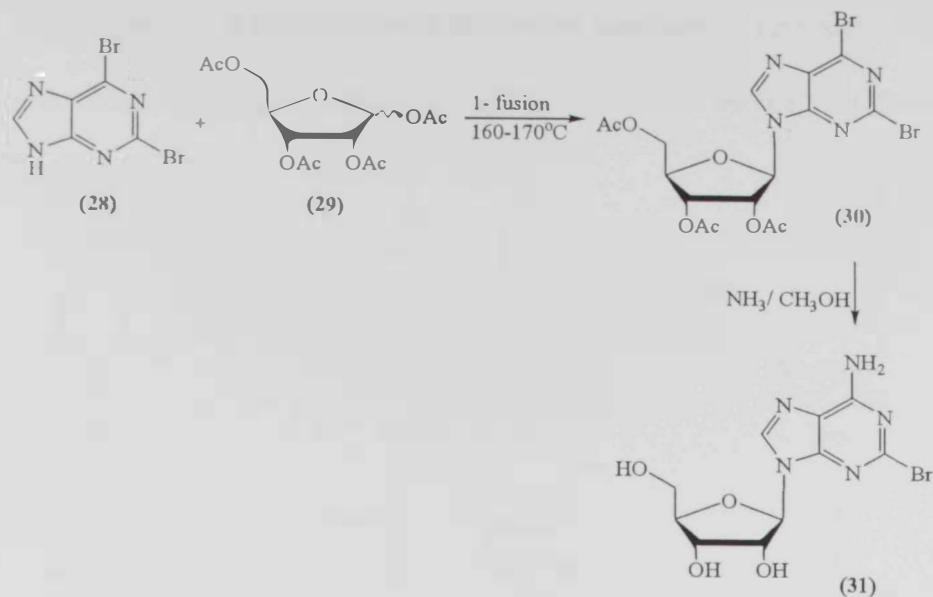
derivatives (25) in the presence of a catalytic amount of chloroacetic or dichloroacetic acid followed by the treatment with ammonia (Scheme 4).



Scheme 4: One-step synthesis of α - and β -isomers of deoxyadenosine derivatives

A long number of catalysts have been successfully employed for the fusion reaction including zinc chloride, aluminum chloride, sulfur trioxide, sulfamic acid, iodine and polyphosphoric acid.⁽¹⁴⁻¹⁷⁾

By contrast, a similar reaction of 2,6-dibromopurine (28) with 1,2,3,5-tetra-*O*-acetylribofuranose (29) at 160-170 °C produced a protected nucleoside (30) in a good yield. The corresponding nucleoside (31) was obtained by treatment of (30) with ammonia^(13, 18) (Scheme 5).

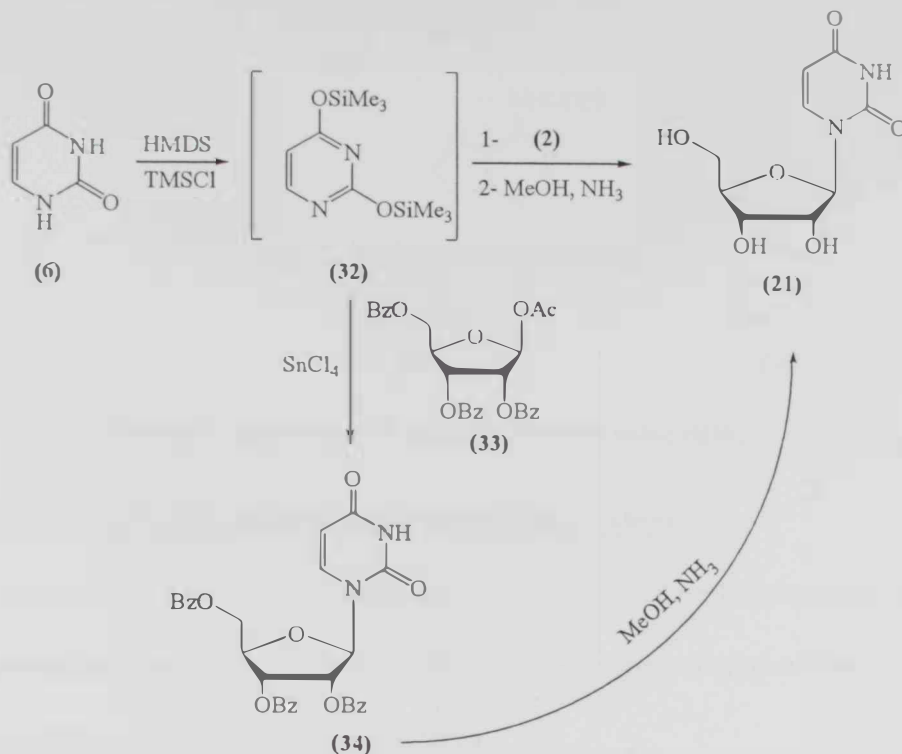


Scheme 5: Synthesis of substituted adenosine *via* fusion

1.1.2.4 The Silyl Method

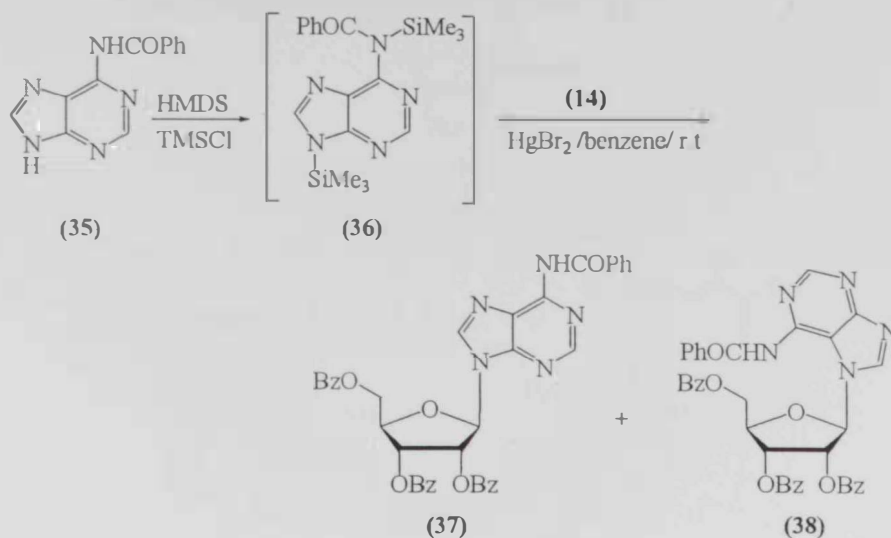
Use of trimethylsilyl derivatives of heterocyclic bases as reagents in nucleoside synthesis was reported by Brikhofe⁽¹⁹⁾ and by Nishimura and co-workers.⁽²⁰⁾ The synthesis of nucleosides involves two steps: the first is the formation of the silyl intermediate while the second is the condensation between the resultant silyl derivatives with an activated sugar. The major silylating agents are: chlorotrimethylsilane Me_3SiCl , (TMSCl), hexamethyl disilazane $\text{Me}_3\text{SiNHSiMe}_3$ (HMDS), silylated acylamides such as $\text{Me}(\text{OSiMe}_3)\text{C}=\text{NSiMe}_3$ and aminotriethyl silane Et_3SiNH_2 . In the preparation of uridine (21), uracil (6) was treated with excess of HMDS and TMSCl; then the silyl intermediate (32) was allowed to react, without isolation, with 2,3,5-tri-*O*-benzoyl-D-ribofuranosyl chloride (2) followed by hydrolysis with base to produce the same product (21) (Scheme 6). An especially useful modification of the trimethylsilyl method is the use of silylated pyrimidines (32) with 1-*O*-

acetyl-2,3,5-tri-*O*-benzoyl- β -D-ribofuranose (**33**) in the presence of a Friedel-Crafts catalyst, such as stannic chloride SnCl_4 , to prepare 2',3',5'-tri-*O*-benzoyluridine (**34**) (Scheme 6).



Scheme 6: Synthesis of uracil by two different methods

In general, the silyl method is particularly useful for the synthesis of pyrimidine nucleosides, which can be used to complement the fusion synthesis which is generally more suitable for preparing purine nucleosides. The use of mercuric salts in the reaction holds a great potential to extend the method to purine nucleosides. Two isomeric nucleosides (**37**) and (**38**) were obtained by the reaction between the bistrimethylsilyl purine derivative (**36**) and 2,3,5-tri-*O*-benzoyl-D-ribofuranosyl bromide (**14**) in benzene at room temperature in the presence of mercuric bromide (Scheme 7).



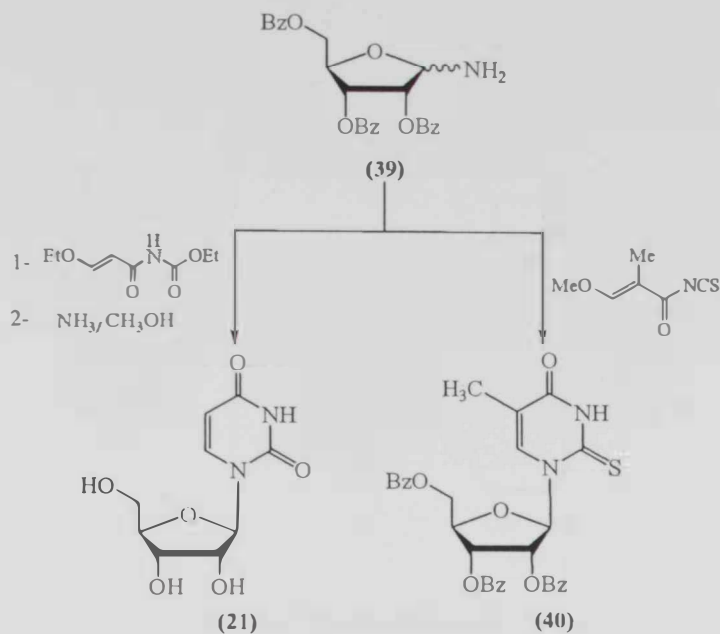
Scheme 7: Synthesis of N^7 and N^6 nucleosides using HgBr_2

1.1.3 Construction of the Pyrimidine and Purine Ring System

The methods discussed above involve a reaction between a heterocyclic base and a sugar. This general method has been used to prepare both purine and pyrimidine nucleosides.

1.1.3.1 Construction of Pyrimidine Ring System

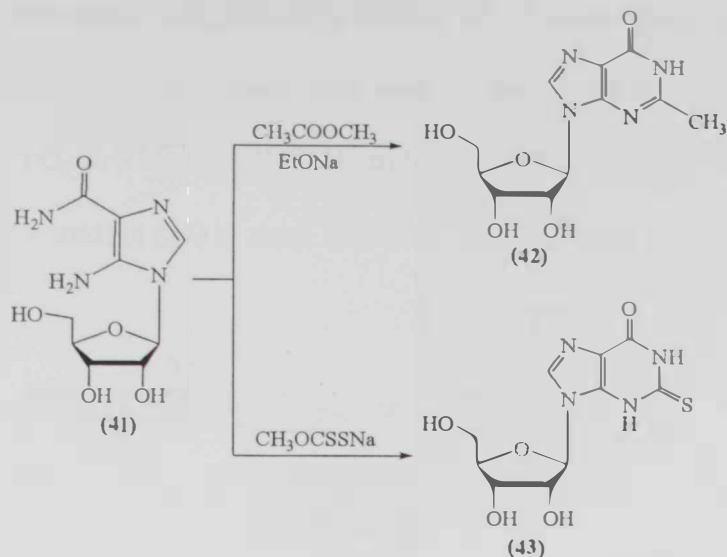
The first pyrimidine nucleoside synthesis using ring closure was reported in 1958 by Show^(21, 22) Uridine (**21**) was obtained by the reaction between the ribosylamine derivative (**39**) and β -ethoxy- N -ethoxycarbonylacrylamide followed by hydrolysis. A thio nucleoside derivative (**40**) was obtained by using α -methoxy- β -methoxyacryloyl isothiocyanate.⁽²⁰⁾ β -isomer was isolated in both cases even though the anomeric mixture of (**39**) was used (Scheme 8).



Scheme 8: Synthesis of pyrimidine nucleosides using ring closure

1.1.3.2 Construction of the Purine Ring System

A number of purine nucleosides have been prepared by the construction of the heterocyclic system after the C-N glycosidic linkage had been formed. The imidazol nucleoside **(41)** is a pivotal intermediate in the synthesis of the purine nucleoside by ring annulation. The preparation of nucleoside **(42)**⁽²¹⁾ and **(43)**⁽⁶⁾ are given as examples in scheme 9.



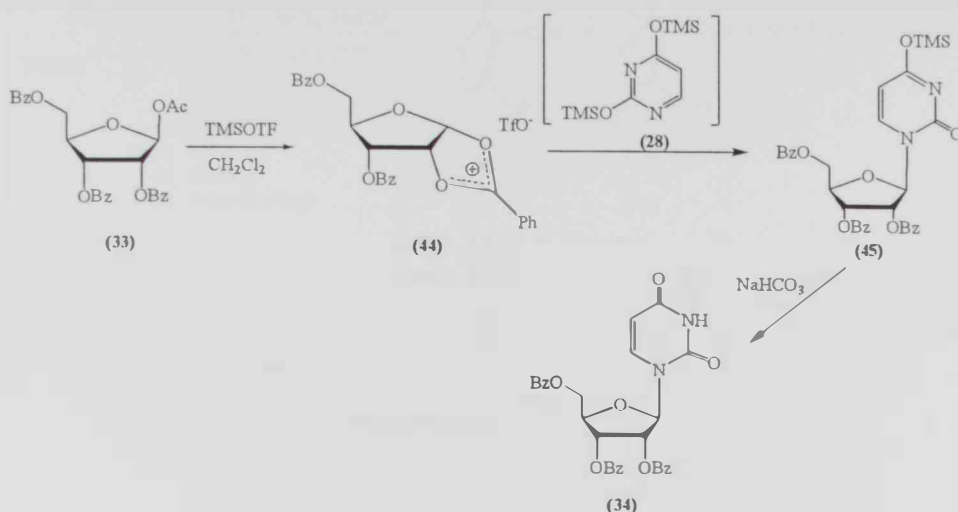
Scheme 9: Synthesis of purine nucleosides using ring construction

1.1.4 Effects of Catalyst and Solvent

Pyrimidine and purine nucleosides can be synthesized by the reaction of silyl heterocyclic bases with peracetylated sugars in the presence of Friedel-Crafts catalysts.⁽²³⁾ However, these procedures still demand the prior silylation of the heterocyclic bases to the highly moisture-sensitive silyl derivatives. Furthermore the perfluoroalkane sulfonic and perchloric acids or their corresponding salts have to be converted to trimethylsilyl triflate.⁽²⁴⁾

It is also found that, Lewis acid catalysts such as $(\text{CH}_3)_3\text{SiSO}_3\text{CF}_3$ or SnCl_4 and the peracetylated sugars derivatives can be combined to effect nucleoside formation in one simple synthetic step in high yield (85%)⁽²⁵⁾. Under this one step condition, the solvation affects the reactivity of the nucleophilic centers even stronger than any other factors. Since Friedel-Crafts catalysts such as SnCl_4 or TiCl_4 had been used successfully for the Silyl-Hilbert-Johnson nucleoside synthesis⁽²⁵⁾ these new silylated Lewis acids TMSClO_4 and TMSOTf were reacted with silylated uracil (28) and (33). It was found that catalytic amounts of TMSClO_4 or TMSOTf in 1,2-dichloroethane or acetonitrile were adequate for generating the

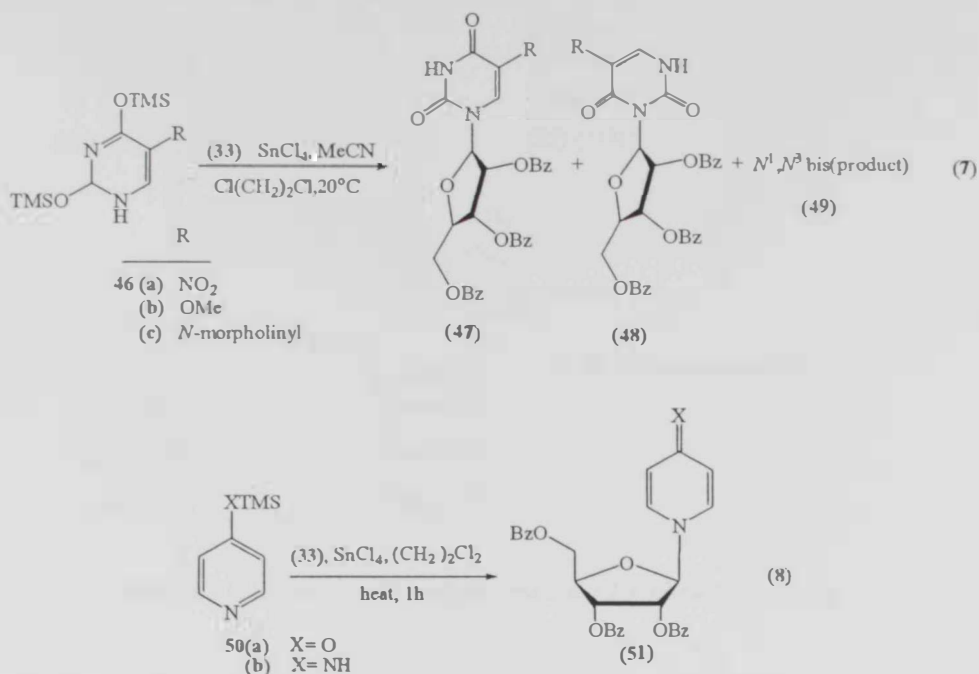
reactive intermediate cation (**44**), although the use of 1.1 equivalents was more efficient. Reaction of (**44**) with silylated uracil (**28**) lead to the silylated intermediate (**45**) and regenerated TMSO⁺ or TMSOTf.^(26,27) Hydrolysis of (**45**) in aqueous NaHCO₃ produced 2',3',5'-tri- *O*-benzoyluridine (**34**) in more than 80% yield (Scheme 10).



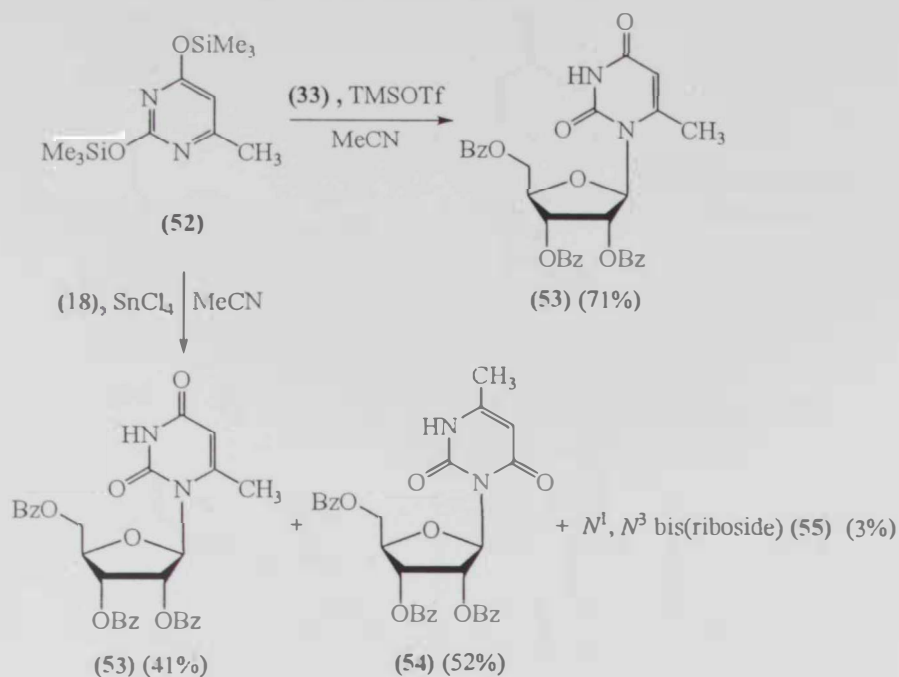
Scheme 10: Schematic mechanism of tribenzoyluracil formation

In contrast to TMSO₄ and TMSOTf, the weaker Lewis acids⁽²⁸⁾ (TMS)₂SO₄ and TMSCl do not promote nucleoside formation, since they do not convert (**33**) into the sugar cation (**44**). However, the even weaker Lewis acid TMSI, which can be prepared *in situ* from TMSCl and NaI in acetonitrile, does catalyze the formation of nucleosides.^(29,30) The use of TMSOTf as a catalyst dramatically increases the yields of the 5-methoxy- or 5-morpholino-2',3',5'-uridine tri-*O*-benzoates (**47b**) and (**48c**) from the silylated uracils (**46b,c**) and (**33**). This is even significant in 1,2-dichloroethane; 89% of (**47b**) (compared to 53% using SnCl₄) and 95% of (**47c**) (compared to 39% using SnCl₄) are obtained. Analogously, use of catalytic TMSOTf with the rather basic silylated 4-trimethylsilyloxy-pyridine (**50a**) and 4-trimethylsilylamino-pyridine (**50b**) gave the corresponding nucleosides (**51a**) and (**51b**) in 87%

and 80% yields,⁽²⁷⁾ whereas (51 a) is obtained only in 63% yield with SnCl₄⁽³¹⁾ (Equations 7 and 8)

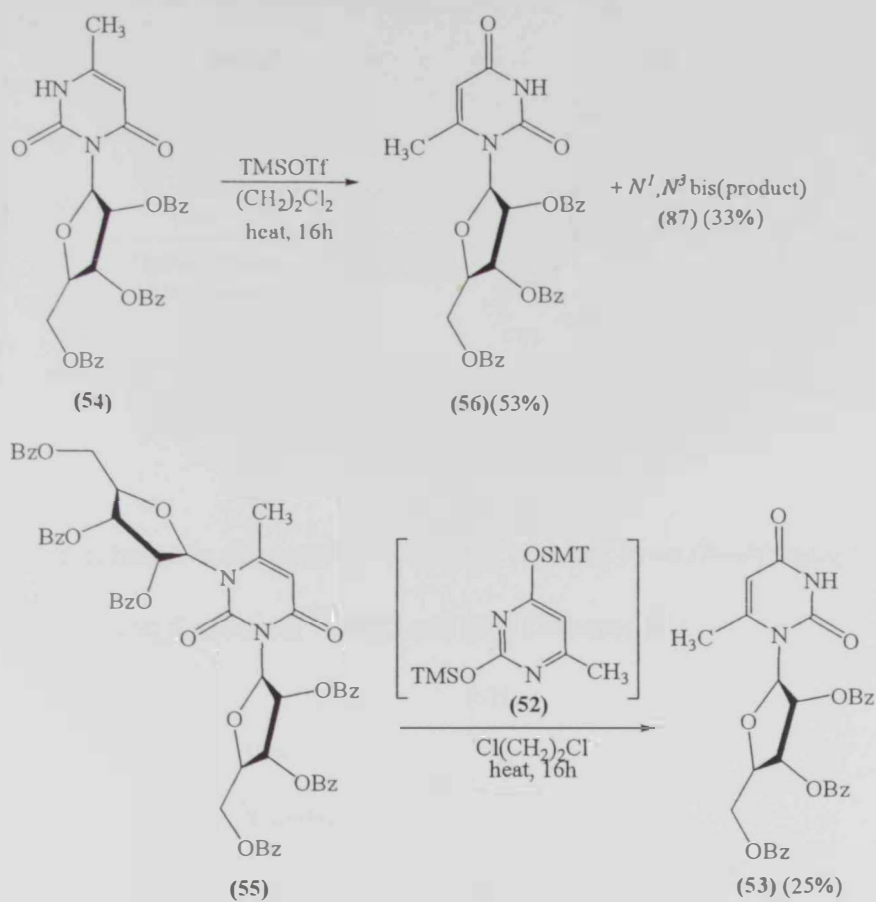


Under carefully controlled conditions using TMSOTf in purified acetonitrile, silylated 6-methyluracil (52) produced the desired protected 6-methyluridine (53) in 71% yield compared to 41% with SnCl₄ (Scheme 11).



Scheme 11: Synthesis of 6-methylpyrimidine-2,4-dione nucleosides

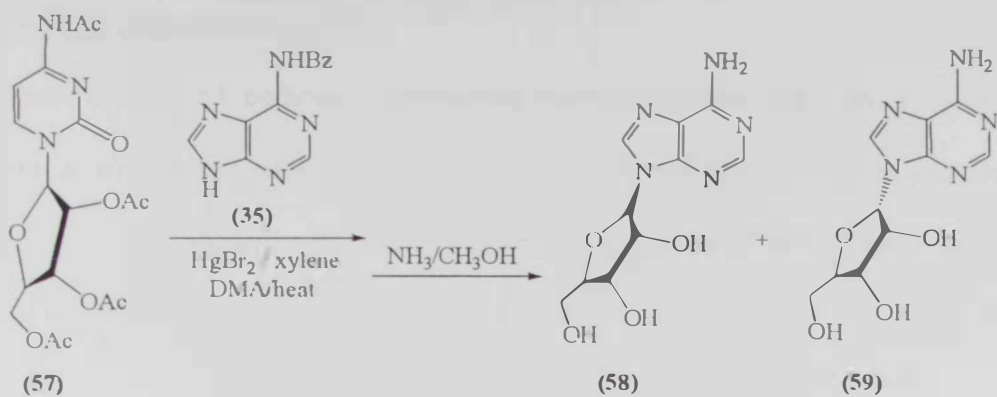
Furthermore, the undesired N^3 -nucleoside (54) rearranges by heating with TMSOTf to give a 53% yield of the protected N^1 -nucleoside (56) and a 33% yield of the N^1, N^3 -bis(riboside) (55). The sterically hindered (55) reacts on heating with silylated 6-methyluracil (52) and TMSOTf to give the corresponding N^1 -nucleoside (53)⁽²⁷⁾ (Scheme 12).



Scheme 12: Synthesis of 6-methylpyrimidine-2,4-dione nucleosides

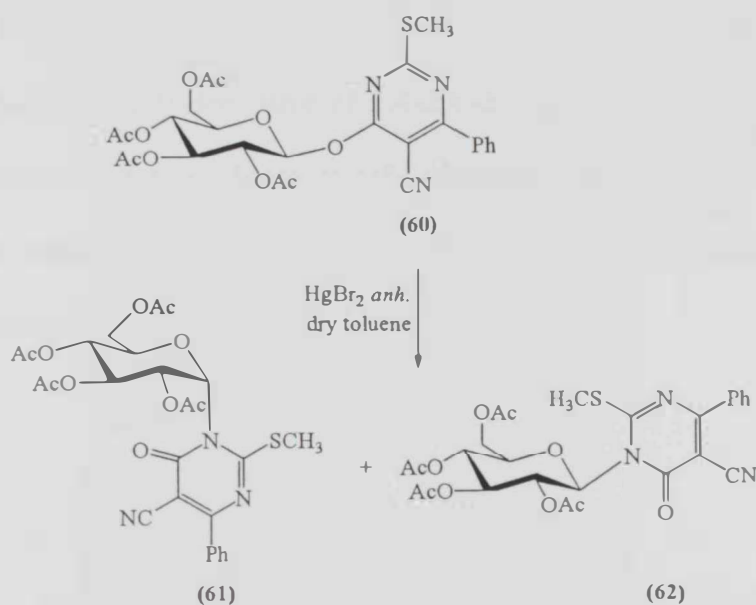
1.1.5 Transglycosylation

Transglycosylation was first investigated by Lichtenthaler and co-workers⁽³²⁾ by treating peracylated cytidine (57) with N^6 -benzoyladenine (35) in the presence of HgBr_2 and DMA in xylene to afford after saponification (58) and its α -isomer (59)⁽³²⁾ (Scheme 13).



Scheme 13: Pyrimidine-purine transglycosylation

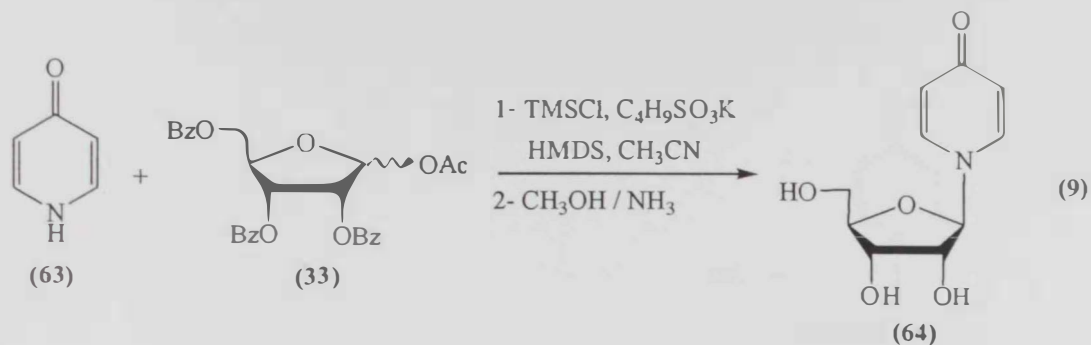
Heating of (60) in toluene in the presence of HgBr_2 resulted in an $O \rightarrow N$ transglycosidation to give a mixture of α - and β - isomers⁽³³⁾ (61) and (62) (Scheme 14).



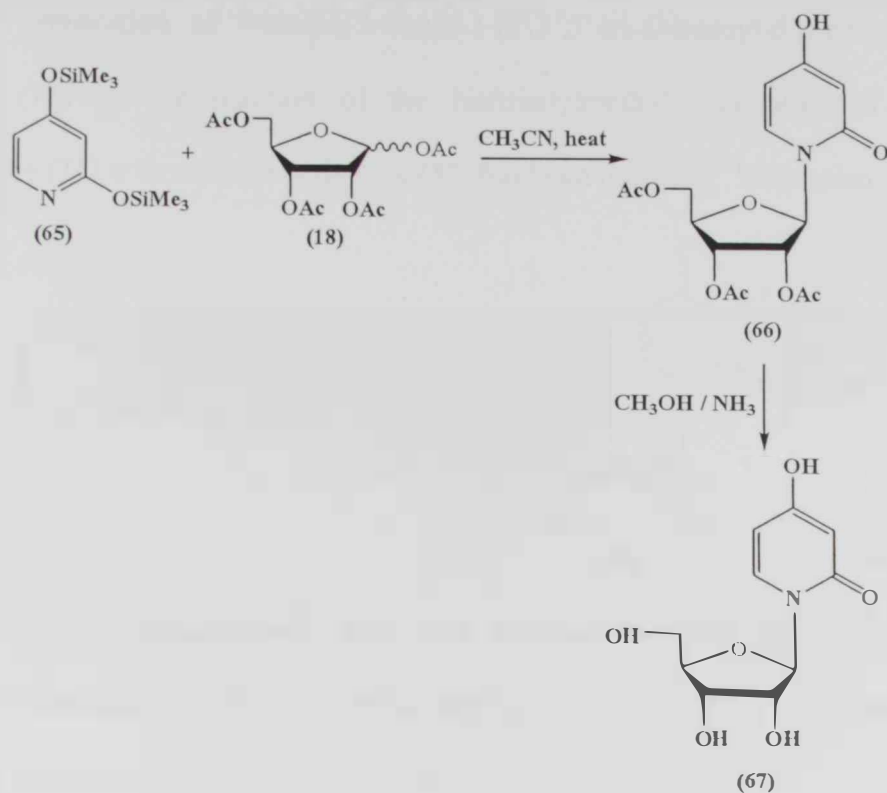
Scheme 14: Synthesis of an α - and β - isomers ($O \rightarrow N$ transglycosidation)

1.1.6 Synthesis of Deazanucleosides

There are several methods to synthesize deazanucleoside. The basic 4-pyridone (63) reacts *via* a silyl intermediate with 1-*O*-acetyl-2,3,5-tri-*O*-benzoyl-D-ribofuranose (33), followed by saponification to yield the free pyridine nucleoside (64) in 50 % yield (Equation 9)

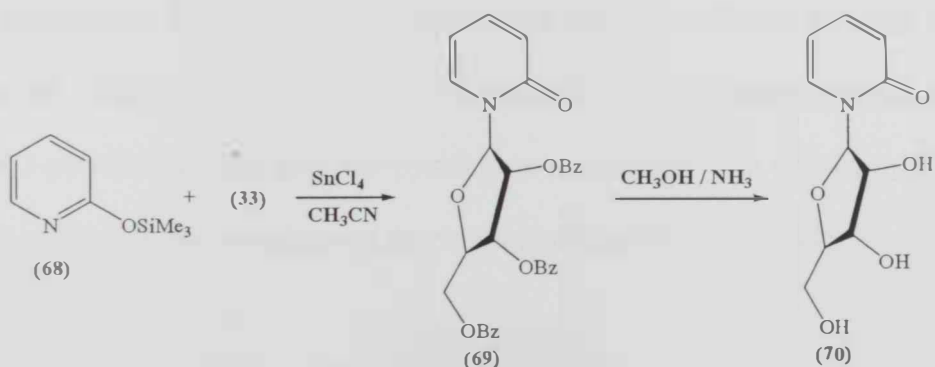


The bis(trimethylsilyl) derivative of 2,4-dihydropyridine (65) is condensed with 2,3,5-tri-*O*-acetyl-D-ribofuranosyl bromide (18) to afford a protected nucleoside (66) in a 78% yield. The corresponding free nucleoside (67) is obtained by treatment of (66) with ammonia⁽³⁴⁾ (Scheme 15).



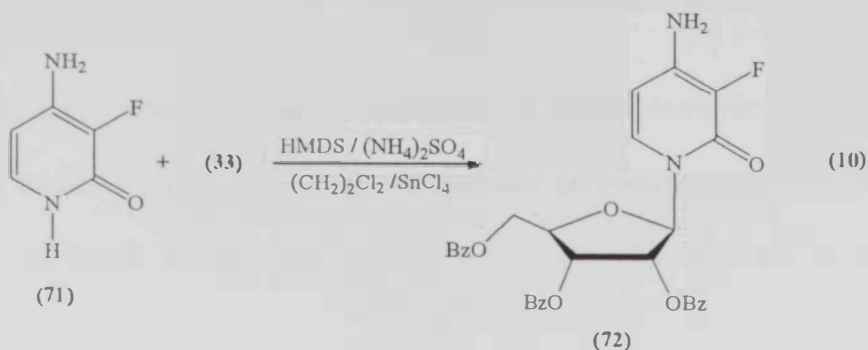
Scheme 15: Synthesis of 4-hydroxy-2-pyridinone nucleoside

Niedballa and Vorbruggen⁽³¹⁾ reported that the reaction of 2-trimethyl silyloxy pyridine (68) with 1-*O*- acetyl-2,3,5-tri-*O*-benzoyl- β -D-ribofuranose (33) in the presence of SnCl_4 gave the corresponding pyridinone nucleoside (69). Subsequent treatment of (69) with methanolic ammonia yielded the free nucleoside (70) (Scheme 16).

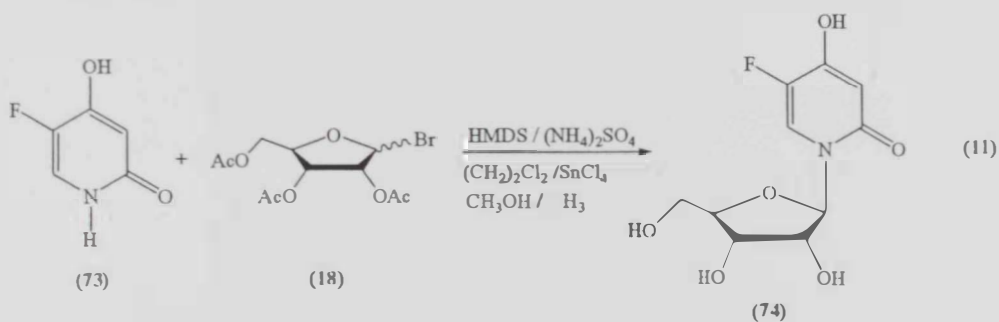


Scheme 16: Synthesis of 2-pyridinone nucleoside

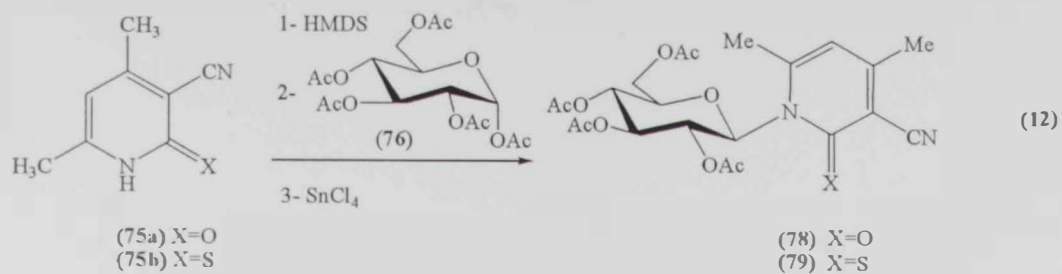
The preparation of 4-amino-3-fluoro-1-(2',3',5'-tri-*O*-benzoyl- β -D-ribofuranosyl)-2-pyridinone (72) by the reaction of the bis(trisilylmethyl) derivative of 4-amino-3-fluoropyridine (71) with a ribose derivative (33) has been reported⁽³⁵⁾ (Equation 10)



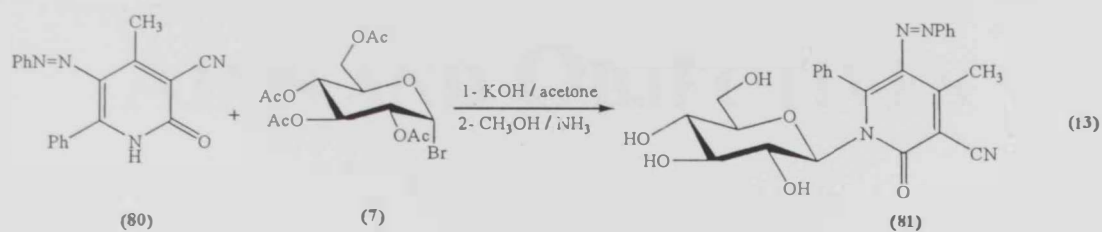
5-Fluoro-3-deazauridine⁽³⁶⁾ (74) was obtained by the reaction between the trimethylsilyl derivative of (73) and a ribose derivative (18), followed by the treatment with ammonia in methanol to produce (74) (Equation 11).



A comparative study that involved two silyl pyridines (75a,b) differing in the C-2 substituent and a bulky sugar derivative (76) has attracted a lot of interest (Equation 12). The reaction of 2-pyridinone (74) gave the pyridinone nucleoside (78). Similarly, the 2-thiono isomer (75) resulted in the formation of the thionopyridine nucleoside (79).



In addition, it was found that for preparation of deazapyrimidine nucleosides reported by Elqemeie and co-workers,^(37,38) 3-deazapyrimidine glycosides (**81**) were obtained by the reaction of the K-salt of (**80**) with an activated sugar derivative (**7**) in 70-85% yield (Equation 13).



AIMS AND OBJECTIVES

1.2 Aims and Objectives

The aims of the present study are:

1. To synthesize some novel 3-deazapyrimidines and their nucleosides using an easy direct method
2. To test the purity and to study the mechanisms of the obtained products.
3. To confirm the obtained structures using different techniques such as FT-IR spectroscopy, 1D- and 2D-NMR, ¹³C-NMR, elemental analysis as well as quantum mechanics calculations..
4. To study the biological activity of the obtained products.

MATERIALS AND METHODS

2. Materials and Methods

General: All air sensitive materials were handled under a nitrogen atmosphere. Mp's (Pyrex capillary) are not corrected. Infrared spectra were recorded with a Thermo Nicolet Nexus 470 FT-IR spectrometer in the range 4000-400 cm^{-1} on samples in potassium bromide disks. ^1H -NMR spectra (200 MHz) and ^{13}C -NMR spectra (75.0 MHz) were obtained on a Varian 200 MHz instrument; chemical shifts were recorded in δ (ppm) units, relative to Me_4Si as an internal standard at 0.0 ppm. The spin multiplicities are indicated by the symbols s (singlet), d (doublet), t (triplet), m (multiplet) and b (broad). Optical rotations were measured with a Perkin-Elmer digital polarimeter at 589 nm (sodium D line) in a 1 dm cell. Thin-layer chromatography (TLC) was carried out on precoated Merck silica gel F₂₅₄ plates and UV light was used for visualization. Column chromatography was performed on a Merck silica gel. Microanalytical data (C, H, N, S) were performed on a Flash-EA-1112 series analyzer and were within $\pm 0.5\%$ for (C, H, N) and $\pm 0.8\%$ for S of the theoretical values. All other reagents were purchased from Aldrich and used without further purification.

2.1 General Procedure for the Synthesis of 2(1H)-Pyridinones

4,6-Disubstituted-3-cyano-2(1H)-pyridinones (82a-i): A mixture of an aromatic aldehyde (10 mmol), ethyl cyanoacetate (10 mmol), or 2-cyanoacetamide, (0.01 mol, acetophenone derivatives (10 mmol) and ammonium acetate (0.1 mol) in ethanol (50 mL) was heated under reflux for 6 h. The mixture was cooled, and the resultant precipitate was filtered off and washed with cold H_2O (3 x 50 mL) to give a solid mass. The solid was crystallized from appropriate solvent (ethanol or DMSO) and dried to give the desired 2-pyridinone (**82a-i**).

4,6-Diphenyl-3-cyano-2(1H)-pyridinones (82a): Pale yellow crystals; yield 85% from DMSO, mp 333°C; $R_f = 0.533$ (6:4 hexane / ethylacetate), IR (KBr, cm^{-1}) 1600 (CO), 2220 (CN), 3440 (NH), $^1\text{H-NMR}$ [DMSO- d_6 , 200 MHz]: (δ , ppm) 6.82 (s, 1H, H-5), 7.54-7.89 (m, 10H, aromatic), 12.81 (bs, 1H, NH); $^{13}\text{C-NMR}$ [DMSO- d_6 , 200 MHz]: (δ , ppm) 106.3 (C-5), 116.5 (CN), 116.0 (C-3), 127.8-136.0 (Aromatic carbons), 151.5 (C-6), 159.8 (CO of pyridine), 162.0 (C-4); Anal. Calcd for $\text{C}_{18}\text{H}_{12}\text{N}_2\text{O}$ (272.30): C, 79.39; H, 4.44; N, 10.29 %, found: C, 79.0; H, 4.46; N, 10.20 %

4-(o-Tolyl)-6-phenyl-3-cyano-2(1H)-pyridinones (82b): Pale yellow crystals; yield 67% from DMSO, mp 284°C; $R_f = 0.38$ (6:4 hexane / ethylacetate), IR (KBr, cm^{-1}) 1641 (CO), 2350 (CN), 3420 (NH); $^1\text{H-NMR}$ [DMSO- d_6 , 200 MHz]: (δ , ppm) 2.36 (s, 3H, CH_3), 6.71 (s, 1H, H-5), 7.31-7.89 (m, 12H, aromatic), 12.81 (bs, 1H, NH); $^{13}\text{C-NMR}$ [DMSO- d_6 , 200 MHz]: (δ , ppm) 107.5 (C-5), 116.6 (CN), 116.0 (C-3), 126.7-137.1 (aromatic carbons), 151.9 (C-6), 161.8 (C-2), 162.4 (C-4); Anal. Calcd for $\text{C}_{19}\text{H}_{14}\text{N}_2\text{O}$ (286.33): C, 79.70; H, 4.93; N, 9.78; found: C, 79.90; H, 5.06; N, 9.87%

4-(m-Tolyl)-6-phenyl-3-cyano-2(1H)-pyridinones (82c): Yellow crystals; yield 76% from DMSO, mp 263°C, $R_f = 0.26$ (6:4 hexane / ethylacetate), IR (KBr, cm^{-1}) 1650 (CO), 2229 (CN), 3442 (NH), $^1\text{H-NMR}$ [DMSO- d_6 , 200 MHz]: (δ , ppm) 2.36 (s, 3H, CH_3), 6.77 (s, 1H), 7.34-7.89 (m, 12H, aromatic), 12.81 (bs, 1H, NH); $^{13}\text{C-NMR}$ [DMSO- d_6 , 200 MHz]: (δ , ppm) 98.4 (C-3), 106.3 (C-5), 116.6 (CN), 125.4-138.3 (aromatic carbons), 151.4 (C-6), 159.9 (C-2), 162.2 (C-4); Anal. Calcd for $\text{C}_{19}\text{H}_{14}\text{N}_2\text{O}$ (286.33): C, 79.70; H, 4.93; N, 9.78 %, found: C, 79.70; H, 5.04; N, 9.77 %

4-(Thiophen-2-yl)-6-phenyl-3-cyano-2(1H)-pyridinones (82d): Yellow crystals; yield 73% from DMSO, mp 315°C; $R_f = 0.62$ (6:4 hexane / ethylacetate), IR (KBr, cm^{-1}) 1643 (CO),

2220 (CN), 3425 (NH), ¹H-NMR [DMSO-*d*₆, 200 MHz]: (δ, ppm) 6.9 (s, 1H), 7.30-7.88 (m, 5H, aromatic), 7.90 (d, 1H, J = 8.6 Hz, CH aromatic), 8.05-8.06 (m, 2H), 12.70 (bs, 1H, NH); ¹³C-NMR [DMSO-*d*₆, 200 MHz]: (δ, ppm) 95.5 (C3), 104.5 (C5), 117.0 (CN), 127.8-136.7 (Ar-C), 150.8 (C6), 151.2 (CO of pyridine), 162.2 (C4); Anal. Calcd for C₁₆H₁₀N₂OS (278.33): C, 69.04; H, 3.62; N, 10.06; S, 11.52 %, found: C, 68.70; H, 3.63; N, 10.0; S, 11.50 %

4-(Thiophen-2-yl)-6-(*p*-chlorophenyl)-3-cyano-2(1H)-pyridinones (82e): Pale yellow crystals; yield 82% from DMSO, mp 342-343°C; R_f = 0.32 (6:4 hexane / ethylacetate), IR (KBr, cm⁻¹) 1660 (CO), 2220 (CN), 3430 (NH); ¹H-NMR [DMSO-*d*₆, 200 MHz]: (δ, ppm) 6.98 (s, 1H, C-5), 7.29-7.34 (m, 1H, aromatic), 7.57-7.62 (d, 2H, J = 8.6 Hz), 7.88-7.93 (d, 2H, J = 8.6 Hz), 7.98-8.07 (m, 2H, 2-thienyl), 12.74 (bs, 1H, NH); ¹³C-NMR [(DMSO-*d*₆), 200 MHz]: (δ, ppm) 104.8 (C-5), 116.9 (CN), 116.0 (C-3), 128.7-136.7 (aromatic carbons), 150.2 (C-6), 150.7 (C-2), 162.3 (C-4). Anal. Calcd for C₁₆H₉N₂OCIS (312.77): C, 61.44; H, 2.90; N, 8.96; S, 10.25 %. found: C, 61.40; H, 2.90; N, 8.94; S, 10.30 %

4-(2-Trifluoromethylphenyl)-6-phenyl-3-cyano-2(1H)-pyridinones (82f): Yellow crystals; yield 80% from DMSO, mp 306-307°C; R_f = 0.34 (6:4 hexane / ethylacetate), IR (KBr, cm⁻¹) 1637 (CO), 2349 (CN), 3446 (NH); ¹H-NMR [DMSO-*d*₆, 200 MHz]: (δ, ppm) 3.82 (s, 3H, *p*-OCH₃), 6.84 (s, 1H, C-5), 7.02-7.10 (d, 2H, J = 9.0 Hz), 7.67-7.70 (d, 2H, J = 4.4 Hz), 8.75-8.78 (d, 2H, J = 4.4 Hz), 12.81 (bs, 1H, NH); ¹³C-NMR [DMSO-*d*₆, 200 MHz]: (δ, ppm) 55.6 (OCH₃), 104.8 (C-5), 116.1 (CN), 114.4, 124.1, 129.6, and 157.1 (aromatic carbons at C-6), 122.6, 150.2, and 152.0 (aromatic carbons at C-4), 143.6 (C-6), 161.8 (C-4), 161.9 (C-2). Anal. Calcd for C₁₉H₁₁N₂OF₃ (340.30): C, 67.06; H, 3.26; N, 8.23 %, found: C, 67.4; H, 3.30; N, 8.30 %

4-(Pyridin-4'-yl)-6-(p-methoxyphenyl)-3-cyano-2(1H)-pyridinones (82g): Yellow crystals; yield 60% from DMSO, mp 329-330°C; $R_f = 0.236$ (6:4 hexane / ethylacetate); IR (KBr, cm^{-1}) 1640 (CO), 2222 (CN), 3448 (NH); $^1\text{H-NMR}$ [DMSO- d_6 , 200 MHz]: (δ , ppm) 6.87 (s, 1H, H-5), 7.45-8.00 (m, 9H, aromatic), 12.91 (bs, 1H, NH); $^{13}\text{C-NMR}$ [DMSO- d_6 , 200 MHz]: (δ , ppm) 106.3 (C-5), 116.2 (CN), 122.0 (CF_3), 125.7-132.3 (aromatic carbons), 140.1 (C-6), 158.4 (C-4'), 161.3 (C-2). Anal. Calcd for $\text{C}_{18}\text{H}_{13}\text{N}_3\text{O}_2$ (303.31): C, 71.28; H, 4.32; N, 13.85 % , Found C, 71.4; H, 4.18; N, 13.8 %.

4-(p-Tolyl)-6-(p-chlorophenyl)-3-cyano-2(1H)-pyridinones (82h): Yellow crystals; yield 80% from DMSO, mp 312-313°C; $R_f = 0.180$ (6:4 hexane / ethylacetate); IR (KBr, cm^{-1}) 2349 (CN), 1636 (CO), 3433 (NH), $^1\text{H-NMR}$ [DMSO- d_6 , 200 MHz]: (δ , ppm) 2.37 (s, 3H, CH_3), 6.83 (s, 1H, H-5), 7.33-7.92 (m, 12H, aromatic), 12.81 (bs, 1H, NH); $^{13}\text{C-NMR}$ [DMSO- d_6 , 200 MHz]: (δ , ppm) 107.2 (C-5), 117.2 (CN), 117.0 (C-3), 128.9-136.6 (aromatic carbons), 141.2 (C-6), 160.2 (C-2), 162.8 (C-4); Anal. Calcd for $\text{C}_{19}\text{H}_{13}\text{ClN}_2\text{O}$ (320.77): C, 71.14; H, 4.08; N, 8.73 % found: C, 71.20; H, 4.03; N, 8.67 %

4-Phenyl-6-(p-chlorophenyl)-3-cyano-2(1H)-pyridinones (82i): yellow crystals; yield 80% from ethanol, mp 305-306°C; $R_f = 0.22$ (6:4 hexane / ethylacetate); IR (KBr, cm^{-1}) 2216 (CN), 1635 (CO), 3446 (NH); $^1\text{H-NMR}$ [DMSO- d_6 , 200 MHz]: (δ , ppm) 6.87 (s, 1H, H-5), 7.52-7.95 (m, 10H, aromatic), 12.81 (bs, 1H, NH); $^{13}\text{C-NMR}$ [DMSO- d_6 , 200 MHz]: (δ , ppm) 107.4 (C-5), 117.1 (CN), 117.0 (C-3), 128.9-136.7 (Aromatic carbons), 151.2 (C-6), 160.3 (CO of pyridine), 162.8 (C-4); Anal. Calcd for $\text{C}_{18}\text{H}_{11}\text{ClN}_2\text{O}$ (306.75): C, 70.48; H, 3.61; N, 9.13 %; found: C, 70.80; H, 3.62; N, 9.13 %.

2.2 General Procedure for Nucleoside Synthesis

2.2.1 Method A (The Potassium Salt Method)

1-(2'',3'',4'',6''-Tetra-O-acetyl-β-D-glycopyranosyl)-3-cyano-4,6-substituted-2-pyridinones (83a-e) and (87a-e): To a solution of 4,6-disubstituted-3-cyano-2(1*H*)-pyridinones (0.01 mol) in aqueous KOH [0.56 g (0.01 mol)] in 6 ml distilled water, a solution of 2,3,4,6-tetra-*O*-acetyl-α-D-hexapyranosyl bromide (0.011 mol, 4.12 g) in acetone 30 ml was added. The reaction mixture was stirred at room temperature until the reaction was judged completed by TLC (4–6h); 30 ml of CH₂Cl₂ was then added. The organic layers were dried over Na₂SO₄, filtered and the organic solvent was removed under reduced pressure at room temperature to afford the crude nucleoside products. The residue was recrystallized from ethanol to give the nucleosides (83a-e) (Scheme 18) and (87a-e) (Scheme 21)

1.2.2.2 Method B (The Silyl Method)

1-(2'', 3'', 4'', 6''-Tetra-O-acetyl-β-D-glucopyranosyl)-3-cyano-4-(thiophen-2-yl)-6-(4'-chlorophenyl)-2-pyridinone (83d): A mixture of 2-pyridinone (82d) (0.01 mol), 1,1,1,3,3,3 hexamethyldisilazane (HMDS, 60 mL), ammonium sulfate (0.125 g) and drops of chlorotrimethylsilane was heated under nitrogen for 4-8 h. Excess HMDS was removed by distillation, and the residue was dried under a reduced pressure for 6 h. The resulting intermediate bis-silyl derivative (84) was dissolved in anhydrous MeCN (20 mL) and a solution of a 1,2,3,4,6-penta-*O*-acetyl-α-D-glycopyranose (0.01 mol, 3.91 g) in 20 mL of MeCN was added with stirring. The mixture was cooled to 5 °C during the subsequent addition of TMSOTf (2.17 ml, 0.015 mol). The stirring at room temperature was continued for 16-18h until the reaction was completed as observed by TLC analysis (1:1 chloroform; acetone). The mixture was diluted with CHCl₃ (150 mL), and the organic solution was washed

with a saturated NaHCO₃ solution (50 mL) and then H₂O (2x50 mL). The organic layer was dried (anhydrous Na₂SO₄). The solvent was removed under a reduced pressure and a crude product thus obtained was purified by column chromatography on a silica gel column using 5% MeOH in CHCl₃ as an eluent to give the pure product (83d) in a yield of 61% (Scheme 19)

1-(2'',3'',4'',6''-Tetra-O-acetyl-β-D-glucopyranosyl)-3-cyano-4,6-diphenyl-2-pyridinone (83a):

White crystals; yield 66% (method A); mp 193°C, from ethanol; R_f = 0.48 (6:4 hexane / ethylacetate), IR (KBr, cm⁻¹) 1600 (C-2), 1752 (acetyl carbonyl CO), 2220 (CN); [α]²⁵ = 25.4° (c = 4.92 mg/mL, chloroform); ¹H-NMR [CDCl₃, 200 MHz]: (δ, ppm) 1.91-2.07 (4s, 12H, 4CH₃CO), 4.03-4.25(m, 3H, H-5'', H-6''a,H-6''b), 5.22 (t, 1H, H-4''), 5.41-5.47 (m, 3H, H-2'',H-3''), 6.33 (d, 1H, H-1'', J = 7.8 Hz), 7.49-8.00 (m, 10H, aromatic); ¹³C-NMR [CDCl₃, 200 MHz]: (δ, ppm) 20.3-20.5 (4CH₃), 62.0 (C-6'), 68.3 (C-4'), 70.3 (C-2'), 72.6 (C-3'), 72.8(C-5'), 94.3 (C-1''), 94.3(C-5), 113.9 (C-3), 115.5 (CN), 127.2-136.8 (aromatic carbons), 157.3 (C-6), 157.8 (C-2), 162.3 (C-4), 168.9-170.6 (four acetoxy carbonyl carbon). Anal. Calcd for C₃₂H₃₀N₂O₁₀ (602.59): C, 63.78; H, 5.02; N, 4.65 %, found: C, 64.00; H, 5.14; N, 4.61 %.

1-(2'',3'',4'',6''-Tetra-O-acetyl-β-D-glucopyranosyl)-3-cyano-4-(o-tolyl)-6-phenyl-2-

pyridinone (83b): White crystals; yield 65%, (method A); mp 189-190°C, from ethanol; R_f = 0.381 (6:4 hexane / ethylacetate), IR (KBr, cm⁻¹) 1659 (C-2), 1765 (acetoxycarbonyl), 2352 (CN); [α]²⁵ = 26.1° (c = 3.84 mg/ml, chloroform); ¹H-NMR [CDCl₃, 200 MHz]: (δ, ppm) 1.93-2.08 (4s, 12H, 4CH₃), 2.28 (s, 3H, o-CH₃), 4.00 (m, 1H, H-5'), 4.25-4.27 (m, 2H, H-6''a, H-6''b), 5.23-5.47 (m, 3H, H-2'', H-3'', H-4''), 6.32-6.36 (d, 1H, H-1'', J = 7.8 Hz), 7.25-8.05 (m, 10H, aromatic); ¹³C-NMR [CDCl₃, 200 MHz]: (δ, ppm) 20.1 (ortho-CH₃), 20.8 (4 CH₃), 62.3 (C-6''), 68.6 (C-4''), 70.6 (C-2''), 72.9 (C-3''), 73.0 (C-5''), 94.7 (C-1''), 96.1 (C-5), 114.0 (C-3), 116.5 (CN), 126.4-136.9 (aromatic carbons), 157.8 (C-6), 158.5 (C-2), 162.0 (C-4), 170.9 (four

acetoxy carbonyl carbon); Anal. Calcd for $C_{33}H_{32}N_2O_{10}$ (616.61): C, 64.28; H, 5.23; N, 4.54 %, found: C, 64.50; H, 5.23; N, 4.70 %.

1-(2'',3'',4'',6''-Tetra-O-acetyl- β -D-glucopyranosyl)-3-cyano-4-(thiophen-2'-yl)-6-phenylpyridinone (83c): White crystals; yield 72%, (method A); mp 188-189°C, from ethanol, $R_f = 0.921$ (6:4 hexane / ethylacetate), IR (KBr, cm^{-1}) 1680 (CO), 1752 (acetoxy carbonyl), 2354 (CN); $[\alpha]^{25} = 7.1^\circ$ ($c = 4.28$ mg/ml, chloroform), 1H -NMR [$CDCl_3$, 200 MHz]: (δ , ppm) 1.92-2.07 (4s, 12H, 4CH₃), 4.06 (m, 1H, H-5''), 4.21-4.22 (m, 2H, H-6''a, H-6''b) 5.18-5.50 (m, 3H, H-2'', H-3'', H-4''), 6.29 (d, 1H, H-1'', $J = 9.0$ Hz), 7.20-7.56 (m, 5H, aromatic), 7.69 (s, 1H, H-5), 7.98-8.06 (m, 2H, thienyl H-2, 3); ^{13}C -NMR [$CDCl_3$, 200 MHz]: (δ , ppm) 20.6-20.7 (4CH₃), 62.0 (C-6''), 68.4 (C-5''), 70.3 (C-4''), 72.98 (C-3''), 73.0 (C-2''), 91.8 (C5), 94.4 (C-1''), 114.2 (C-3), 114.5 (CN), 127.3-137.2 (aromatic carbons), 148.6 (thienyl C-2), 158.0 (C-6), 162.9 (C-2), 168.9, 170.9, 170.4, and 170.6 (four acetoxy carbonyl carbon); Anal. Calcd for $C_{30}H_{28}N_2O_{10}S$ (608.62): C, 59.20; H, 4.64; N, 4.60; S, 5.27 %, found: C, 60.20; H, 4.70; N, 4.60; S, 5.20 %.

1-(2'',3'',4'',6''-Tetra-O-acetyl- β -D-glucopyranosyl)-3-cyano-4-(thiophen-2'-yl)-6-(4-chlorophenyl)-2-pyridinone (83d): White crystals; yield 48% (method A), 61% (method B); mp 155-156°C, from ethanol, $R_f = 0.625$ (6:4 hexane / ethylacetate), IR (KBr, cm^{-1}) 1641 (C-2), 1752 (acetoxy carbonyl), 2330 (CN); $[\alpha]^{25} = 17.9^\circ$ ($c = 9.2$ mg/ml, chloroform); 1H -NMR [$CDCl_3$, 200 MHz]: (δ , ppm) 1.93-2.07 (4s, 12H, 4CH₃), 4.00 (m, 1H, H-5''), 4.19-4.25 (m, 2H, H-6''a, H-6''b), 5.20-5.25 (m, 1H, H-4''), 5.39-5.45 (m, 2H, H-2'', H-3''), 6.25-6.30 (d, 1H, H-1'', $J = 8.2$ Hz), 7.19-7.22 (d, 2H, $J = 3.8$ Hz), 7.45-7.51 (m, 1H, thienyl H-5), 7.56-7.59 (d, 2H, CH, $J = 4.2$ Hz), 7.63 (s, 1H, H-5), 7.94-7.99 (m, 2H, thienyl H-2, H-3); ^{13}C -NMR [$CDCl_3$, 200 MHz]: (δ , ppm) 20.6-20.7 (4CH₃), 61.7 (C-6''), 67.1 (C-5''), 67.8 (C-4''), 70.9 (C-3''), 71.7

(C-2''), 95.0 (C-1''), 91.9 (C-5), 113.9 (C-3), 114.5 (CN), 128.5-137.2 (aromatic carbons), 148.7 (C-6), 156.7 (C-2), 163.1 (C-4), 168.9, 170.2, 170.3 and 170.4 (four acetoxy carbonyl carbon) Anal Calcd for C₃₀H₂₇ClN₂O₁₀S (643.06): C, 56.03; H, 4.23; N, 4.36; S, 4.99 %, found: C, 56.00; H, 4.20; N, 4.21; S, 4.99 %

1-(2'',3'',4'',6''-Tetra-O-acetyl-β-D-glucopyranosyl)-3-cyano-4-[2-(trifluoromethyl)-phenyl]-6-phenyl-2-pyridinone (83e): White crystals; yield 30% (method A); mp 167-168°C, from ethanol, R_f = 0.86 (6:4 hexane / ethylacetate), IR (KBr, cm⁻¹) 1660 (C-2), 1760 (acetoxy carbonyl), 2400 (CN); [α]²⁵ = 9.5° (c = 8.4 mg/mL, chloroform); ¹H-NMR [CDCl₃, 200 MHz]: (δ, ppm) 1.91, 2.05, 2.06, 2.08 (4s, 12H, 4CH₃), 4.05-4.11 (m, 1H, H-5''), 4.22-4.25 (m, 2H, H-6''a, H-6''b), 5.18-5.27 (m, 1H, H-4''), 5.42-5.47 (m, 2H, H-2'', H-3''), 6.33-6.37 (d, 1H, H-1'', J = 8 Hz), 7.26-8.01 (m, 9H, aromatic); ¹³C-NMR [CDCl₃, 200 MHz]: (δ, ppm) 20.5-20.6 (4s, 4CH₃), 62.0 (C-6''), 68.3 (C-5''), 70.3 (C-4''), 72.7 (C-3''), 94.2 (C-2''), 94.4 (C-1''), 113.6 (C-5), 115.3 (C-3), 116.5 (CN), 126.1 (CF₃), 127.3-139.3 (aromatic carbons), 162.3 (C-6), 155.7 (C-2), 158.4 (C-4), 168.9-170.6 (four acetoxy carbonyl carbon); Anal. Calcd for C₃₃H₂₉F₃N₂O₁₀ (670.59): C, 59.11; H, 4.36; N, 4.18 %, found: C, 59.8; H, 4.30; N, 4.12 %.

1-(2'',3'',4'',6''-Tetra-O-acetyl-β-D-galactopyranosyl)-3-cyano-4,6-diphenyl-2-pyridinone (87a): White crystals; yield 49%, mp 174-175°C, from ethanol, R_f = 0.391 (6:4 hexane / ethylacetate), IR (KBr, cm⁻¹) 1642 (C-2), 1748 (acetoxy carbonyl), 2225 (CN); [α]²⁵ = 21.8° (c = 3.2 mg/mL, chloroform); ¹H-NMR [CDCl₃, 200 MHz]: (δ, ppm) 1.88-2.22 (4s, 12H, 4CH₃), 4.17-4.28 (m, 3H, H-5'', H-6''a, H-6''b), 5.21-5.28 (m, 1H, H-4''), 5.51-5.74 (m, 2H, H-2'', H-3''), 6.27-6.31 (d, 1H, H-1'', J = 8 Hz), 7.50-7.70 (m, 8H, aromatic), 7.66 (s, 1H, H-5), 8.04-8.09 (m, 2H, aromatic); ¹³C-NMR [CDCl₃, 200 MHz]: (δ, ppm) 20.5, 20.6, 20.6 and 20.7 (4CH₃), 61.8 (C-6''), 67.2 (C-5''), 67.9 (C-3''), 70.9 (C-4''), 71.8 (C-2''), 94.0 (C-5),

94.9 (C-1''), 114.0 (C-3), 115.4 (CN), 127.3-136.8 (aromatic carbons), 157.2 (C-6), 157.8 (C-2), 162.4 (C-4), 168.9, 170.2, 170.3, and 170.4 (four acetoxy carbonyl carbon). Anal. Calcd for C₃₂H₃₀N₂O₁₀ (602.59): C, 63.78; H, 5.02; N, 4.65 %, found: C, 64.20; H, 5.20; N, 4.70 %

1-(2'',3'',4'',6''-Tetra-O-acetyl-β-D-galactopyranosyl)-3-cyano-4-(m-tolyl)-6-phenyl-2-

pyridinone (87b): White crystals; yield 74%, mp 196-197°C, from ethanol; R_f = 0.43

(6:4 hexane/ethylacetate), IR (KBr, cm⁻¹) 1652 (C-2), 1748 (acetoxy carbonyl), 2235 (CN); [α]²⁵ = 7.5° (c = 4.0 mg/ml, chloroform); ¹H-NMR [CDCl₃, 200 MHz]: (δ, ppm) 1.93-2.08 (4s, 12H, 4CH₃), 2.28 (s, 3H, *ortho*-CH₃), 4.17-4.28 (m, 3H, H-5'', H-6''a, H-6''b), 5.21-5.28 (m, 1H, H-4'', J = 3.4), 5.51-5.53 (d, 1H, H-3'', J = 3.8 Hz), 5.64-5.74 (dd, 1H, H-2'', J = 8.2 Hz), 6.27-6.31 (d, 1H, H-1'', J = 8.2 Hz), 7.26 (s, 1H, H-2'), 7.32-7.90 (m, 7H, aromatic), 8.07-8.09 (m, 2H, aromatic); ¹³C-NMR [CDCl₃, 200 MHz]: (δ, ppm) 20.5-20.7 (4CH₃), 21.4 (O-CH₃), 61.8 (C-6''), 67.2 (C-5''), 67.9 (C-3''), 70.9 (C-4''), 71.7 (C-2''), 94.0 (C-1''), 94.9 (C-5), 114.0 (C-3), 116.5 (CN), 125.2-138.8 (aromatic carbons), 157.8 (C-6), 158.5 (C-2), 162.0 (C-4), 170.9 (four acetoxy carbonyl carbon); Anal. Calcd for C₃₃H₃₂N₂O₁₀ (616.61): C, 64.28; H, 5.23; N, 4.54 %, found: C, 64.20; H, 5.14; N, 4.61 %

1-(2'',3'',4'',6''-Tetra-O-acetyl-β-D-galactopyranosyl)-3-cyano-4-(thiophen-2-yl)-6-phenyl-

pyridinone (87c): white crystals; yield 68%, mp 216-217°C, from ethanol; R_f = 0.33

(6:4 hexane/ethylacetate), IR (KBr, cm⁻¹) 1650 (C-2), 1753 (acetoxy carbonyl), 2241 (CN); [α]²⁵ = 8.8° (c = 4.0 mg/ml, chloroform); ¹H NMR [CDCl₃, 200 MHz]: (δ, ppm) 1.88, 2.03, 2.04 and 2.22 (4s, 12H, 4CH₃), 4.16-4.23 (m, 3H, H-5'', H-6''a, H-6''b), 5.19-5.26 (dd, 1H, H-4'', J = 3.6 Hz), 5.49-5.52 (d, 1H, H-3'', J = 3.6 Hz), 5.63-5.73 (dd, 1H, H-2'', J = 8.2 Hz), 6.24-6.28 (d, 1H, H-1'', J = 8.2 Hz), 7.51-7.56 (m, 3H, aromatic), 7.58-7.59 (m, 1H, thienyl H-4), 7.69 (s, 1H, H-5), 7.96-7.98 (m, 1H, thienyl H-3), 8.02-8.07 (m, 2H, aromatic); ¹³C-NMR

[CDCl₃, 200 MHz]: (δ, ppm) 20.5-20.7 (4CH₃), 61.8 (C-6''), 67.2 (C-5''), 67.8 (C-3''), 70.9 (C-4''), 71.7 (C-2''), 91.6 (C-1''), 94.9 (C5), 114.1 (C-3), 114.5 (CN), 127.2-137.2 (aromatic carbons), 148.5 (thienyl C-2), 157.9 (C-6), 162.9 (C-2), 168.9, 170.2, 170.3, and 170.4 (four acetoxy carbonyl carbon); Anal Calcd for C₃₀H₂₈N₂O₁₀S (608.62): C, 59.20; H, 4.64; N, 4.60; S, 5.27 %, found C, 60.6; H, 4.7; N, 4.6; S, 5.3 %

1-(2'',3'',4'',6''-Tetra-O-acetyl-β-D-galactopyranosyl)-3-cyano-4-(thiophen-2'-yl)-6-(p-chlorophenyl)-2-pyridinone (87d): white crystals; yield 48%, mp 155-156°C, from ethanol, R_f = 0.63 (6:4 hexane / ethylacetate), IR (KBr, cm⁻¹) 1590 (C-2), 1760 (acetoxy carbonyl), 2230 (CN); [α]²⁵ = 8.7° (c = 4.0 mg/ml, chloroform); ¹H NMR [CDCl₃, 200 MHz]: (δ, ppm) 1.92, 2.04, 2.06 and 2.23 (4s, 12H, 4CH₃), 4.17-4.26 (m, 3H, H-5'', H-6''a, H-6''b), 5.20-5.27 (dd, 1H, H-4'', J = 3.2 Hz), 5.51-5.52 (d, 1H, H-3'', J = 3.4 Hz), 5.64-5.73 (dd, 1H, H-2'', J = 8.2 Hz), 6.20-6.25 (d, 1H, H-1'', J = 8.2 Hz), 7.49-7.53 (m, 2H, aromatic), 7.56-7.61 (dd, 1H, J = 3.4 Hz, aromatic), 7.65 (s, 1H, H-5), 7.98-8.02 (m, 3H, aromatic); ¹³C-NMR [CDCl₃, 200 MHz]: (δ, ppm) 20.6-20.7 (4CH₃), 61.7 (C-6''), 67.1 (C-5''), 67.8 (C-3''), 70.9 (C-4''), 71.7 (C-2''), 91.9 (C-5), 95.0 (C-1''), 113.9 (C-3), 114.5 (CN), 128.5-137.1 (aromatic carbons), 156.7 (C-6), 163.1 (C-2), 168.9 (C-4), 170.4 (four acetoxy carbonyl carbon). Anal. Calcd for C₃₀H₂₇ClN₂O₁₀S (643.06): C, 56.03; H, 4.23; N, 4.36; S, 4.99 %; found: 56.10, H, 4.22; N, 4.35; S, 4.90 %.

1-(2'',3'',4'',6''-Tetra-O-acetyl-β-D-galactopyranosyl)-3-cyano-4-(p-trifluoromethyl-phenyl)-6-phenyl-2-pyridinone (87e): white crystals; yield 48%, mp 155-156°C, from ethanol; R_f = 0.63 (6:4 hexane / ethylacetate), IR (KBr, cm⁻¹) 1635 (C-2), 1743 (acetoxy carbonyl), 2353 (CN); [α]²⁵ = 14.4° (c = 8.0 mg/ml, chloroform); ¹H-NMR [CDCl₃, 200 MHz]: (δ, ppm) 2.20 (m, 12H, 4CH₃), 4.17-4.25 (m, 3H, H-5'', H-6''a, H-6''b), 5.26-5.27 (dd, 1H, H-3'', J = 3.4 Hz),

5.51-5.53 (d, 1H, H-4'', J = 2.6 Hz), 5.64-5.73 (dd, 1H, H-2'', J = 8.2 Hz), 6.27-6.31 (d, 1H, H-1'', J = 8.2 Hz), 7.52-7.55 (m, 3H, aromatic), 7.60 (s, 1H, H-5), 7.78-7.80 (m, 4H, aromatic), 8.04-8.08 (m, 2H, aromatic), ¹³C-NMR [CDCl₃, 200 MHz]: (δ, ppm) 20.5-20.7 (4CH₃), 61.8 (C-6''), 67.2 (C-5''), 67.8 (C-3''), 70.9 (C-4''), 71.8 (C-2''), 94.0 (C-1''), 95.0 (C-5), 115.0 (C-3), 115.2 (CN), 126.1 (CF₃), 127.3-136.5 (aromatic carbons), 155.6 (C-6), 158.4 (C-2), 162.0 (C-4), 168.9-170.4 (four acetoxy carbonyl); Anal. Calcd for C₃₃H₂₉F₃N₂O₁₀ (670.59): C, 59.11; H, 4.36; N, 4.18%, found: C, 60.1; H, 4.38; N, 4.12%.

2.3 General Procedure for Nucleoside Deacylation

2.3.1 Method A (Transesterification-Saponification Using Saturated Methanolic Ammonia)

Dry gaseous ammonia was passed through a solution of acetylated nucleoside (**83a-e**) (0.5 g) in dry methanol (10 mL) at 0°C for about 0.5 h. The reaction mixture was stirred at 0°C until complete as shown by TLC; the residue was purified by flash chromatography eluting with 2% EtOH in CH₂Cl₂ to give a white crystalline product (**85a-e**).

2.3.2 Method B (Transesterification-Saponification Using Triethylamine)

Acetylated nucleoside (**87a-e**) was dissolved in a mixture of (MeOH/H₂O/Et₃N) in ratio of (1:1:1) and the mixture was stirred over night at room temperature. The reaction mixture was monitored by TLC (2% methanol and 98% CH₂Cl₂) and stirring was continuous until the reaction completed. The solvent was removed under reduced pressure at room temperature and the residue was purified by column chromatography eluting with 2% EtOH in CH₂Cl₂ to give a white crystalline product of the deacetylated nucleosides (**88a-d**).

1-(β-D-glucopyranosyl)-3-cyano-4,6-diphenyl-2-pyridinone (85a): White crystals; yield 52% (method A); mp 182°C, from methanol; R_f = 0.35 (CH₂Cl₂), IR (KBr, cm⁻¹) 1590 (CO), 2230 (CN), 3430 sugar-OH; [α]²⁵ = 116.8° (c = 10.4 mg/ml, methanol); ¹H-NMR [DMSO-d₆, 200 MHz]: (δ, ppm) 3.26-3.67 (m, 6H, H-2'', H-3'', H-4'', H-5'', H-6''a, H-6''b), 4.57-5.43 (4 OH, exchangable with D₂O), 6.13-6.16 (d, 1H, H-1'', J = 7.4 Hz), 7.51-7.60 (m, 6H, aromatic), 7.73-7.76 (m, 2H, aromatic), 7.88 (s, 1H, H-5), 8.22-8.27 (m, 2H, aromatic); ¹³C-NMR [DMSO-d₆, 200 MHz]: (δ, ppm) 60.6 (C-6'), 69.7 (C-5'), 72.9 (C-4'), 77 (C-3'), 78.0 (C-2'), 96.6 (C-1''), 92.8 (C-5), 114.9 (C-3), 115.0 (CN), 127.6-136.5 (aromatic carbons), 156.8 (C-6), 157.4 (C-2), 162.9 (C-4). Anal. Calcd for C₂₄H₂₂N₂O₆ (434.44): C, 66.35; H, 5.10; N, 6.45, found: C, 65.99; H, 4.98; N, 6.41%.

1-(β-D-glucopyranosyl)-3-cyano-4-(m-tolyl)-6-phenyl-2-pyridinone (85b): White crystals; yield 63% (method A); mp 163°C, from methanol; $R_f = 0.51$ (CH_2Cl_2), IR (KBr, cm^{-1}) 1585 (CO), 2450 (CN), 3400 sugar-OH; $[\alpha]^{25} = 88^\circ$ ($c = 6.52$ mg/ml, methanol), $^1\text{H-NMR}$ [$\text{DMSO-}d_6$, 200 MHz] (δ , ppm) 2.52 (s, 3H, CH_3), 3.36-3.66 (m, 6H, H-2'' H-3'', H-4'', H-5'', H-6''a, H-6''b), 4.65-5.27 (4 OH, exchagable with D_2O), 6.12-6.15 (d, 1H, H-1'', $J = 7.8$ Hz), 7.39-7.57 (m, 7H, aromatic), 7.87 (s, 1H, H-5), 8.24-8.28 (m, 2H, aromatic); $^{13}\text{C-NMR}$ [$\text{DMSO-}d_6$, 200 MHz] (δ , ppm) 21.7 (s, CH_3), 61.0 (C-6''), 68.8 (C-5''), 70.6 (C-4''), 74.2 (C-3''), 77.1 (C-2''), 93.4 (C-1''), 97.8 (C-5), 115.4 (C-3), 115.7 (CN), 126.4-139.0 (aromatic carbons), 157.5 (C-6), 157.9 (C-2), 163.7 (C-4). Anal. Calcd for $\text{C}_{25}\text{H}_{24}\text{N}_2\text{O}_6$ (448.47): C, 66.95; H, 5.39; N, 6.25 %, found: C, 66.89; H, 5.37; N, 6.31 %.

1-(β-D-glucopyranosyl)-3-cyano-4-(thiophen-2-yl)-6-phenyl-2-pyridinone (85c): White crystals; yield 74% (method A); mp 219°C from methanol; $R_f = 0.34$ (CH_2Cl_2), IR (KBr, cm^{-1}) 1595 (CO), 2300 (CN), 3445 sugar-OH; $[\alpha]^{25} = 202^\circ$ ($c = 8.4$ mg/ml, methanol); $^1\text{H NMR}$ [$\text{DMSO-}d_6$, 200 MHz]: (δ , ppm) 3.25-3.68 (m, 6H, H-2'', H-3'', H-4'', H-5'', H-6''a, H-6''b), 4.59-5.45 (4 OH, exchagable with D_2O), 6.11-6.15 (d, 1H, H-1'', $J = 7.8$ Hz), 7.32-7.37 (dd, 1H, thienyl H-5, $J = 3.4$ Hz), 7.54-7.56 (m, 3H, aromatic), 7.97 (s, 1H, H-5), 7.98-7.99 (dd, 1H, thienyl H-3, $J = 1.2$ Hz), 8.03-8.06 (dd, 1H, thienyl H-2, $J = 1.2$ Hz), 8.22-8.27 (m, 2H, aromatic); $^{13}\text{C-NMR}$ [$\text{DMSO-}d_6$, 200 MHz]: (δ , ppm) 60.5 (C-6''), 69.6 (C-5''), 72.7 (C-4''), 76.9(C-3''), 78.0 (C-2''), 90.4 (C-3), 96.7(C-1''), 113.4 (C-5), 115.3 (CN), 127.6-136.5 (aromatic carbons), 148.3 (C-6), 157.4 (C-2), 163.5 (C-4). Anal. Calcd for $\text{C}_{22}\text{H}_{20}\text{N}_2\text{O}_6\text{S}$ (440.47): C, 59.99; H, 4.58; N, 6.36; S, 7.28 %, found: C, 60.10; H, 4.59; N, 6.20; S, 7.32 %.

1-(β-D-glucopyranosyl)-3-cyano-4-(thiophen-2-yl)-6-(4-chlorophenyl)-2-pyridinone (85d): White crystals; yield 60% (method A); mp 250°C, from methanol; $R_f = 0.38$ (CH_2Cl_2), IR

(KBr, cm^{-1}) 1645 (CO), 2240 (CN), 3440 sugar-OH; $[\alpha]^{25} = 331.2^\circ$ ($c = 8.8$ mg/ml, methanol); $^1\text{H-NMR}$ [DMSO- d_6 , 200 MHz]: (δ , ppm) 3.24-3.68 (m, 6H, H-2'' H-3'', H-4'', H-5'', H-6''a, H-6''b), 4.59-5.46 (4 OH, exchangable with D_2O), 6.08-6.12 (d, 1H, H-1'', $J = 7.4$ Hz), 7.32-7.37 (dd, 1H, thienyl H-5, $J = 3.6$ Hz), 7.59-7.63 (d, 2H, $J = 8.6$ Hz), 7.98-8.31 (m, 3H), 8.26-8.31 (d, 2H, $J = 8.6$ Hz); $^{13}\text{C-NMR}$ [DMSO- d_6 , 200 MHz]: (δ , ppm) 60.6 (C-6''), 69.6 (C-5''), 72.8 (C-4''), 76.9 (C-3''), 78.0 (C-2''), 90.7 (C-5), 96.8 (C-1''), 113.3 (C-3), 115.2 (CN), 128.6-136.4 (aromatic carbons), 148.5 (C-6), 156.1 (C-2), 163.5 (C-4). Anal. Calcd for $\text{C}_{22}\text{H}_{19}\text{ClN}_2\text{O}_6\text{S}$ (474.91): C, 55.64; H, 4.03; N, 5.90; S, 6.75 %, found: C, 55.59; H, 3.99; N, 6.01; S, 6.74 %.

1-(β -D-glucopyranosyl)-3-cyano-4-[2-(trifluoromethyl)phenyl]-6-phenyl-2-pyridinone (85e):

White crystals; yield 32% (method A); mp 168°C , from methanol; $R_f = 0.87$ (CH_2Cl_2), IR (KBr, cm^{-1}) 1650 (CO), 2220 (CN), 3445 sugar-OH; $[\alpha]^{25} = 100.6^\circ$ ($c = 8$ mg/ml, methanol); $^1\text{H-NMR}$ [DMSO- d_6 , 200 MHz]: (δ , ppm) 3.24-3.69 (m, 6H, H-2'' H-3'', H-4'', H-5'', H-6''a, H-6''b), 4.58-5.45 (4 OH, exchangable with D_2O), 6.15-6.18 (d, 1H, H-1'', $J = 7.4$ Hz), 7.54-7.57 (m, 3H, aromatic), 7.97-7.99 (m, 5H, aromatic), 8.28-8.29 (m, 2H, aromatic); $^{13}\text{C-NMR}$ [DMSO- d_6 , 200 MHz]: (δ , ppm) 60.5 (C-6''), 69.6 (C-5''), 72.7 (C-4''), 76.9 (C-3''), 78.0 (C-2''), 92.9 (C-3), 96.7 (C-1''), 114.7 (C-5), 115.0 (CN), 125.7-139.8 (aromatic carbons), 155.3 (C-6'), 157.7 (C-2), 162.8 (C-4). Anal. Calcd for $\text{C}_{25}\text{H}_{21}\text{F}_3\text{N}_2\text{O}_6$ (502.44): C, 59.76; H, 4.21; N, 5.58 %, found: C, 59.65; H, 4.30; N, 5.59 %

1-(β -D-galactopyranosyl)-3-cyano-4,6-diphenyl-2-pyridinone (88a): White crystals; yield

43% (method B); mp 219°C , from methanol; $R_f = 0.16$ (CH_2Cl_2), IR (KBr, cm^{-1}) 1652 (CO) 2241 (CN), 3430 sugar-OH; $[\alpha]^{25} = 61^\circ$ ($c = 7.36$ mg/ml, methanol); $^1\text{H-NMR}$ [DMSO- d_6 , 200 MHz]: (δ , ppm) 3.24-3.67 (m, 6H, H-2'' H-3'', H-4'', H-5'', H-6''a, H-6''b), 4.59-5.45 (4 OH, exchangable with D_2O), 6.13-6.17 (d, 1H, H-1'', $J = 8$ Hz), 7.51-7.59 (m, 6H, aromatic), 7.73-

7.77 (m, 2H, aromatic), 7.88 (s, 1H, H-5), 8.22-8.27 (m, 2H, aromatic); ^{13}C -NMR [DMSO- d_6 , 200 MHz]: (δ , ppm) 60.4 (C-6''), 68.2 (C-5''), 69.9 (C-3''), 73.5 (C-4''), 76.4 (C-2''), 90.5 (C-1''), 97.3 (C-5), 113.2 (C-3), 115.4 (CN), 127.6-136.5 (aromatic carbons), 148.3 (C-6), 157.5 (C-2), 163.7 (C-4). Anal. Calcd for $\text{C}_{24}\text{H}_{22}\text{N}_2\text{O}_6$ (434.44): C, 66.35; H, 5.10; N, 6.45 %, found: C, 66.29; H, 5.03; N, 6.47 %.

1-(β -D-galactopyranosyl)-3-cyano-4-(*m*-tolyl)-6-phenyl-2-pyridinone (88b): White crystals; yield 57% (method B); mp 192°C, from methanol; $R_f = 0.21$ (CH_2Cl_2), IR (KBr, cm^{-1}) 1640 (CO), 2354 (CN), 3439 sugar-OH; $[\alpha]^{25} = 223.8^\circ$ ($c = 8.4$ mg/ml, methanol); ^1H -NMR [DMSO- d_6 , 200 MHz]: (δ , ppm) 3.26-3.75 (m, 6H, H-2'' H-3'', H-4'', H-5'', H-6''a, H-6''b), 2.41 (s, 3H, CH_3), 4.65-5.28 (4 OH, exchangable with D_2O), 6.11-6.15 (d, 1H, H-1'', $J = 7.8$ Hz), 7.39-7.57 (m, 7H, aromatic), 7.86 (s, 1H, H-5), 8.26-8.28 (m, 2H, aromatic); ^{13}C -NMR [DMSO- d_6 , 200 MHz]: (δ , ppm) 61.0 (C-6''), 68.8 (C-5''), 70.6 (C-3''), 74.2 (C-4''), 77.1 (C-2''), 93.4 (C-1''), 97.8 (C-5), 115.4 (C-3), 115.7 (CN), 126.4-139.0 (aromatic carbons), 157.5 (C-6), 157.9 (C-2), 163.7 (C-4). Anal. Calcd for $\text{C}_{25}\text{H}_{24}\text{N}_2\text{O}_6$ (448.47): C, 66.95; H, 5.39; N, 6.25 %, found. C, 66.88; H, 5.41; N, 6.19 %.

1-(β -D-galactopyranosyl)-3-cyano-4-(thiophen-2-yl)-6-phenyl-2-pyridinone (88c): White crystals; yield 47% (method B); mp 195°C, from methanol; $R_f = 0.29$ (CH_2Cl_2), IR (KBr, cm^{-1}) 1680 (CO), 2234 (CN), 3438 sugar-OH; $[\alpha]^{25} = 104.4^\circ$ ($c = 8$ mg/ml, methanol); ^1H NMR [DMSO- d_6 , 200 MHz]: (δ , ppm) 3.25-3.68 (m, 6H, H-2'' H-3'', H-4'', H-5'', H-6''a, H-6''b), 4.59-5.45 (4 OH, exchangable with D_2O), 6.11-6.14 (d, 1H, H-1'', $J = 7.8$ Hz), 7.33-7.37 (m, 1H, thienyl-H3), 7.55-7.59 (m, 3H, aromatic), 7.97-8.01 (m, 3H, aromatic), 8.23-8.27 (m, 2H, aromatic); ^{13}C -NMR [DMSO- d_6 , 200 MHz]: (δ , ppm) 60.5 (C-6''), 69.6 (C-5''), 72.8 (C-3''), 76.9 (C-4''), 78.0 (C-2''), 96.8 (C-1''), 90.4 (C-5), 113.2 (C-3), 115.3 (CN), 127.6-

136.5(aromatic carbons), 148.3(C-6), 157.4 (C-2), 163.5 (C-4). Anal. Calcd for C₂₂H₂₀N₂O₆S: C, 59.99, H, 4.58, N, 6.36; S, 7.28 %; found: C, 60.01; H, 4.61; N, 6.29; S, 7.29 %.

1-(β-D-galactopyranosyl)-3-cyano-4-(thiophen-2-yl)-6-(4'-chlorophenyl)-2-pyridinone (88d):

White crystals, yield 77% (method B); mp 280°C, from methanol; R_f = 0.51(CH₂Cl₂), IR (KBr, cm⁻¹) 1645 (CO), 2230 (CN), 3443 sugar-OH; [α]²⁵ = 300° (c = 8.4 mg/ml, methanol); ¹H NMR [DMSO-*d*₆, 200 MHz]: (δ, ppm) 3.49-3.73 (m, 6H, H-2'', H-3'', H-4'', H-5'', H-6''a, H-6''b), 4.65-5.30 (4 OH, exchangable with D₂O), 6.02-9.06 (d, 1H, H-1'', J = 8.2 Hz), 7.29-7.34 (dd, 1H, J = 4.0 Hz), 7.54-7.59 (d, 2H, J = 8.6 Hz), 7.91-7.97 (m, 2H, thienyl H-2, 3), 7.99 (s, 1H, H-5), 8.21-8.25 (d, 2H, J = 8.8 Hz); ¹³C-NMR [DMSO-*d*₆, 200 MHz]: (δ, ppm) 60.4 (C-6''), 68.2 (C-5''), 69.9 (C-3''), 73.5(C-4''), 76.5 (C-2''), 90.7 (C-1''), 97.4 (C5), 113.3(C-3), 115.4 (CN), 128.7-136.4 (aromatic carbons), 148.5 (C-6), 156.1 (C-2), 163.6 (C-4). Anal. Calcd for C₂₂H₁₉ClN₂O₆S: C, 55.64; H, 4.03; N, 5.90; S, 6.75 %; found: C, 55.63; H, 3.98; N, 5.87; S, 6.72 %.

2.4 General Procedure for the Synthesis of 4,6-Diaryl-1-(*p*-Fluorobenzoyl)-3-Cyano-2-Pyridinone (89a-d)

To a solution of 3-Deazopyrimidine (5 mmol) in 50 ml acetonitrile and 2 ml of pyridine, a solution of 10 mmol of *p*-fluorobenzoyl chloride in acetonitrile was added gradually with stirring at room temperature until the reaction was completely judged by TLC (30 min.). The reaction mixture was evaporated under reduced pressure to yield a solid. The solid was washed with water (2×20ml), and crystallized in DMSO to give the desired compound (89a-d) (Scheme 23).

1-(p-Fluorobenzoyl)-4-(thiophen-2-yl)-6-(p-chlorophenyl)-3-cyano-2-pyridinones (89a):

White crystals; yield 62%; mp 180°C, from DMSO; $R_f = 0.85$ (6:4 Hexane:ethyl acetate), IR (KBr, cm^{-1}) 1580 (CO), 1770 (CO at pyridine N), 2230 (CN); $^1\text{H-NMR}$ [DMSO- d_6 , 200 MHz]: (δ , ppm) 7.36-7.38 (t, 1H), 7.46-7.62 (m, 5H), 8.12-8.13 (d, 1H, $J = 4.0$ Hz), 8.14-8.22 (d, 1H, $J = 3.8$ Hz), 8.24-8.33 (m, 5H); $^{13}\text{C-NMR}$ [DMSO- d_6 , 200 MHz]: (δ , ppm) 95.4 (C-1), 104.5 (C-5), 116.9 (C-3"), 117.4 (CN), 125.8 (C-2'), 126.7 (C-2, thienyl), 128.7 (C-3, thienyl), 128.9 (C-3'), 131.2 (C-2"), 131.4 (C-1"), 131.9 (C-4, thienyl), 132.2 (C-1'), 135.7 (C-1, thienyl), 136.3 (C-2), 148.5 (C-4), 157.9 (CO at pyridine N), 162.4 (C-4"), 168.9 (C-6); Anal Calcd for $\text{C}_{23}\text{H}_{13}\text{FN}_2\text{O}_2\text{S}$ (400.43): C, 68.99; H, 3.27; N, 7.00; S, 8.01 %, found: C, 68.90; H, 3.25; N, 6.99; S, 7.90 %.

1-(p-Fluorobenzoyl)-4-(thiophen-2-yl)-6-(p-chlorophenyl)-3-cyano-2-pyridinones (89b):

White crystals; yield 65%; mp 185°C, from DMSO; $R_f = 0.86$ (0.5 % CH_3OH in CH_2Cl_2), IR (KBr, cm^{-1}) 1592 (CO), 1754 (CO at pyridine N), 2240 (CN), $^1\text{H-NMR}$ [DMSO- d_6 , 200 MHz]: (δ , ppm) 7.33-7.37 (t, 1H), 7.46-7.59 (m, 4H), 8.012-8.04 (d, 1H, $J = 5$ Hz), 8.12-8.14 (d, 1H, $J = 3.8$ Hz), 8.21-8.33 (m, 5H); $^{13}\text{C-NMR}$ [DMSO- d_6 , 200 MHz]: (δ , ppm) 96.8

(C-1), 116.5 (C-3"), 117 (C-5), 117.4 (CN), 123.7(C-1"), 128.9 (C-2"), 129.1 (C-2'), 129.5 (C-3'), 131.5 (C-1, thienyl), 132.2 (C-1'), 133.3 (C-4'), 133.5 (C-2), 134.3 (C-4, thienyl), 135.7 (C-2, thienyl), 136.3 (C-3, thienyl), 124 (C-1'), 129 (C-2'), 132.2 (C-2"), 133.3 (C-4), 133.5 (C-1"), 150.2 (C-3""), 150.4 (C-1""), 154 (C-6), 158 (CO at pyridine N), 158.2 (C-3"), 161 (C-4'), 162 (C-4); Anal. Calcd for C₂₃H₁₂ClFN₂O₂S (434.87): C, 63.52; H, 2.78; N, 6.44; S, 7.37%, found: C, 63.02; H, 2.73; N, 6.45; S, 7.4 %.

1-(p-Fluorobenzoyl)-4-(4'-pyridyl)-6-(p-methoxyphenyl)-3-cyano-2-pyridinones (89c):

White crystals; yield 65%; mp 222°C, from DMSO; R_f = 0.63 (0.5 % CH₃OH in CH₂Cl₂), IR (KBr, cm⁻¹) 1590 (CO), 1750 (CO at pyridine N), 2233 (CN); ¹H-NMR [DMSO-*d*₆, 200 MHz]: (δ, ppm) 3.84 (s, 3H, OCH₃), 7.07-7.11 (d, 1H, J = 8.6 Hz), 7.47-7.57 (t, 2H), 7.81-7.84 (m, 4H), 8.22-8.32 (m, 4H), 8.83-8.86 (d, 2H, J = 5.8 Hz); ¹³C-NMR [DMSO-*d*₆, 200 MHz]: (δ, ppm) 55.5 (OCH₃), 114.5 (C-1), 114.6 (C-3'), 116.5 (C-3"), 117 (CN), 118 (C-3), 123.2 (C-2""), 124 (C-1'), 129 (C-2'), 132.2 (C-2"), 133.3 (C-4), 133.5 (C-1"), 150.2 (C-3""), 150.4 (C-1""), 154 (C-6), 158 (CO at pyridine N), 158.2 (C-3"), 161 (C-4'), 162 (C-4). Anal. Calcd for C₂₄H₁₃ClFN₃O₂ (429.83): C, 67.06; H, 3.05; N, 9.78 %, found: C, 67.02; H, 3.01, N, 9.76 %.

1-(p-Fluorobenzoyl)-4-(3,4-dimethoxyphenyl)-6-(p-methoxyphenyl)-3-cyano-2-

pyridinones (89d): White crystals; yield 72%; mp 197°C, from DMSO; R_f = 0.8 (6:4 hexane / ethyl acetate), IR (KBr, cm⁻¹) 1600 (CO), 1768 (CO at pyridine N), 2215 (CN), ¹H NMR [DMSO-*d*₆, 200 MHz]: (δ, ppm) 3.82-3.86 (3s, 9H, OCH₃), 7.04-7.09 (d, 1H, J = 9.00 Hz), 7.14-7.18 (d, 2H, J = 8.60 Hz), 7.42-7.54 (m, 4H), 8.16-8.32 (m, 5H); ¹³C-NMR [DMSO-*d*₆, 200 MHz]: (δ, ppm) 55.43-55.72 (OCH₃), 98.9 (C-5), 111.8 (C-1), 112.3 (C-2, *p*-3,4-dimethoxyphenyl), 114.4 (C-3'), 116.9 (C-5, *p*-3,4-dimethoxyphenyl), 117.9 (C-5'), 121.7

(CN), 123.9 (C-6, 3,4-dimethoxyphenyl), 127.2 (C-2'), 128.2 (C-1, 3,4-dimethoxyphenyl), 129.5 (C-6'), 133.2 (C-1"), 133.4 (C-2), 148.8 (C-4, 3,4-dimethoxyphenyl), 150.2 (C-3, 3,4-dimethoxyphenyl), 150.8 (C-1"), 156.0 (C-4'), 158.3 (C-4), 159.2 (CO at pyridine N), 161.8 (C-4"), 162.7 (C-6). Anal. Calcd for $C_{28}H_{21}FN_2O_5$ (484.48): C, 69.42; H, 4.37; N, 5.78 %, found: C, 69.20; H, 4.36; N, 5.80 %.

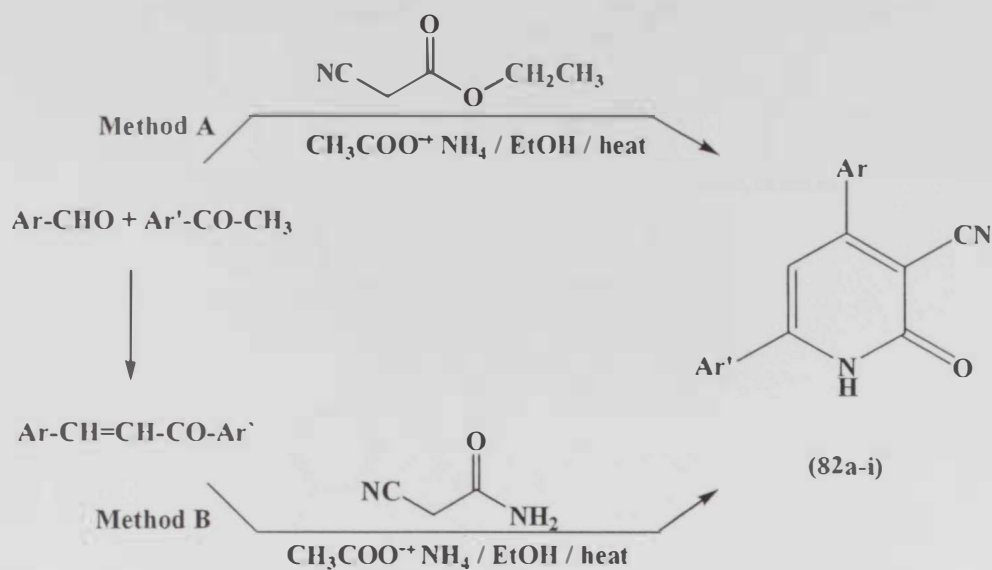
RESULTS AND DISCUSSION

3 Results and Discussion

3.1 Synthesis of 3-Deazapyrimidine Derivatives:

α,β -Unsaturated ketones are versatile reagents that have been extensively utilized in heterocyclic synthesis. Several new synthetic methods of 3-deazapyrimidine derivatives have been reported using α,β -unsaturated ketones as starting materials.^(37,38) It is of interest to study these reactions and to report the results of our investigations into the potential use readily obtained 3-deazapyrimidines in the field of nucleoside synthesis and their respective biological applications. The investigations have resulted in the development of a new modified synthetic method of medically important nucleoside derivatives (For more details see 4.3.1).

As an initial target for the assembly of new nucleosides, 3-deazapyrimidine derivatives (**82a-i**) are prepared⁽³⁸⁾ as outlined in scheme 17. The synthesized 3-deazapyrimidinones were allowed to react with various activated sugar moieties to produce the targeted products (**83-88**). The incorporation of any new group will result in change of size and shape of the products. In addition, it may introduce a chiral center, which will result in the formation of stereoisomers which may have different pharmacological activities. As a result, the introduction of a new group may increase the biological activity. The synthesized analogues may have different activities with respect to changing the size and the shape. Changing the number of substituents or the degree of unsaturation may result in new properties. These types of structural change result in analogues that exhibit either different potency or different types of activity.



Compound No.	Ar	Ar'
82a	phenyl	phenyl
b	2-tolyl	phenyl
c	3-tolyl	phenyl
d	2-thienyl	phenyl
e	2-thienyl	4-chlorophenyl
f	2-trifluoromethyl phenyl	phenyl
g	4-pyridyl	4-methoxyphenyl
h	4-tolyl	4-chlorophenyl
i	phenyl	4-chlorophenyl

Scheme 17: Synthesis of 3-cyano-4,6-disubstituted pyridine-2(1H)-ones (82a-i)

The corresponding nucleoside analogous (83-88) and *N*-(*p*-fluorobenzoyl) derivatives (89a-d) were synthesized and their structures are shown in figure 5. Compounds (82a-i) contain two nucleophilic centers, the oxygen at C-2 and the *N*-pyridine. The quantum mechanics calculations show that the nucleophilicity of the nitrogen atom in the pyridine ring system is higher than the exocyclic oxygen at C-2.

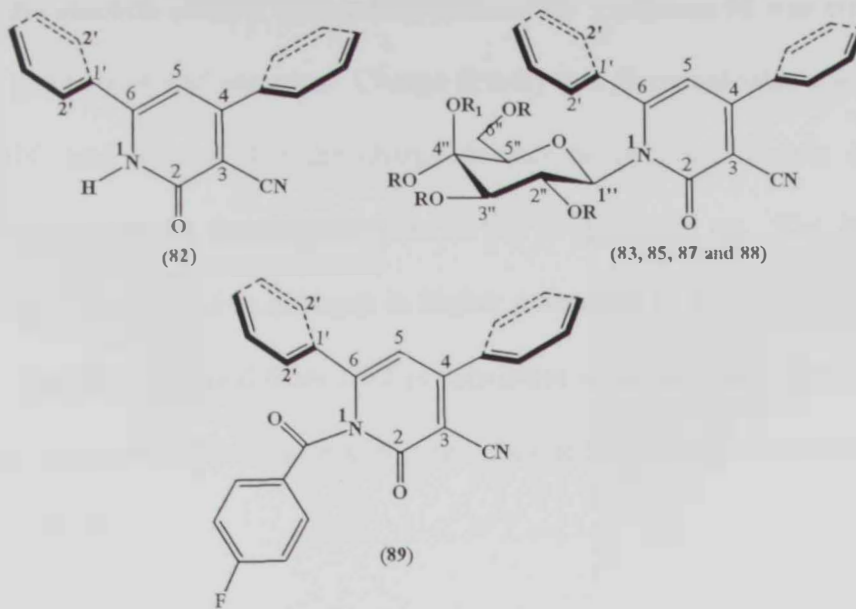


Figure 5: General structures of 3-deazapyrimidinone (82), related nucleosides (83, 85, 87, and 88) and non-nucleoside (89)

Quantum Mechanics (QM) calculations using density functional theory (DFT) were used to study the electron affinity of 3-deazapyrimidines. Gaussian 98 was employed for the calculation of geometries and energies. Charge density gas phase calculations were performed at B3LYP/6-31G and showed that the charge density on pyridine *N*-atom is 0.549066 au while the charge density on the oxygen atom at C-2 is 0.408723 au. The *HOMO* electron density topology on the pyridine nitrogen is higher compared to the *HOMO* of the carbonyl oxygen atom. The data obtained from DFT is consistent with the data obtained from spectral analyses. The results show that the nucleosides obtained are the *N*- nucleosides not the *O*- nucleosides (Figure 6).

HOMO Electron Density

LUMO Electron Density

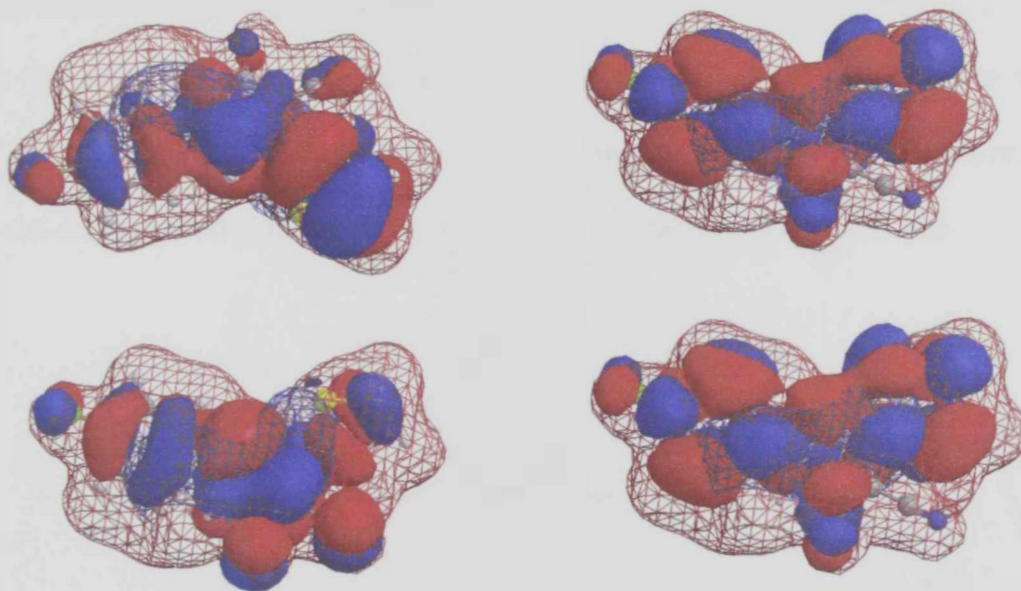
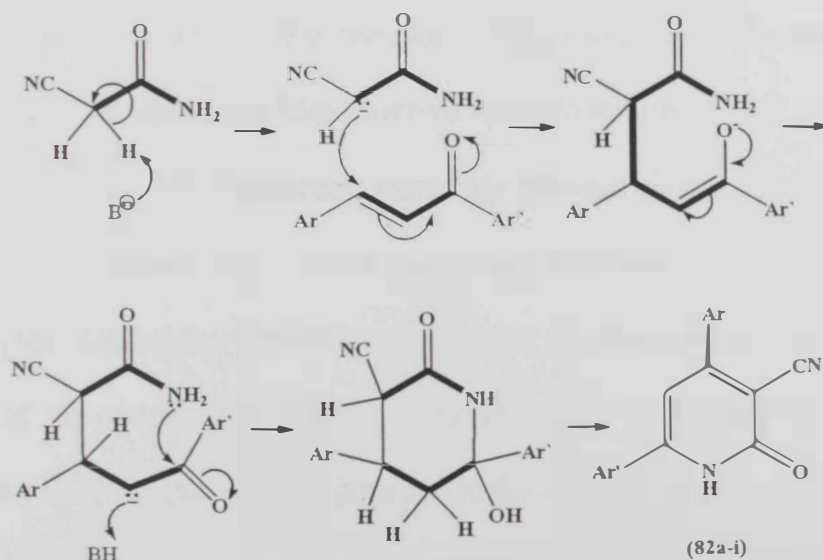


Figure 6: Molecular Orbital Calculations for compound 82e: Wire structures show that the total charge density while, solid colors (red and blue) show *HOMO* and *LUMO* electron density

The present part deals with the synthesis of some novel 3-cyano-4,6-disubstituted pyridine-2(1*H*)-ones (**82a-i**) by the reaction of α,β -unsaturated ketones with ethylcyanoacetate in the presence of ammonium acetate. 3-cyano-4,6-disubstituted pyridine-2(1*H*)-ones (**82a-i**) are synthesized in a one-pot reaction using substituted acetophenones, aldehydes and ethyl cyanoacetate in a catalytic amount of ammonium acetate (Method A). While in Method B, cyanoacetamide is used to synthesize the same products. To examine the two methods, A and B, two parallel experiments have been conducted under the same conditions to synthesize compound (**82a**). It was found that in Method A, the yield was higher than in Method B. Method A was selected to synthesize all compounds (**82a-i**) not only because of the higher yield but also to avoid the handling of the lachrymator chalcones and to save time since no prior condensation reaction was needed (Scheme 17).

It has been found that α,β -unsaturated ketones react with cyanoacetamide through conjugate-addition followed by cyclization in refluxing ethanol to give the corresponding 3-cyano-4,6-disubstituted pyridine-2(1*H*)-ones (**82a-i**) in good yield (Scheme 18).



Scheme 18: Suggested mechanism of 3-cyano-4,6-disubstituted pyridine-2(1*H*)-ones (**82a-i**)

Compounds (**82a-i**) were obtained and their structures were confirmed on the basis of their elemental analysis and spectral data (IR, $^1\text{H-NMR}$, $^{13}\text{C-NMR}$) as well as data obtained from modeling calculations. The analytical data for (**82e**) show that the molecular formula is $\text{C}_{16}\text{H}_9\text{N}_2\text{OSCl}$. IR, $^1\text{H-NMR}$ and $^{13}\text{C-NMR}$ were used to confirm the structure. The IR spectrum of (**82e**) showed the most significant absorption band for the presence of the carbonyl group at 1600 cm^{-1} . A strong band at 2220 cm^{-1} corresponding to the CN group at C-3 and a NH signal appeared at 3430 cm^{-1} .

The structure of compound (**82e**) was confirmed using $^1\text{H-NMR}$ and $^{13}\text{C-NMR}$ as follows: $^1\text{H-NMR}$ spectrum (δ , ppm) [DMSO-*d*₆, 200 MHz] of compound (**82e**) showed a strong singlet at $\delta = 6.98$ corresponding to the pyridine H-5. Protons at the 3', 4', and 5'-positions of 2-thiophene showed a sharp splitting pattern. This is true for the protons at the 3' and 5'-positions which appear as a pattern of doublet-doublet peaks. The thiophen H-3' appears as a doublet at $\delta = 8.06$ ppm with a coupling constant $J_{\text{H}3'-\text{H}4'} = 3.8$ Hz. H-5' appears as another doublet at a higher field at $\delta = 7.99$ ppm with $J_{\text{H}5'-\text{H}4'} = 5.0$ Hz. The higher the coupling constant may be attributed to the close contact with more electronegative sulfur atom. Thus, no cross coupling has been observed between thiophene H-3' and pyridine H-5 using NMR techniques. The interaction exist only between protons at the 3', 4' and 5'-positions of the thiophene ring. These results are supported by Quantum Mechanics calculations (QM). Optimizing the energy showed that the thiophene H-3' is present on the opposite side of the pyridine H-5 with a dihedral angle = -146.9° (Figure 7). The pyridine H-5 appears as a sharp singlet at $\delta 6.98$ ppm due to the distance between H-5 and thiophene H-3' which is 4.595 \AA . Aromatic protons at 6-position appear as two doublets at $\delta 7.58$ and 7.89 ppm respectively with equivalent coupling constants ($J = 8.6$ Hz). A broad band appears

at 12.74 ppm exchangeable with D₂O due to the presence of NH (Figure 7). ¹³C-NMR [DMSO-*d*₆, 200 MHz], gives the correct and the exact number of carbons with the correct chemical shifts for each carbon.

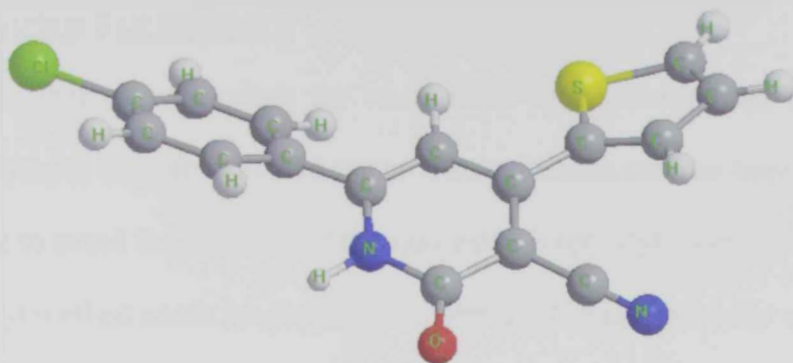


Figure 7: Optimizing structure for compound (82e) using DFT at B3YLP level using the 6-31G basis set

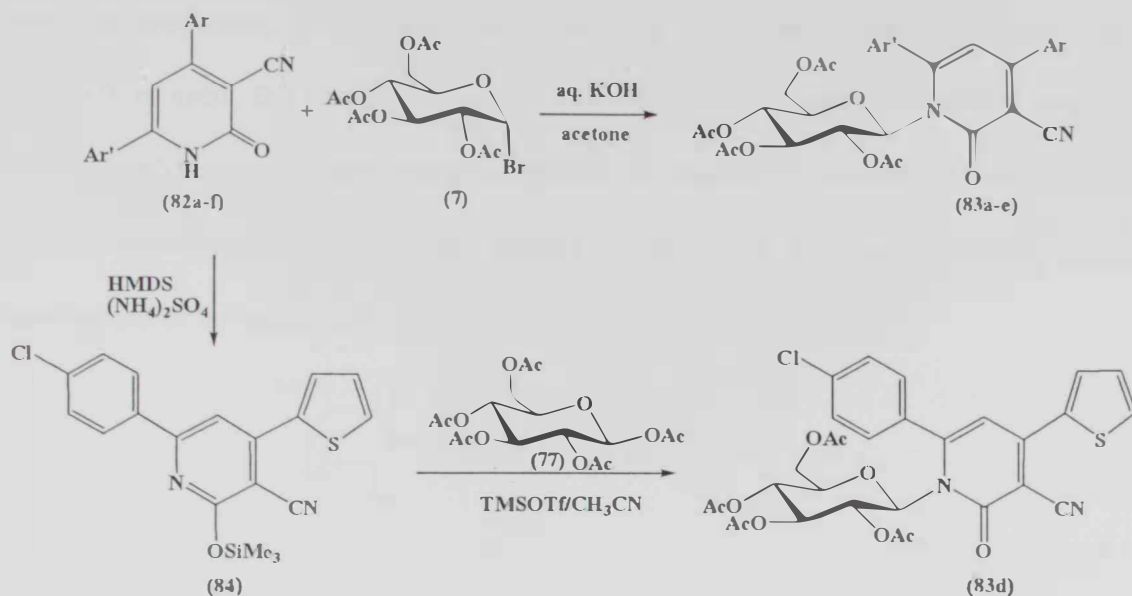
3.2 Nucleosides Derived from 3-Deazapyrimidines

3.2.1 Pyridinone Glucosides (83a-e)

3.2.1.1 Potassium Salt Method

This subsection describes the reaction of the potassium salt of deazapyrimidine derivatives (82a-f) with an activated sugar. The potassium salt has been chosen as reactive intermediate to avoid the handling of the easily hydrolyzed silyl compounds and to save time since the silyl method needs longer to be completed. The use of a polar solvent such as H₂O accelerates the reaction rate and saves time. In the 3-deazapyrimidine potassium salt, there are two reactive centers, the pyridine ring nitrogen and the carbonyl oxygen at C-2. A sole *N*-nucleoside product has been isolated in high yield without any contamination of the *O*-nucleoside. An additional approach in trying to understand the reactivity difference between *N* and *O* is by using the DFT method implemented into the Gaussian program at the BL3YP level with the 6-31G* basis set. It is clear that the experimental results are fully consistent with data obtained from the higher level of theory as the BL3YP level with the 6-31G* basis set. These results showed higher electron density on the pyridine ring nitrogen over exocyclic oxygen atom at C-2. The NMR data for *H-1''* appear at the higher field corresponding to the *N*-nucleosides and not the *O*-nucleosides. For the sake of simplicity of presentation, the synthesis and the structure determination of the nucleosides (83a-e) will be discussed in detail. α -acetobromoglucose (7) is reacted with the appropriate 3-deazapyrimidine derivatives (82a-f) in the presence of aqueous potassium hydroxide presumably through a Walden inversion, to yield the corresponding glucosides (83a-e) (Scheme 19). Since Walden inversion occurs in the halogen replacement reaction, the halide

with the α -configuration yields the β -isomer. The remaining 3-deazapyrimidine galactosides (87a-e) are synthesized and analyzed in a similar way.



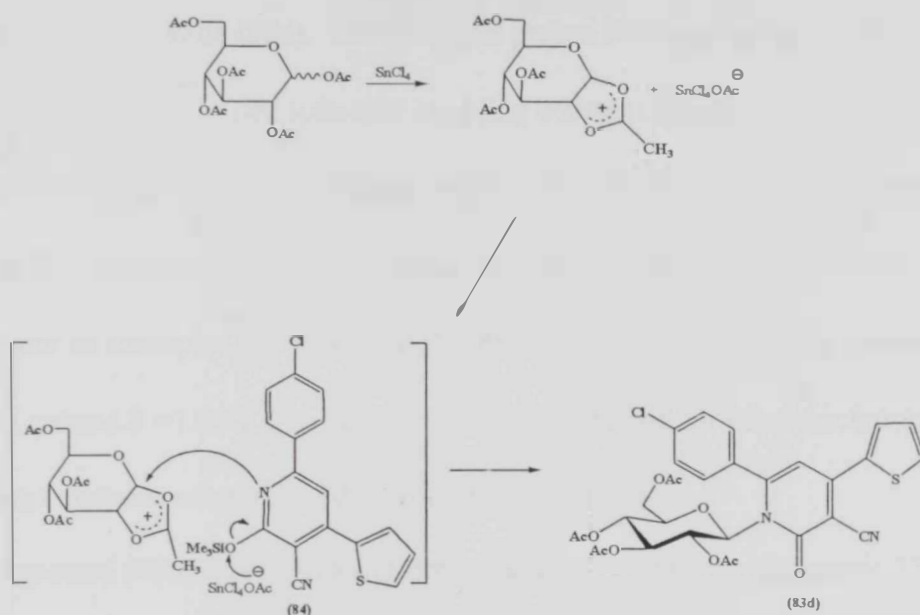
Compound No.	Ar	Ar'
83a	phenyl	phenyl
b	2-tolyl	phenyl
c	2-thienyl	phenyl
d	2-thienyl	4-chlorophenyl
e	2-trifluoromethyl phenyl	phenyl

Scheme 19: Two ways synthesis of the pyridinone glucosides (83a-e)

3.2.1.2 The Silyl Method

This subsection describes the reaction of the silyl derivative (84) with an activated sugar to give the corresponding *N*-nucleosides (83d). A likely mechanism for the formation of the nucleoside (83d) involves an intermediate cyclic carbonium ion, as shown in Scheme 20. The reaction of a nucleophilic base should take place from the less sterically hindered β -

face of the cation to give the β -nucleoside, as observed. The reaction is carried out under dry nitrogen and without isolation of the silyl intermediate. The use of polar solvents such as acetonitrile accelerates the reaction rate. When a stoichiometric amount of the catalyst (TMSOTf) is used, the reaction proceeds smoothly to give typical $^1\text{H-NMR}$ spectra of compound (83d) with the same chemical shift of the anomeric proton $H-1''$ that is obtained by K-salt procedure and the same melting point. The synthesis and the structure determination of the nucleoside (83d) are discussed in detail here in.



Scheme 20: Schematic Mechanism of the Silyl Method

The structure of the obtained nucleoside is determined as follows: First, compound (83d) is optically active and is characterized by a specific rotation $[\alpha]^{25} = 17.9^\circ$ ($c = 9.2$ mg/ml, chloroform). The IR spectrum of (83d) showed the presence of acetoxy carbonyl groups at 1752 cm^{-1} . A strong band appeared at 1641 cm^{-1} corresponding to the pyridine carbonyl at C-2. The structure of the compound (83d) was further confirmed by $^1\text{H-NMR}$ and COSY. The COSY spectrum was used to assign intra-proton interactions (Figures 8-10).

Clear interaction between H-5 of the pyridine ring and *ortho*-protons at 6-position is shown. A cross peak interaction of aromatic region is observed. In addition, the cross-peak interaction between anomeric proton H-1'' and H-2'' is also observed. No cross-peak interaction between thiophene H-3' and pyridine H-5 was obtained which is consistent with data obtained from quantum mechanics calculation.

Since ¹H-NMR spectroscopy is powerful tool, it was used routinely for the determination of the relative configurations (α , β). The ¹H-NMR (CDCl₃) showed the β -configuration of nucleoside (83d). The anomeric proton H-1'' appears as doublet at relatively low field ($\delta = 6.25$ - 6.30). The spin-spin coupling constant $J_{H1''-H2''} = 8.20$ Hz indicates that the protons H-1'' and H-2'' are in diaxial orientation. The H-2'' and H-3'' signal appear as multiplet at $\delta = 5.39$ - 5.45 . The H-5'' signal appears as multiplet at $\delta = 4.00$. The H₂-6'' signal appears as multiplet at $\delta = 4.19$ - 4.25 . Protons of the four acetoxy groups appear as four singlet around $\delta = 1.93$ - 2.07 . Similar results are obtained for other nucleosides (83a-e). All coupling constants are given in the experimental section.

Compound (83d) was further confirmed using ¹³C-NMR spectroscopy. These results are in agreement with the assigned structure. The ¹³C-NMR (CDCl₃) spectrum of (83d) was characterized by a signal at $\delta = 95.0$ ppm corresponding to the C-1'' atom of the β -configuration. The signals appear at $\delta = 148.7$, 163.1 ppm assigned for C-6 and C-4, respectively. Signals at $\delta = 168.9$, 170.2 , 170.3 and 170.4 ppm assign for the acetoxy carbonyl carbon. Signals corresponding to pyridine C-5 and C-3 resonate at $\delta = 91.9$ and 113.9 ppm, respectively. Another five signals at $\delta = 71.7$, 70.9 , 67.8 , 67.1 and 61.7 ppm assign for the sugar carbons as C-2'', C-3'', C-4'', C-5'' and C-6'' respectively. On the other

hand, the carbonyl carbon of pyridine appears at $\delta = 163.1$ ppm and the nitrile carbon appears at $\delta = 114.5$ ppm.

STANDARD 1H OBSERVE

expt COSY

SAMPLE		SPECIAL	
date	Sep 20 2004	temp	not used
solvent	CDCl3	gain	30
sample		spin	0
ACQUISITION		GRADIENTS	
sw	3201.0	PRGf1g	n
dt	0.160	hsglvt	2000
np	1024	hsgt	0.005000
fb	1800	F2 PROCESSING	
cs	32	sb	-0.080
hl	1.000	sbs	not used
nl	4	fn	1024
2D ACQUISITION		F1 PROCESSING	
sw1	3201.0	sb1	-0.040
nl	128	sbs1	not used
TRANSMITTER		PROC1	
tl	HI	fn1	1024
strq	200.057	DISPLAY	
lor	255.9	sp	633.7
tpwr	55	wp	1127.0
pw	13.300	ep1	608.4
PRESATURATION		wp1	1096.2
setmode	n	rf1	400.2
satpwr	0	rfp	6
satdly	0	rf11	400.2
satfrq	0	rfp1	0
DECOUPLER		PLOT	
dn	C13	wc	124.0
da	FLAS	ncn	6.2
hs		wc2	124.0
sspul		nc2	0
		***	332
			7

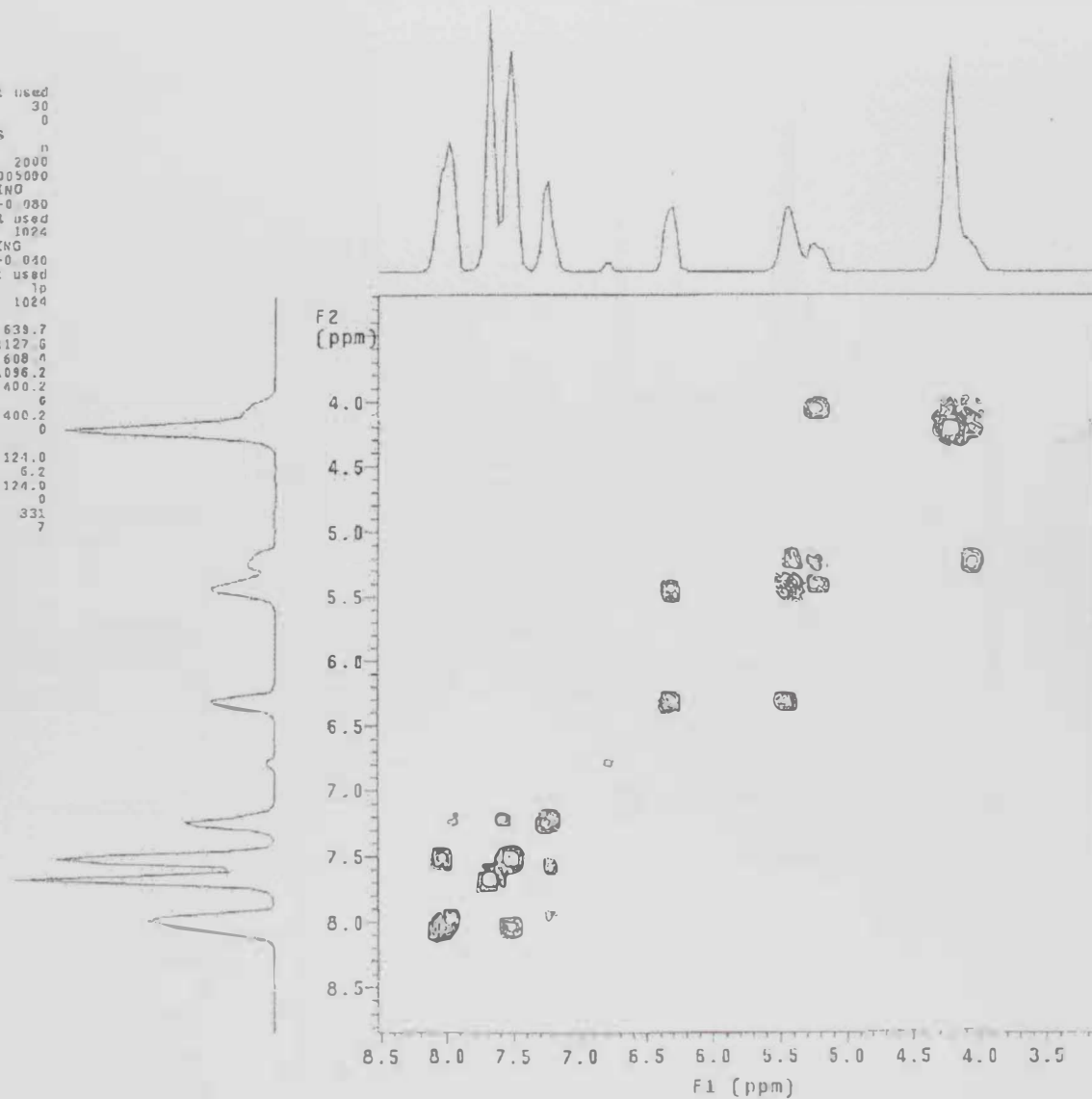
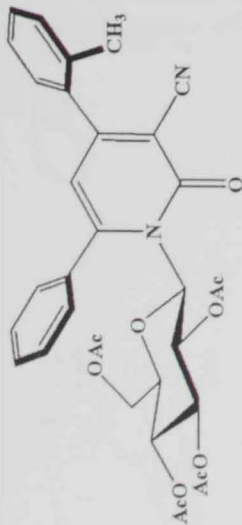


Figure 8: COSY spectrum of compound (83b)


```

STANDARD 1H OBSERVE
exp1 COSY

SAMPLE SPECIAL
date Sep 20 2004 temp not used
solvent CDCl3 gain 30
sample spin 0

ACQUISITION GRADIENTS
sw 3201.0 PRG14 n
at 0.180 hsglv1 2000
np 1024 hegt 0.005000
fb 1800 F2 PROCESSING
ss 32 sb -0.080
dl 1.000 ebs not used
nt 4 fn 1024

2D ACQUISITION F1 PROCESSING
sw1 3201.0 su1 -0.040
nl 128 cu1 not used

TRANSMITTER lp
in H1 fn1 1024
sfrq 200.057 DISPLAY -224.8
tof 255.0 ep -1992.0
tpr 55 wn -155.3
pw 13.300 sp1 1866.7
PRESATURATION wp1 400.2
xatmode n rf1 0
satp-r 0 rfp 0
satdly 0 rf11 400.2
satfrq 0 rfp1 0

DECOUPLER PLOT
dn C13 wc 124.0
dm nnn sc 6.2
FLAGS wc2 124.0
hs nn sc2 c
sepu n vs 331

```

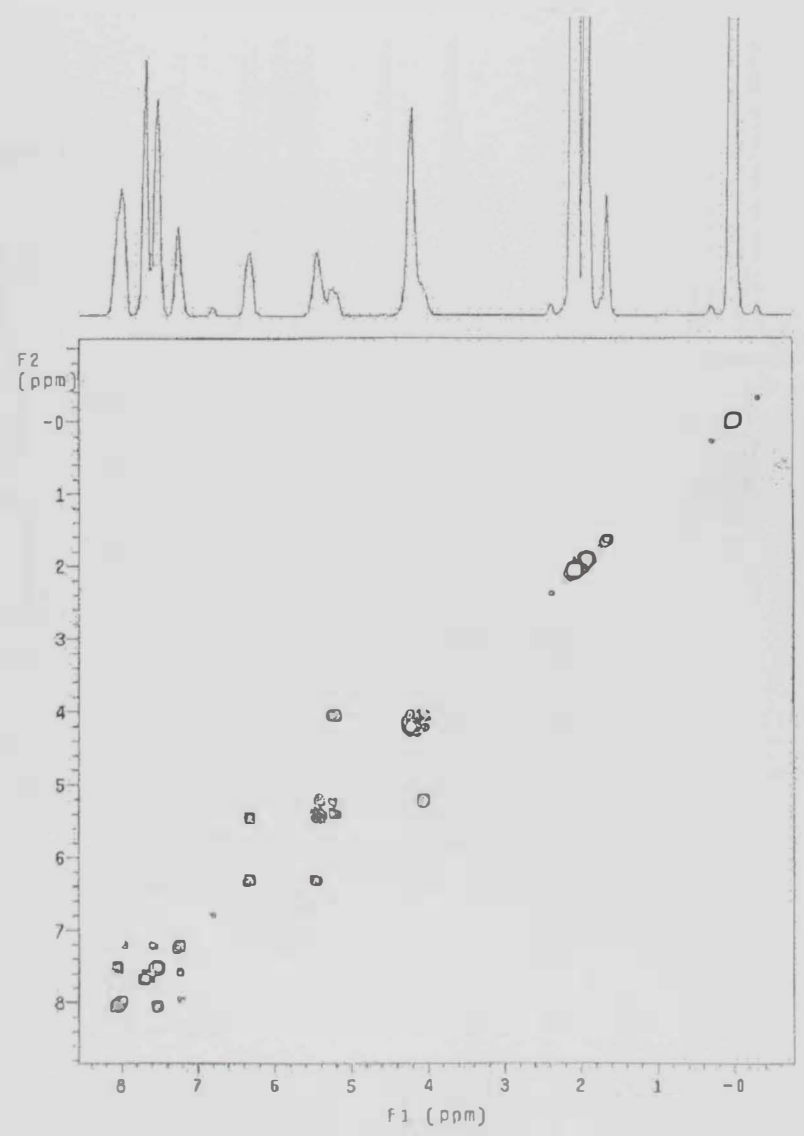
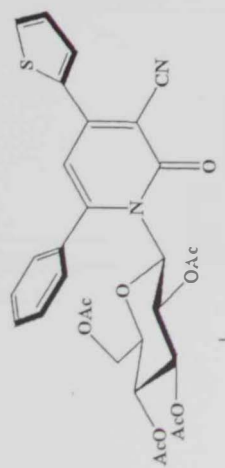


Figure 9: COSY spectrum of compound (83c)

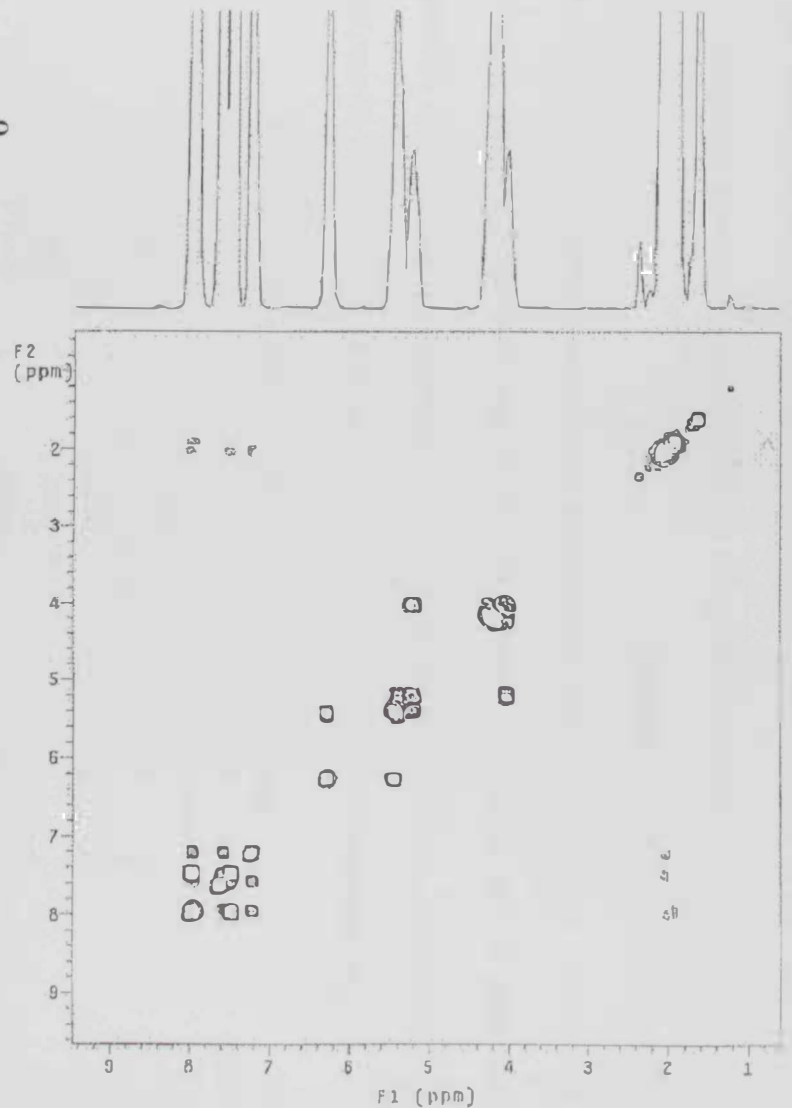
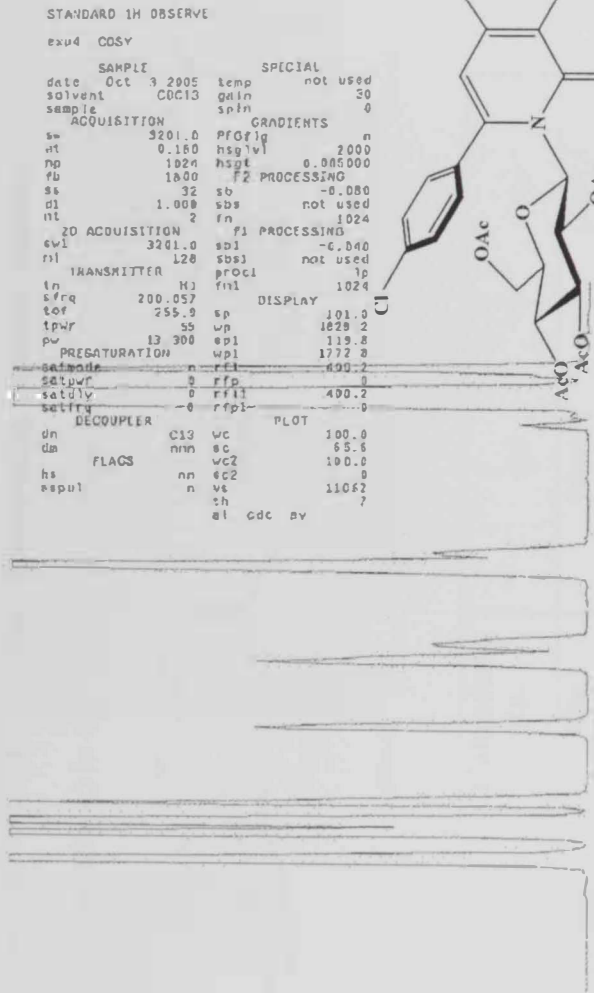
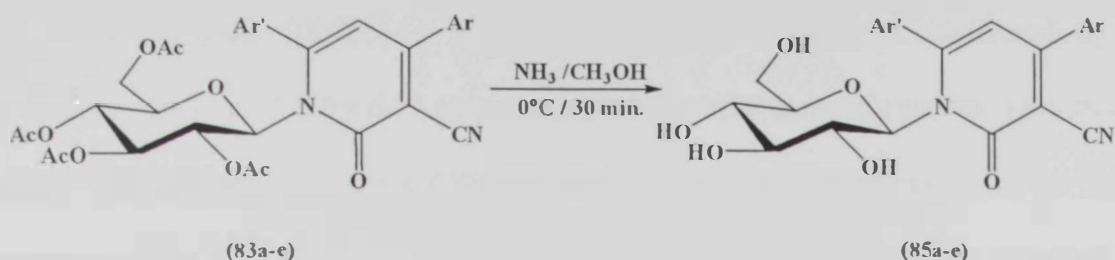


Figure 10: COSY spectrum of compound (83d)

3.2.2 Ammonolysis of Nucleosides (83a-e)

Ammonolysis of the nucleosides (83a-e) using saturated ammonia in methanol gives free nucleosides (85 a-e) in 42-75% yield (Scheme 21).



Compound No.	Ar	Ar'
85a	phenyl	phenyl
b	2-tolyl	phenyl
c	2-thienyl	phenyl
d	2-thienyl	4-chlorophenyl
e	2-trifluoromethyl phenyl	phenyl

Scheme 21: Ammonolysis step of the Prydinone glucosides

The structures of the obtained nucleosides (85 a-e) are elucidated by studying their IR, ^1H NMR and ^{13}C NMR spectra which are in accordance with the structures proposed from the result of the elemental analysis as well as the data obtained from the modeling calculation. The NOESY (two dimensional nuclear overhauser spectroscopy) is used to assign the inter-protons interaction.

The IR (KBr) absorption spectra of compounds (85a-e) showed a characteristic band at 3441 cm^{-1} due to the sugar hydroxy groups. Another band at 2924 cm^{-1} can be assigned to the nitrile group. A strong absorption band at 1637 cm^{-1} is attributed to the stretching vibration of the carbonyl group at C-2. In addition to these bands, the ether linkage of the

glucopyranoside ring system shows a broad band at 1050 cm^{-1} . It is clear that, the stretching vibration band of the four acetoxy carbonyl groups within the $1700\text{-}1750\text{ cm}^{-1}$ range have disappeared.

The $^1\text{H-NMR}$ ($\text{DMSO-}d_6$) spectrum of compound (85e) is confirmed by the appearance of a doublet at $\delta = 6.17\text{ ppm}$ corresponding to the anomeric proton of the glucose moiety with a spin-spin coupling constant equal to 7.40 Hz corresponding to the diaxial orientation of the H-1'' and H-2'' protons indicating the formation of only one β -isomer. The $^{13}\text{C-NMR}$ ($\text{DMSO-}d_6$) spectrum of (85e) is characterized by a signal at $\delta = 96.7\text{ ppm}$ corresponding to the C-1'' atom of glucose residue. No more signals appear in the region $\delta = 1.9\text{-}2.0\text{ ppm}$ corresponding to the methyl of acetoxy groups. See experimental part for more details.

The phase sensitive NOESY spectrum of (85a) was collected at 25°C in CDCl_3 (Figure 12). All inter ring NOESY cross peak between the anomeric proton at C-1'' and the *ortho*-phenyl protons at C-6 are also seen. This conclusion obtained from the NOESY study was fully supported by quantum mechanics calculations using the Gaussian 98 program. The conformation analysis gave the most stable conformer, whereby the plane of the pyridine ring bisects the sugar moiety while the aromatic substituent at position-6 appears twisted relative to the pyridine plane (Figure 11). The calculated average distance between H-1' and the *ortho*-aromatic protons is 2.71 and 3.71 \AA respectively. These calculated distances between H-1 and the *ortho*-aromatic protons are fully consistent with the observed NOESY results.

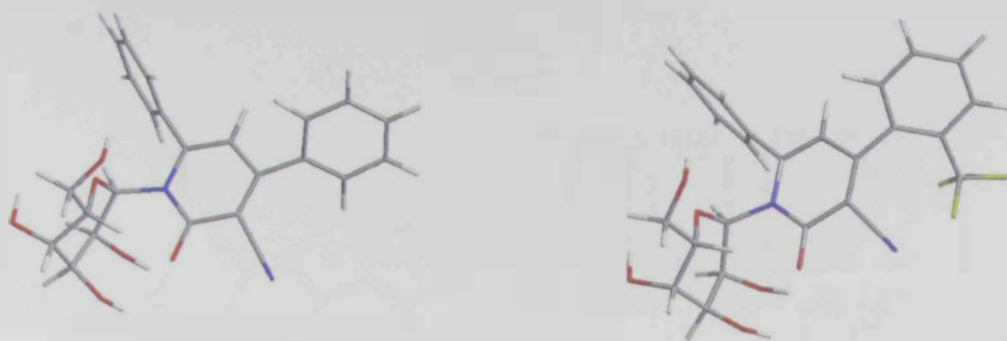


Figure 11: Optimizing structure for compounds (85a,e) using DFT at B3YLP level using the 6-31G basis set

STANDARD III OBSERVE

exp4 NOESY

SAMPLE		FLAGS	
date	Sep 9 2005	hs	n
solvent	ONSO	sapul	n
sample		PROflg	n
ACQUISITION		hsq1v1	2000
sw	3201.0	SPECIAL	
at	0.160	temp	not used
rp	1024	gain	30
fb	1800	spin	0
ss	32	F2 PROCESSING	
d1	1.000	gf	0.074
nt	128	gfs	not used
2D ACQUISITION		fn	2048
sw1	3201.0	f1	PROCESSING
ni	200	gf1	0.058
TRANSMITTER		gfs1	not used
tn	H1	procl	lp
sfrq	200.058	fn1	2048
tof	255.3	DISPLAY	
tpwr	55	sp	22.3
pw	13.300	wp	1855.5
	NOESY	sp1	56.7
mix	0.200	wpl	1786.7
PRESATURATION		rf1	400.2
solmode	nnnn	ifp	0
solpwr	0	rf11	400.2
satdly	0	rfp1	0
satfrq	0	PLOT	
DECOUPLER		wc	124.0
dn	C13	sc	8.2
dm	nm	wc2	124.0
		sc2	0
		vs	480

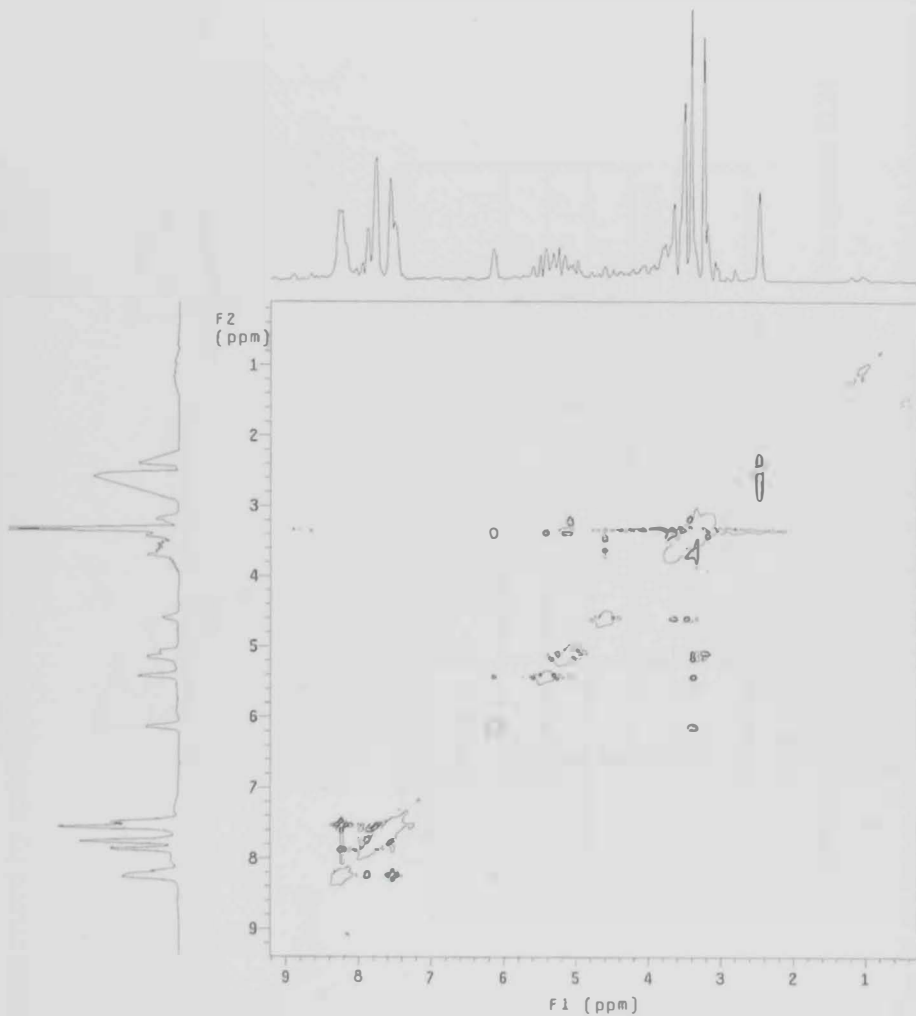
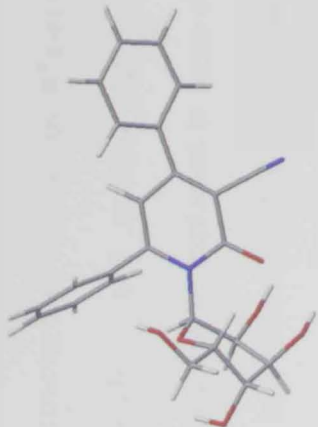
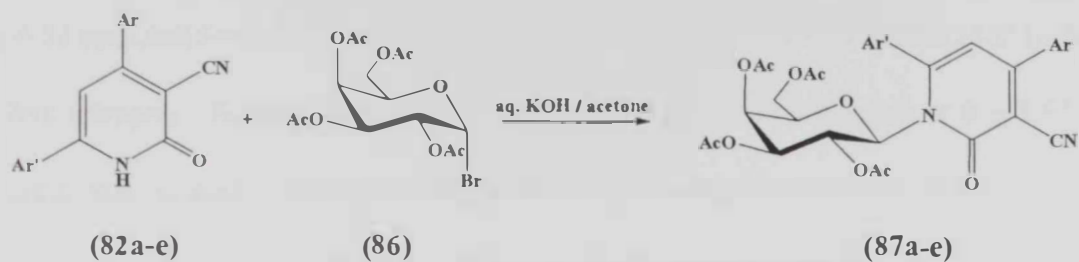


Figure 12: NOESY spectrum of compound (85a)

3.2.3 Pyridinone Galactosides

The structures of compounds (87a-e) were established unambiguously on the basis of elemental analysis and spectral data. All these compounds are β -anomers. The stereochemistry can be explained in terms of the S_N2 substitution reaction between the α -bromosugar and the nucleophilic Pyridinone anion. All products are optically active and were characterized by specific rotation (Scheme 22).



Compound No.	Ar	Ar'
87a	phenyl	phenyl
b	3-tolyl	phenyl
c	2-thienyl	phenyl
d	2-thienyl	4-chlorophenyl
e	2-trifluoromethyl phenyl	phenyl

Scheme 22: Synthesis of Pyridinone Galactoside (87a-e) in aqueous KOH

The IR (KBr) spectra of compounds (87a-e) are characterized by the presence of the carbonyl group in the $1750\text{-}1780\text{ cm}^{-1}$ region and the presence of a strong band at 1641 cm^{-1} corresponding to the carbonyl group at pyridine C-2. In addition to these bands the galactopyranoside ring shows strong bands at 1064 and 1105 cm^{-1} corresponding to ether linkage.

As has already been discussed, $^1\text{H-NMR}$ spectroscopy is routinely used to determine the relative configuration (α - or β -) of nucleosides. In the β -configuration, the anomeric proton H-1'' at $\delta = 6.31$ ppm is in a diaxial relationship with H-2'' of the hexapyranosyl ring system with a coupling constant greater than 7.5 Hz which indicates that the configuration of the hexapyranose is β .

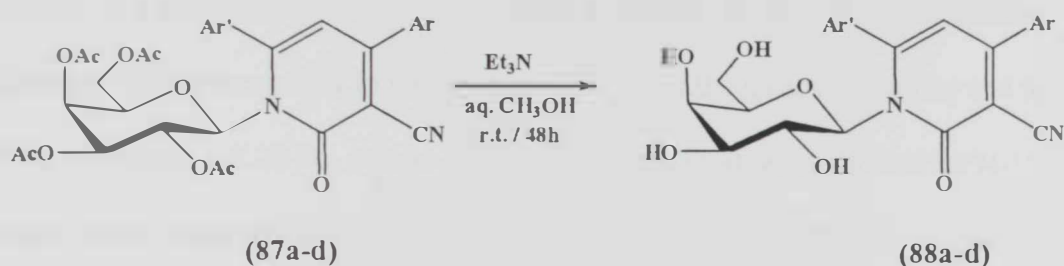
Analysis of the $^1\text{H-NMR}$ spectrum of (87a) reveals the presence of a doublet at δ 6.27-6.31 ppm and $J = 8.00$ Hz which can be attributed to the anomeric proton H-1'' linked to pyridine nitrogen. Signals for H-2'' and H-3'' are observed as multiplets at $\delta = 5.51$ -5.74 ppm and, and the signal corresponding to H-4'' as a multiplet at 5.21-5.28 ppm in CDCl_3 respectively. This indicates that the protons are axially oriented and that they exist in ${}^4\text{C}_1(\text{D})$ conformation and the β -configuration. Then H-6' and H-6'' signals were observed as a multiplet at 4.17-4.28 ppm. The 12 protons of the four acetoxy groups appear at $\delta = 1.88$, 2.04, 2.05 and 2.22 ppm within the range expected for the equatorial acetoxy groups. The pyridinone protons appear in the region $\delta = 7.26$ -8.09 ppm whereas the H-5 appears as a strong singlet at $\delta = 7.66$ ppm. Signals observed at $\delta = 7.50$ -7.70 ppm and 8.04-8.09 ppm correspond to the aromatic protons.

The structures of compounds (87a-e) are also confirmed by $^{13}\text{C-NMR}$ spectra (See experimental part for more details). The $^{13}\text{C-NMR}$ spectrum of compound (87a), as an example, is characterized by a signal at $\delta = 94.9$ ppm corresponding to the C-1'' atom of the β -anomer. The four signals which appear at $\delta = 168.9$, 170.2, 170.3 and 170.4 ppm (four acetoxy carbonyl carbon) are due to the four acetoxy carbonyl carbon atoms of the sugar moiety. The four signals which are shown at $\delta = 20.5$, 20.6, 20.6 and 20.7 ppm are attributed to the methyl carbons of the same groups. The five signals at $\delta = 71.8$, 67.9, 70.9,

67.2 and 61.8 ppm assigned to β -anomer of C-2'', C-3'', C-4'', C-5'' and C-6' respectively. The pyridinone ^{13}C -NMR signals seen at $\delta = 157.8, 114.0, 162.4, 94.0$ and 157.2 ppm correspond to C-2, C-3, C-4, C-5 and C-6 respectively. A strong signal appears at $\delta = 115.4$ ppm corresponding to the cyano group at C-3. The ^{13}C -NMR signals of the aryl groups at the positions 4 and 6 of pyridinone nucleus appear within the range 127.3 - 136.8 ppm.

3.2.4 Ammonolysis of Nucleosides (87a-d)

1-(β -D-galactopyranosyl)-3-deazapyrimidine derivatives (**88a-d**) were obtained by the ammonolysis of (**87a-d**) using triethylamine in methanol at room temperature for 48 hours. The reaction mixture was purified using column chromatography to give the correct microanalytical results in yield 57-77% (Scheme 23).



Compound No.	Ar	Ar'
88a	phenyl	phenyl
b	3-tolyl	phenyl
c	2-thienyl	phenyl
d	2-thienyl	4-chlorophenyl

Scheme 23: Ammonolysis step of the Pyridinone galactosides

The structures of the obtained galactosides were confirmed by elemental analysis, IR spectra and NMR data. The IR (KBr) spectra of the free galactosides (**88a-d**) were characterized by the absence of the ester carbonyl at 1750 cm^{-1} . The presence of the broad

band within 3200-3700 cm^{-1} is due to the four hydroxyl groups of the galactose moiety while the strong band appears at 1639 cm^{-1} corresponding to the carbonyl group at C-2.

The structure of compound (88a) was confirmed by $^1\text{H-NMR}$ and COSY. The COSY spectrum was used to assign intra-protons interactions. Figures 13 and 14 show a cross peak interaction within the aromatic region between H-5 of the pyridine ring and *ortho*-protons at the 6-position (same as in the acetylated product 87a). The cross-peak interaction between the anomeric proton *H-1''* and *H-2''* is also observed. No cross-peak interaction between the hydroxyl protons at C-2'', C-3'', C-4'', C-6'' and any other protons in the system was observed.

The $^1\text{H-NMR}$ ($\text{DMSO-}d_6$) spectra of the nucleosides (88a-d) are characterized by the appearance of a doublet at $\delta = 6.02\text{-}6.06$ ppm, at a relatively lower field than other sugar ring protons. This corresponds to the anomeric proton of the galactose moiety and the large coupling constant, $J = 8.20$ Hz, can be attributed to the diaxial orientation of the *H-1''* and *H-2''* protons which indicates the β -configuration and the ${}^4\text{C}_1$ (D) conformation. The $^{13}\text{C-NMR}$ ($\text{DMSO-}d_6$) spectrum of (88a) is characterized by a signal at $\delta = 97.4$ ppm corresponding to the C-1'' atom of the glucose residue. No other signals were observed at $\delta \approx 20$ ppm region corresponding to the methyl of the acetoxy groups.

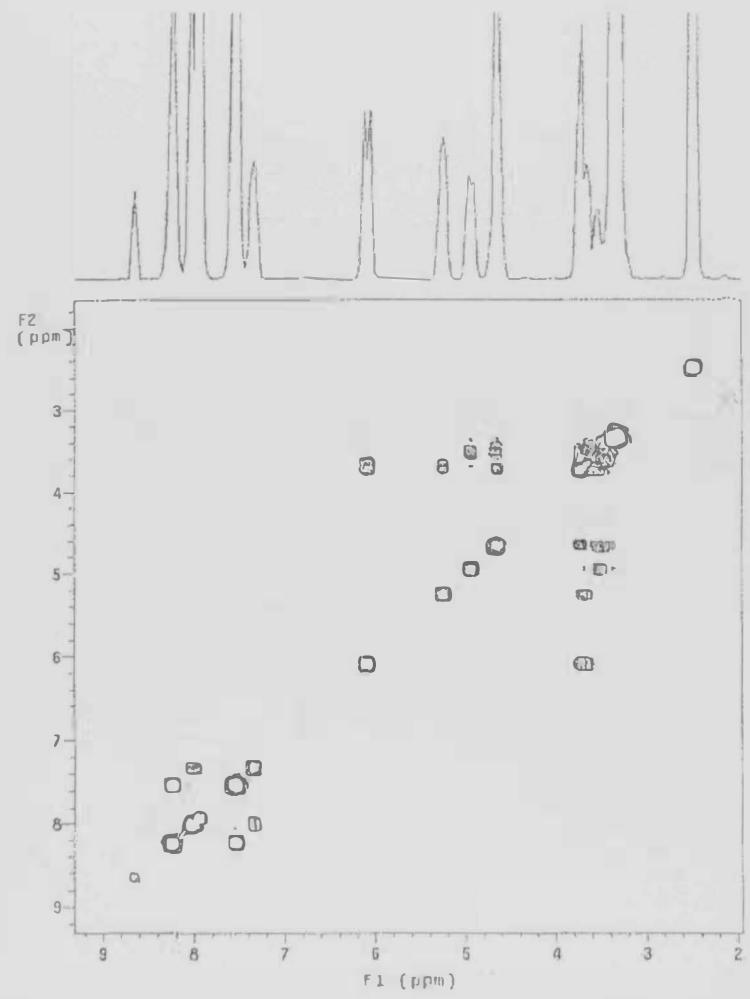
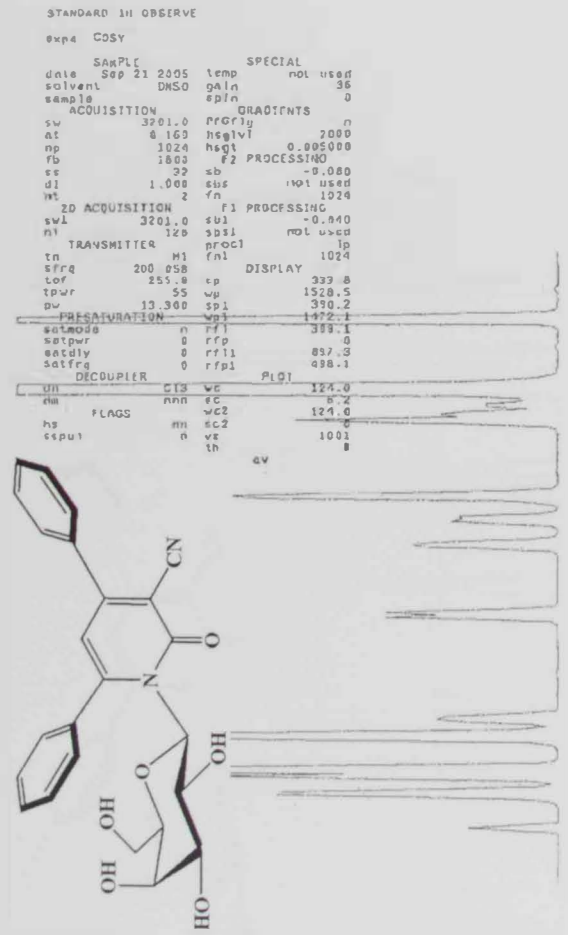
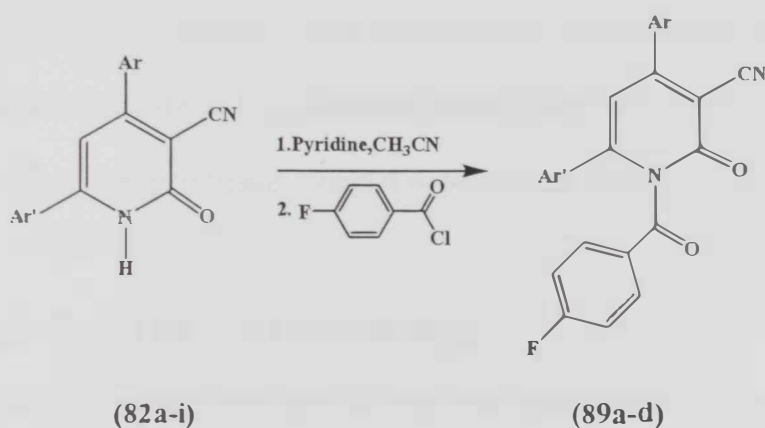


Figure 13: COSY spectrum of compound (88a)

3.3 Synthesis of Non-Nucleoside Derivatives (89a-d):

This part deals with the synthesis of 1-(*p*-fluorobenzoyl)-3-cyano-4,6-diaryl-2-pyridinone (89a-d) by the reaction of 3-deazapyrimidine derivatives (82a-i) with 4-fluorobenzoyl chloride in dry acetonitrile. The reaction afforded a sole product within 30 min. 1-(*p*-fluorobenzoyl)-3-cyano-4,6-diaryl-2-pyridinones (89a-d) were obtained in a 62-72% yield (Scheme 24). The structures of compounds (89a-d) were confirmed by elemental analysis and spectral data (IR, ¹H-NMR, ¹³C-NMR). The analytical data for (89a) reveals a molecular formula, C₂₆H₁₄F₄N₂O₂. The IR spectrum of (89a) shows the presence of two carbonyl groups at 1580 cm⁻¹ and at 1770 cm⁻¹ corresponding to the carbonyl group at C-2 and another one at pyridine-*N*, respectively. The strong band at 2230 cm⁻¹ is due to the CN group at C-3.



Compound. No.	Ar	Ar'
89a	2-thienyl	phenyl
b	2-thienyl	4-chlorophenyl
c	4-pyridyl	4-methoxyphenyl
d	3,4-Dimethoxyphenyl	4-methoxyphenyl

Scheme 24: Synthesis of 1-(*p*-fluorobenzoyl)-3-cyano-4,6-diaryl-2-pyridinone (89a-d)

Summary

This study includes the design and synthesis of some new 3-deazapyrimidines and their nucleoside analogues. Moreover, the reactions with the fluoro derivatives produced new fluorinated pyridine analogues. The structures of all final products were established and confirmed by different spectroscopic tools. Quantum mechanical calculations supported the suggested structures of the obtained nucleosides. The biological activity of the products is incorporated in this study. All our work is summarized in the following points:

A. Synthesis of 3-Deazapyrimidine Derivatives

3-Deazopyrimidine derivatives (**82a-i**) were prepared as outlined in (Scheme 17). They were synthesized by the reaction of α,β -unsaturated ketones and ethylcyanoacetate in the presence of ammonium acetate. The reaction was accomplished *via* the conjugate addition of enolate anion to the α,β -unsaturated ketones followed by cyclization in refluxing ethanol to give the corresponding 3-cyano-4,6-distributed pyridine-2(*1H*)-ones (**82a-i**) in good yield.

B. Nucleosides Derived from 3-Deazapyrimidines

Pyridione nucleosides (**83a-e**) and (**87a-e**) were synthesized by the reaction between the activated deazopyrimidine derivatives (**82a-e**) either through the formation of the K-salt or the silyl intermediate. The activated intermediate was allowed to react *in situ* with activated sugar molecules to produce the target nucleosides (**83a-e**) and (**87a-e**) (Schemes 19 and 22).

C. Formation of Free Pyridione Nucleosides

Removing the acetyl groups from the sugar moiety was carried out using either saturated ammonia in methanol or triethylamine to give free nucleosides (**85a-e**) or (**88a-e**) in high yield (Schemes 21 and 23).

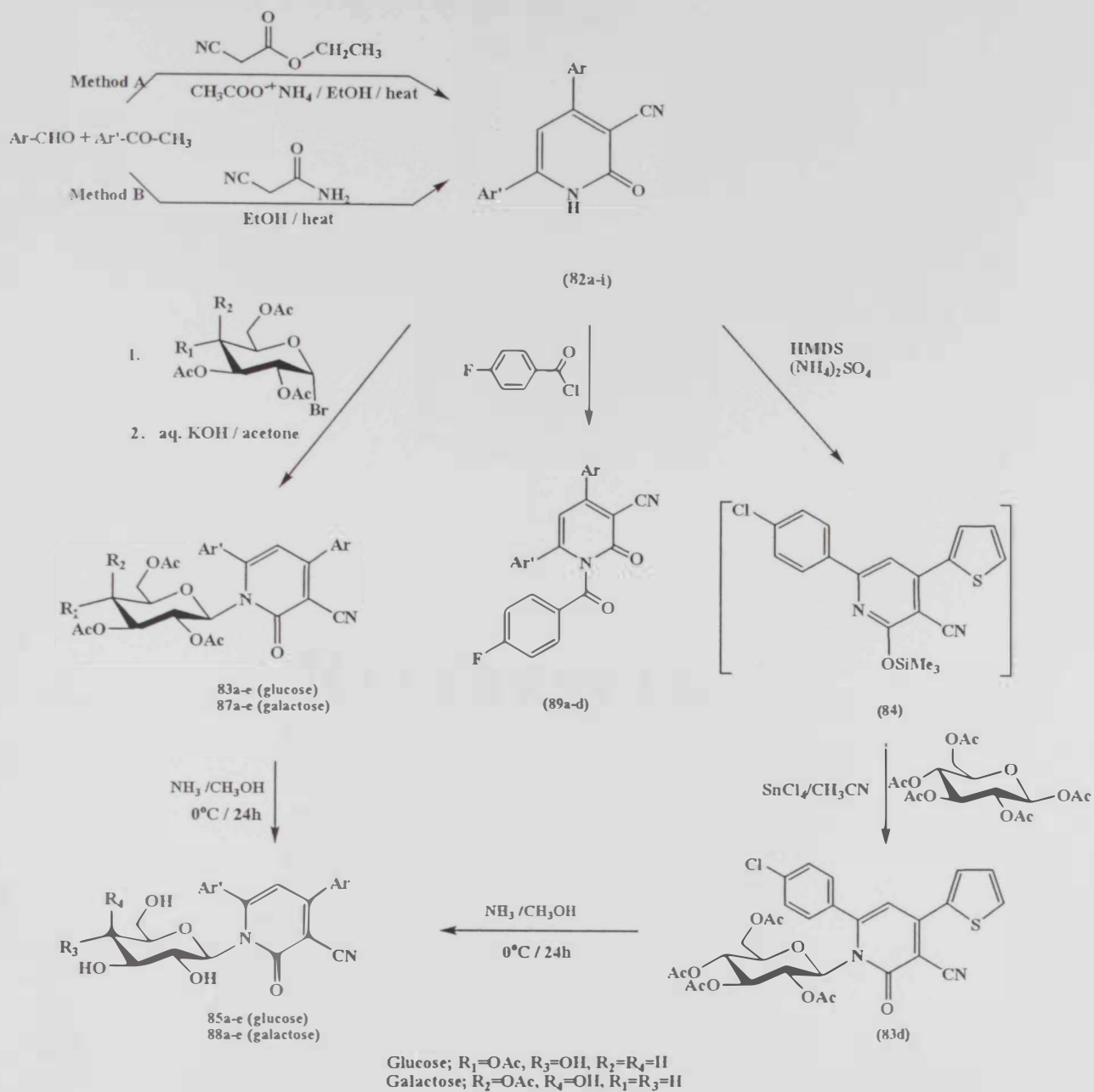
Quantum Mechanics (QM) calculations were used to support the data obtained from the spectral analysis. QM was also used to detect the more reactive center among the pyridinone moiety. Modeling was also used to enhance the 3D-view of these molecules and to examine the obtained conformers.

D. Synthesis of Non-Nucleoside Derivatives

This part deals with the synthesis of new 4,6-diaryl-1-(4'-fluorobenzoyl)-3-cyano-2(*1H*)-pyridinone (**89a-d**). The reaction of pyridine base (**82a-i**) with *p*-fluorobenzoyl chloride afforded the corresponding pyridinone (**89a-d**) (Scheme 25).

E. Biological Application

The synthesized compounds are classified into two main groups according to their biological activity. The most prominent analogue was (**89a**) which resulted in a decrease in the viability of the cells. Therefore (**89a**) could be considered as a potential anticancer agent in which both concentrations were effective (100 and 200 μ M). However analogue (**85c**) was effective at a concentration of 200 μ M only.



Scheme 25: General synthetic scheme for all nucleosides and non-nucleosides derivatives

REFERENCES

References

- (1) Levene, P. A., Jacobs, W. A. *Chem. Ber.*, **1909**, *42*, 2475.
- (2) Paul S. D.; Robert C. H.; Adrian D. H.; Paul D. T.; Patience S.; John G. X.; Dick V. J. *Med. Chem*, **1993**, *36*, 24440-2458.
- (3) John S. W., Williams J. T.; Dona L. B.; Fisher T. E.; Hoffman J. M.; Ronald J. H.; Suzanne C. M.; Clarence S. R.; Walfred S. S.; Craig M. T.; Goldman M. E.; Obrien J. A.; Emini E. A.; Nunberg J. H.; Quintero J. C.; Schleif W. A.; Anderson P. S. *J. Med. Chem*, **1993**, *36*, 249-255.
- (4) Fisher, E.; Helferich, B. *Chem. Ber*, **1914**, *47*, 210.
- (5) Mikhailopulo I. A.; Gunar V. I.; Zavyalov S. I. *Izu. Akad. Nauk SSSR, Ser. Khim*, **1967**, 1811.
- (6) Davoll J.; Lowy, B. *J. Am. Chem. Soc.*, **1951**, *73*, 1650.
- (7) Hilbert G. H.; Johson T. B. *J. Am. Chem. Soc.*, **1930**, *52*, 2001.
- (8) Howard, G. A.; Lythge, B.; Todd, A. R. *J. Am. Chem. Soc., London*, **1947**, 1052.
- (9) Ueda T.; Nishino H. *J. Am. Chem. Soc.*, **1968**, *90*, 1678.
- (10) Shimadate T.; Sato T.; Ishido Y. *Nippon Kagaku Zasshi*, **1960**, *81*, 1440. *C.A.*, **1962**, *56*, 11692g.
- (11) Shimadate T.; Ishido Y.; sato T.; *Nippon Kagaku Zasshi*, **1961**, *82*, 938. *C.A.*, **1962**, *57*, 15216.
- (12) Shimadate T. *Nippon Kagaku Zasshi*, **1961**, *82*, 1268; *C. A.*, **1962**, *57*, 16726.
- (13) Ishido Y.; Sato T. *Bull. Chem. Soe. Jpn.*, **1961**, *34*, 1347.
- (14) Shimadate T. *Nippon Kagaku Zasshi*, **1961**, *82*, 1268, *C. A.*, **1962**, *57*, 19726.

- (15) Ishido Y., Hosono A., Fujii K.; Kikuchi Y.; Sato T. *Nippon Kagaku Zasshi*, 1966, 87, 752. *C. A.*, 1966, 17034c.
- (16) Imai K.; Nohara A.; Honjo M. *Chem. Pharm. Bull.*, 1966, 14, 1377.
- (17) Montgomery J.; Hewson K.; *J. Med. Chem.*; 1969, 12(3), 498.
- (18) Ishido Y., Matsuba T.; Hosono A.; Fujii K.; Sato T.; Isomo S.; Maruyama A. *Bull. Chem. Soc. Jpn.* 1967, 40, 1007.
- (19) Brikhofer L.; Ritter A.; Kuelthau H. P. *Angew. Chem.* 1963, 75, 209.
- (20) Nishimura T.; Shimizu B. I.; Wai I. *Chem. pharm. Bull.*, 1963, 11, 1470.
- (21) Show E. *J. Am. Chem. Soc.*, 1958, 80, 3899.
- (22) Show G.; Wilson D. V. *J. Am. Chem. Soc.*, 1962, 2937.
- (23) Niedballa U.; Vorbruggen H. *J. Org. Chem.* , 1974, 39, 3660.
- (24) Vorbruggen H.; Krolkiewicz K. *Angew. Chem.*, 1975, 87, 417.
- (25) Niedballa U.; Vorbruggen H. *J. Org. Chem.*, 1974, 39, 3654.
- (26) Vorbriiggen H.; Krolkiewicz K. *Angew. Chem., Int. Ed. Engl.* , 1975, 14, 421.
- (27) Vorbriiggen H.; Krolkiewicz K.; Bennua B. *Chem. Ber.*, 1981, 114, 1234.
- (28) Marsmann H. C.; Hom H. G. *Z. Naturforsch*, 1972, 27b, 1448.
- (29) Olah G. A.; Narang S. C.; Balaram Gupta, B. G.; Maihotra R. *J. Org. Chem.*, 1979, 44, 1247.
- (30) Ohsawa K.; Shiozawa T.; Achiwa K.; Terao Y. *Chem. Pharm. Bull.*, 1993, 41, 1906.
- (31) Niedballa U.; Vorbruggen H. *J. Org. Chem.*, 1974, 39, 3668.
- (32) Lichtenthaler F. W.; Kitahara K. *Angew. Chem., Int. Ed. Eng I.*, 1975, 14, 815.
- (33) Stout G. M.; Robins K. R. *J. Org. Chem.*, 1968, 33, 1219.
- (34) McNamara, D. H.; Cook, P. D. *J. Med. Chem.*, 1987, 30, 340.

- (35) Nesnow S.; Miyazaki T.; Kawaja T.; Meyer B.; Heidelberger C. *J. Med. Chem.*, **1973**, *16*, 524.
- (36) Elgemeie G. E. H.; Attia A. M. E.; Fathy N. M. *Liebigs Ann. Chem.*, **1994**, 955.
- (37) Attia A. M. E.; Elgemeie G. E. H. *Nucleosides and Nucleotides*, **1995**, *14*(6), 1211.
- (38) Al-Deeb A. O.; Al-Afify A.; El-Kashef H. *Il Farmaco*, **1999**, *54*, 195–201.

PART TWO

BIOLOGICAL ACTIVITY

4. Biological Activity

4.1 Introduction

Cancer is a class of diseases or disorders characterized by uncontrolled division of cells and the ability of these cells to invade other tissues, either by direct growth into adjacent tissue through *invasion* or by implantation into distant sites by *metastasis*. This unregulated growth is caused by damage to DNA, resulting in mutations to genes that encode for proteins controlling cell division.⁽¹⁾

Development of drug therapy progressed rapidly after the discovery of DNA as the primary genetic material in 1944 and subsequent elucidation of the physical structure in 1953⁽²⁾. Since the nucleic acids DNA and RNA are the initial precursors in the formation of proteins that are responsible for many biological and physiological processes, it is logical that these molecules could be viewed as potential targets for drug design and development.⁽³⁾ DNA and RNA are biopolymers composed of nucleosides held together by phosphodiester linkages and as a result, the nucleosides can also be considered as potential targets.^(2,3)

It was not until the 1960's, that chemistry involving nucleosides and nucleotides provided the fundamental infrastructure and synthetic methodology necessary to produce numerous biologically active naturally occurring and structurally modified nucleosides. The biological activity of anticancer agents such as 5-fluoro-2'-deoxyuridine (FUDR), arabinosylcytidine (ara-C), 8-azainosine, along with the discovery of a potent antiviral nucleoside, arabinosyladenosine (ara-A), and antitumor agent, toyocamycin revealed the potential value of modified nucleoside Analogues as chemotherapeutic agents (Figure 15).^(4,5)

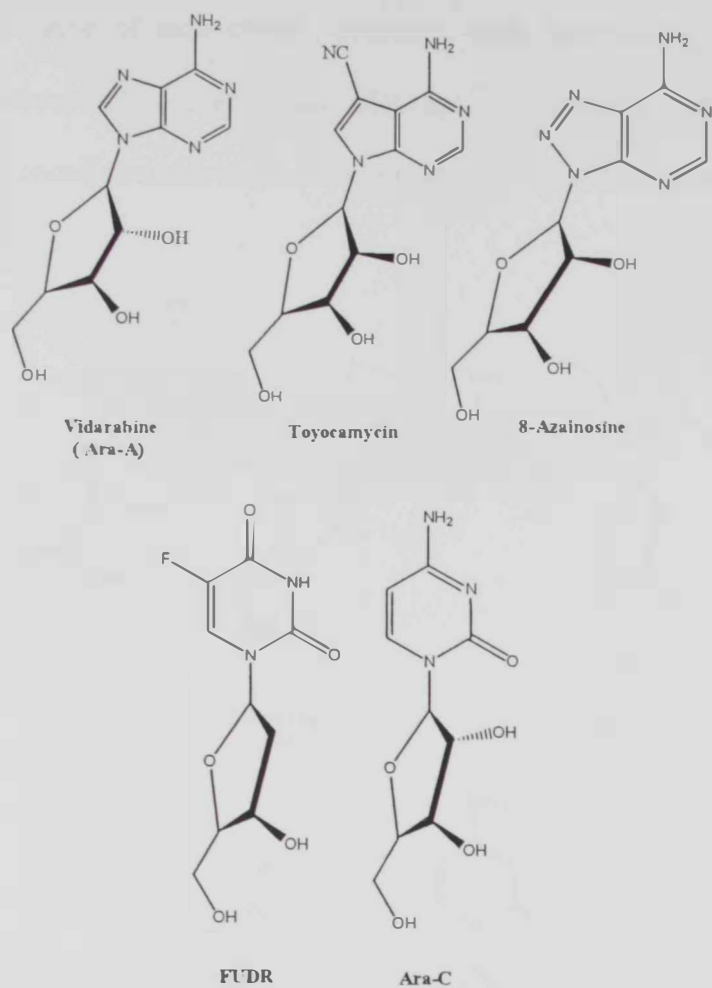


Figure 15: Some FDA-approved nucleoside drugs

The importance of these nucleoside analogues was later confirmed with the emergence of HIV as the main etiological agent of AIDS.⁽⁶⁾ The first drug approved for the treatment of HIV was the modified nucleoside AZT which inhibits HIV-1 reverse transcriptase.⁽⁷⁾ Furthermore, several other nucleoside analogues involved in inhibition of HIV-1 reverse transcriptase, namely ddC, ddI, d4T and 3TC, have provided even more significance to the use of nucleoside analogues as biologically potent chemotherapeutic agents (Figure 16).⁽⁷⁻⁹⁾

Despite these examples, clinical use of these drugs is limited due to several factors, including toxicity, the wide range of side effects, problems with lipophilicity and crossing cell membranes, and susceptibility to enzymatic cleavage.⁽⁹⁾ This has prompted researchers to search for more advanced chemotherapeutic agents that could address these issues

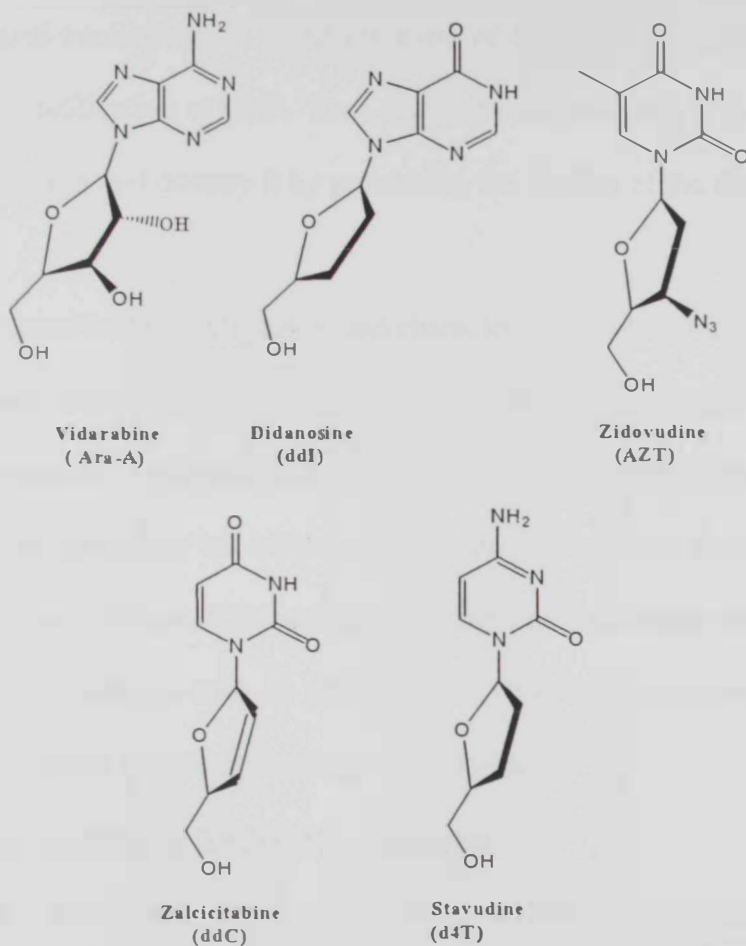


Figure 16: Some potent nucleoside-based inhibitors of HIV-1 RT

4.1.1 Biochemistry of Nucleosides

Cytotoxic nucleoside analogues (NA) were among the first chemotherapeutic agents to be introduced for the medical treatment of cancer.⁽¹⁰⁾ This family of compounds has grown to include a variety of purine and pyrimidine nucleoside derivatives with activity in both solid tumors and hematological malignancies.⁽¹¹⁾ These agents behave as antimetabolites and compete with natural nucleosides. The effectiveness of these agents results from their ability to cause covalent modification of DNA. Thus, they get incorporated into the genetic material during DNA replication and destroy it by preventing the fidelity of the repair system within the DNA.⁽¹²⁾

Recent progress in the identification and characterization of nucleoside mechanisms of anticancer nucleoside activity provides opportunities for possible antitumor effects.⁽¹⁰⁾ Since they are hydrophilic compounds, they require special transporter proteins to enter the cells. Once inside the cells they are activated to become triphosphate derivatives, which can be incorporated within DNA or RNA and damage them by interfering within the enzymes responsible for their synthesis such as polymerases. This results in damaging the genetic component of the cell and eventually leading to apoptosis.⁽¹⁰⁻¹²⁾

4.1.1.1 Purine and Pyrimidine Nucleoside Analogues

Nucleoside analogues (NA) constitute a pharmacologically diverse family, comprising cytotoxic compounds, antiviral agents and immunosuppressive molecules. The anticancer nucleosides include several analogues of physiologic pyrimidine and purine nucleosides. The two primary purine analogues are 2-chlorodeoxyadenosine (2-CdA, cladribine) and 2-fluoro-ara-A-monophosphate (fludarabine).^(10,11) These drugs have mostly been used in the treatment of low-grade hematological malignancies. Among the currently

available pyrimidine nucleobases and analogues cytosine arabinoside (ara-C, cytarabine) is extensively used in the treatment of acute leukemia.

Difluorodeoxycytidine (gemcitabine) has demonstrated activity in a variety of solid tumours and certain hematological malignancies, while 5-fluorouracil and capecitabine have demonstrated activity in colorectal and breast cancers (Figure 17).

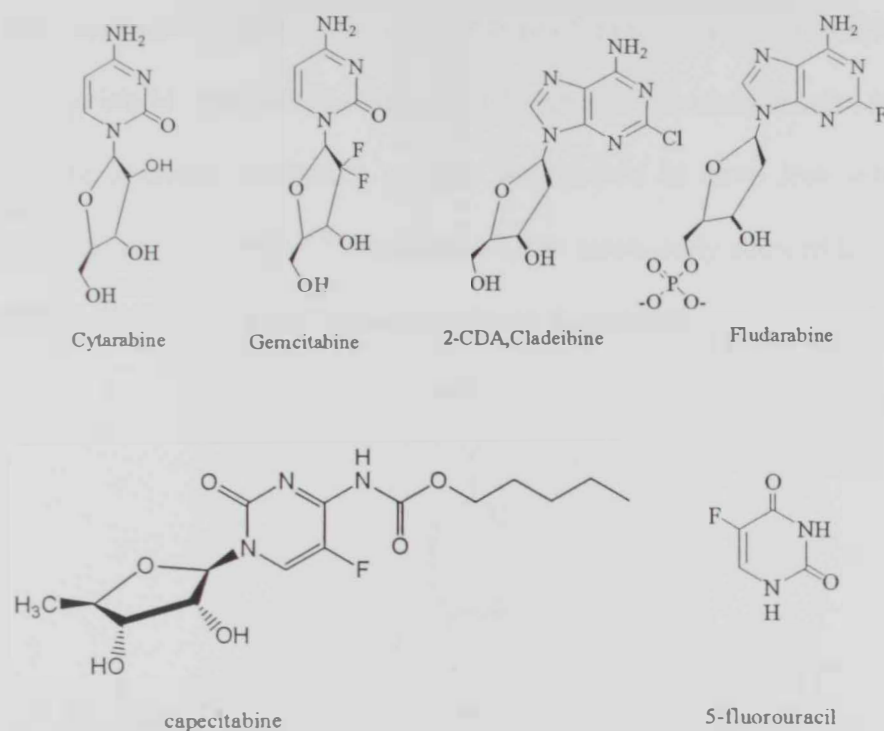
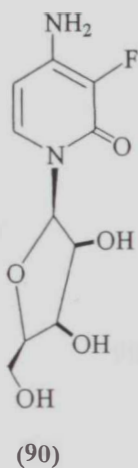


Figure 17: Pyrimidine and purine analogues used in chemotherapy. Gemcitabine, (ara-C, cytarabine) are pyrimidine analogues, whereas fludarabine and (2-CdA, cladribine) are purine analogues. 5-fluorouracil and capecitabine are examples for fluoropyrimidine

4.1.1.2 Pyrimidine Nucleoside Analogues and Nucleobases

4.1.1.2.1 Biological Properties of Pyrimidine Nucleoside

Pyrimidine nucleosides have become the focus of recent research since many of these nucleosides have been found to exhibit significant biological activity. Pyrimidine ribonucleosides and pyrimidine-2'-deoxyribonucleosides which contain an electron withdrawing group at position 3 and/or 5 have been shown to exhibit significant antiviral properties. For example 4-amino-3-fluoro-1-(β -D-ribofuranosyl)-pyridine-2(1*H*)-one (90) has been shown to inhibit the growth of the L1210 Lymphoid Leukemia cell with $IC_{50} = 1.07 \times 10^{-5}$ while the 2'-deoxy derivative of (90) was shown to have less activity against Lymphoid Leukemia L1210 cells⁽¹⁷⁾ Furthermore, the same study showed that the triacetyl derivative exhibited similar but less potent activity to that of (90)

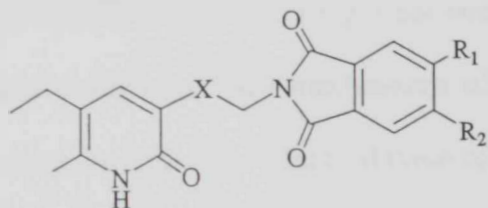


1-Deazaguanine has shown activity against the growth of mouse mammary carcinoma⁽¹⁸⁾ Certain 1- and 3-deazapurines have shown antibacterial, anticancer and antiviral activity.⁽¹⁹⁾ Important biological activity of deaza analogues of guanine is anticipated from the metabolism in microbial and mammalian system. 3-Deazaguanosine has shown potent broad spectrum activity against various DNA and RNA viruses⁽²⁰⁾ while, 3-

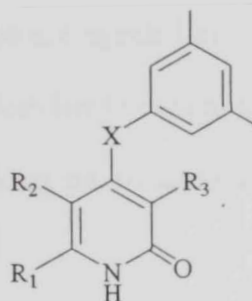
deazauridine has been shown to exhibit significant antiviral properties. It has been shown to inhibit the growth of microorganisms and L1210 leukemia.⁽²¹⁾

4.1.1.2.2 Biological Properties of Deazapyrimidine

Various pyrimidines have been shown to have important biological properties in medicinal and agricultural studies.⁽¹³⁾ For example, selective inhibitors of human immunodeficiency virus type I reverse transcriptase (HIV-IRT) was found to be affected by some deazapyrimidine derivatives with IC_{50} of 19 nm.⁽¹⁴⁾ Compounds 3-[(4,7-dimethyl benzoxazol-2-yl)]- amino-5-ethyl-6-methyl pyridine-2(1*H*)-one and the corresponding 4,7-dichloro analogue (91) have inhibited the spread of HIV-I infection by 95% in MT4 cell culture and were selected for clinical trails as antiviral agents. 4-benzyl pyridinone (92) possess potent HIV-1 specific reverse transcriptase inhibitory properties.⁽¹⁵⁾

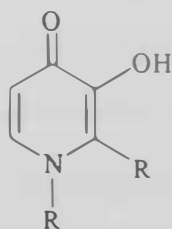


(91) X = NH, CH₂
R₁, R₂ = 4,7-dimethyl
= 4,7-dichloro



(92) X = S, R₁ = H, R₂ = R₃ = CH₃
X = CH₂, R₁ = CH₃, R₂ = Et, R₃ = NH₂

3-Hydroxy-4(1*H*)-pyridione (93) has been used to remove iron from hepatocytes.⁽¹⁶⁾



(93) R = CH₃, R' = H
= CH₂CH₃, R' = H

4.1.1.2.3 Fluoropyrimidines Nucleosides

5-Fluorouracil (5-FU) and 5-fluoro-2'-deoxyuridine (FUDR) have antitumor activity in patients with colorectal, pancreatic, breast and head and neck cancers.⁽²²⁾ These agents require an active intermediate such as 5-fluorodeoxyuridine 5'-monophosphate (5-FdUMP), 5-fluorouridine triphosphate (5-FUTP) or 5-fluorodeoxyuridine triphosphate (5-FdUTP). The cytotoxic effects of these compounds include (i) inhibition of the target enzyme thymidylate synthase (TS) by 5-FdUMP resulting in depletion of thymidine nucleotides and inhibition of DNA synthesis and repair, (ii) incorporation into RNA resulting in abnormal RNA processing and function, and (iii) misincorporation of 5-FdUTP and deoxyuridine triphosphate (dUTP) into DNA, producing damage to nascent DNA.

4.1.2 Nucleosides and Cancer

The growing importance of nucleosides as cytotoxic agents has stemmed both from the development of newer compounds with broad applicability to common cancers, and from an understanding of their mechanisms of action, enabling pharmacological intervention to potentiate the antitumor effects of these compounds.⁽²²⁾

Nucleosides analogues and their corresponding nucleobases and as a result, have been investigated due to their inherent structural resemblance to the naturally occurring nucleosides and nucleobases as the fundamental building blocks of many biological systems. Synthetic nucleoside analogues can be used in chemotherapy to treat cancer, due to the intertwined relationship between physiologic and synthetic nucleosides.⁽²²⁾

Cytotoxic nucleoside analogues are antimetabolites which interfere with nucleic acid synthesis. These agents are generally S-phase specific, and can exert cytotoxic activity either by being incorporated and altering the DNA and RNA macromolecules structures. It can

disrupt the normal replication process by interfering with the normal Watson-Crick base pairing, thereby preferentially kill rapidly dividing cells such as tumor cells. Synthetic nucleoside analogues can also interfere with various enzymes involved in nucleic acid synthesis such as polymerases (e.g. DNA polymerase), phosphorylases (e.g. Thymidine Phosphorylase) and kinases (e.g. nucleoside kinase). However, some family of analogues causes cytotoxic activity by modifying the metabolism of physiologic nucleosides.^(22, 23)

Nucleoside analogues exert their anti cancer potential, if they destroy the cancerous cells by the process of programmed cell death or the disruption of cell cycle progression.⁽²³⁾

4.1.2.1 Apoptosis

Since the mid-nineteenth century, many observations have indicated that cell death plays a considerable role during physiological processes of multicellular organisms, particularly during embryogenesis and metamorphosis.^(24, 25) The term *programmed cell death* was introduced in 1964, proposing that cell death during development is not of an accidental nature but follows a sequence of controlled steps leading to locally and temporally defined self-destruction.⁽²⁶⁾ Eventually, the term *apoptosis* had been coined in order to describe the morphological processes leading to controlled cellular self-destruction and was first introduced in a publication by Kerr, Wyllie and Currie in 1972.⁽²⁷⁾

Apoptosis or programmed cell death is a physiological process that is activated to eliminate unwanted, damaged, aged, or misplaced cells during embryonic development and tissue homeostasis. Apoptotic cells can be recognized by stereotypical morphological changes: the cell shrinks, shows deformation and loses contact to its neighbouring cells. Its chromatin condenses and marginates at the nuclear membrane, the plasma membrane is blebbing or budding, and finally the cell is fragmented into compact membrane-enclosed

structures, called 'apoptotic bodies' which contain cytosol, the condensed chromatin, and organelles (Figure 18). The apoptotic bodies are engulfed by macrophages and thus are removed from the tissue without causing an inflammatory response.⁽²⁸⁾

Apoptosis is in contrast to the necrotic mode of cell-death in which case the cells suffer a major insult, resulting in a loss of membrane integrity, swelling and disruption of the cells. During necrosis, the cellular contents are released uncontrolled into the cell's environment which results in damage to the surrounding cells and a strong inflammatory response in the corresponding tissue.⁽²⁹⁾

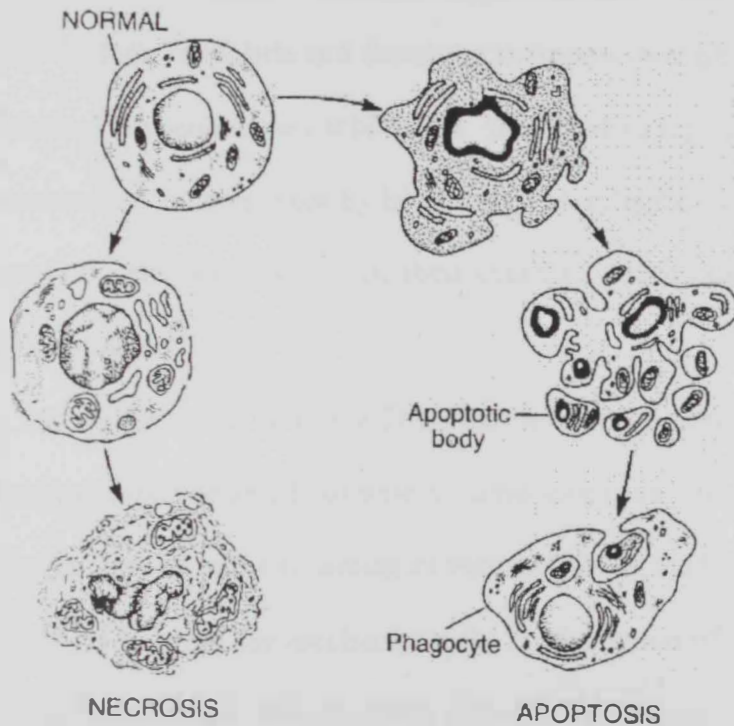


Figure 18: Hallmarks of the apoptotic and necrotic cell death process. Apoptosis includes cellular shrinking, chromatin condensation and margination at the nuclear periphery with the eventual formation of membrane-bound apoptotic bodies that contain organelles, cytosol and nuclear fragments and are phagocytosed without triggering inflammatory processes. The necrotic cell swells, becomes leaky and finally is disrupted and releases its contents into the surrounding tissue resulting in inflammation.

4.1.2.2 Nucleosides and Apoptosis

Many natural and synthetic DNA-targeting agents are now under study. Many of these are quite promising in cancer therapy (i.e., in the treatment of acute promyelocytic leukemia), where new chemotherapeutic agents with different mechanisms of action are tested. DNA topoisomerase enzymes are important nuclear enzymes. They regulate DNA metabolism and affect replication, transcription, chromatin assembly, and consequently also cell division. The functions of the DNA topoisomerases I, II α , and II β thus have significant consequences for cancer development and cancer chemotherapy.^(30, 31) Indeed, important chemotherapeutic agents that are either in clinical use or the subjects of clinical trials target these enzymes. These include etoposide and doxorubicin (topoisomerase II inhibitors) and topotecan and irinotecan (topoisomerase I inhibitors). Inhibitors of topoisomerase II either stabilize DNA-topoisomerase II complexes by blocking DNA religation and thereby cause direct DNA damage (e.g., etoposide) or block their catalytic activity (e.g., dexrazoxane) without causing DNA damage.⁽³¹⁾

It has been known for some time that DNA-damaging topoisomerase II inhibitory anticancer drugs, such as etoposide and doxorubicin, cause apoptosis. Etoposide (VP16), like other drugs, is used in the treatment of various tumors, such as breast and lung cancer and leukemia.⁽³²⁾ However, the mechanisms for the induction of apoptosis are less well understood. It has been shown that apoptosis induced by the chemotherapeutic drug etoposide is caspase-dependent (family of proteins known as cysteine-dependent aspartate-directed proteases). Two classes of caspase-dependent pathways have been identified. The first is dependent on the release of mitochondrial factors, which initiate the apoptosis process. In this case, apoptosis can be inhibited by overexpression of Bcl-2. The second class

is not dependent on mitochondrial factors, and overexpression of Bcl-2 fails to prevent apoptosis.⁽³³⁾

4.2 Material and Methods

4.2.1 Reagents

Nucleoside analogues were synthesized and purified, and then dissolved in di-methyl sulfoxide (DMSO, Sigma Aldrich Chemie GmbH Steinheim, Germany) to prepare 100 and 200 μM solution and stored at -20°C .

4.2.2 Tissue Culture

Human promyelocytic leukemia HL-60 cell line (ATCC, USA) was grown in DMEM medium (GIBCO-BRL) supplemented with 20% fetal calf serum (GIBCO-BRL), 100 units/ml penicillin-streptomycin (GIBCO-BRL). The cells were maintained at 37°C in a 5% CO_2 incubator. After reaching confluency, the cells were subcultured into 96-wells culture plates, allowed to grow for 1 day, and treated with various concentrations of nucleosides and nucleobases.

4.2.3 MTT Cell Proliferation Assay

Cells were plated in 96-well plates at a density 4×10^3 cells/well/100 μL of the appropriate culture medium and treated with the compounds at concentrations of 100-200 μM for 24 hrs. In parallel, the cells were treated with 0.1% of DMSO as a control. A MTT [3-(4,5-dimethylthiazol-2-yl)-2,5-diphenyltetrazolium bromide] assay (Alexis, USA) was performed later according to the manufacturer instructions to examine the cytotoxic effect of these nucleosides. After adding the MTT reagent the plate was further incubated for 1-4 hrs, followed by measuring the absorbance. This assay is based on the cellular cleavage of the tetrazolium salt, MTT, into formazan that is soluble in cell culture medium and is measured at 450 nm directly in 96-well assay plates. The amount of the formazan dye (absorbance) generated by the activity of dehydrogenases in cells by the intact mitochondria is directly

proportional to the number of living cells in culture. All nucleoside compounds tested were dissolved in DMSO and subsequently diluted in the culture medium to obtain the final concentrations that are going to be tested (100-200 μM) before treatment of the cultured cells.

4.3 Results and Discussion

4.3.1 Effects on HL-60 Proliferation and Integrity by Nucleosides

From the MTT cell proliferation assay we can categorize the effects of the tested analogue into three groups as follows (Figures 19-22):

1. Group 1: Protective effect, (% viability 90% and above).
2. Group 2: No effect, (% viability 70-89 %).
3. Group 3: Minimal to moderate effect (% viability 69% and below).

According to this classification the majority of the nucleosides were grouped into group 1 or 2. Compound (89a) was found to be the most prominent analogues which resulted in a decrease in the viability of the cells, and hence can be considered as a potential anti cancer agents in which both concentrations are effective (100 and 200 μM). In contrast, the rest of the analogous displayed only slight anti-tumor activity. However, (85c) was found to be effective at a concentration of 200 μM only. This suggests that all these analogues are capable of protecting against apoptosis or have no effect at all. This finding also suggests that acetylated sugar increases the bioavailability (their delivery into the cell) of the nucleoside and therefore its effectiveness. The initial observations about the apoptotic potential of these drugs in the HL-60 cell line prompted us to further investigate the mechanism of their apoptotic induction. The controls that were used in

these experiments if not specified were untreated cells as negative control and sodium dodecyl sulfate SDS as treated cells.

% Viability in HL-60 Cell Line treated with 3-Deazapyrimidine Derivative

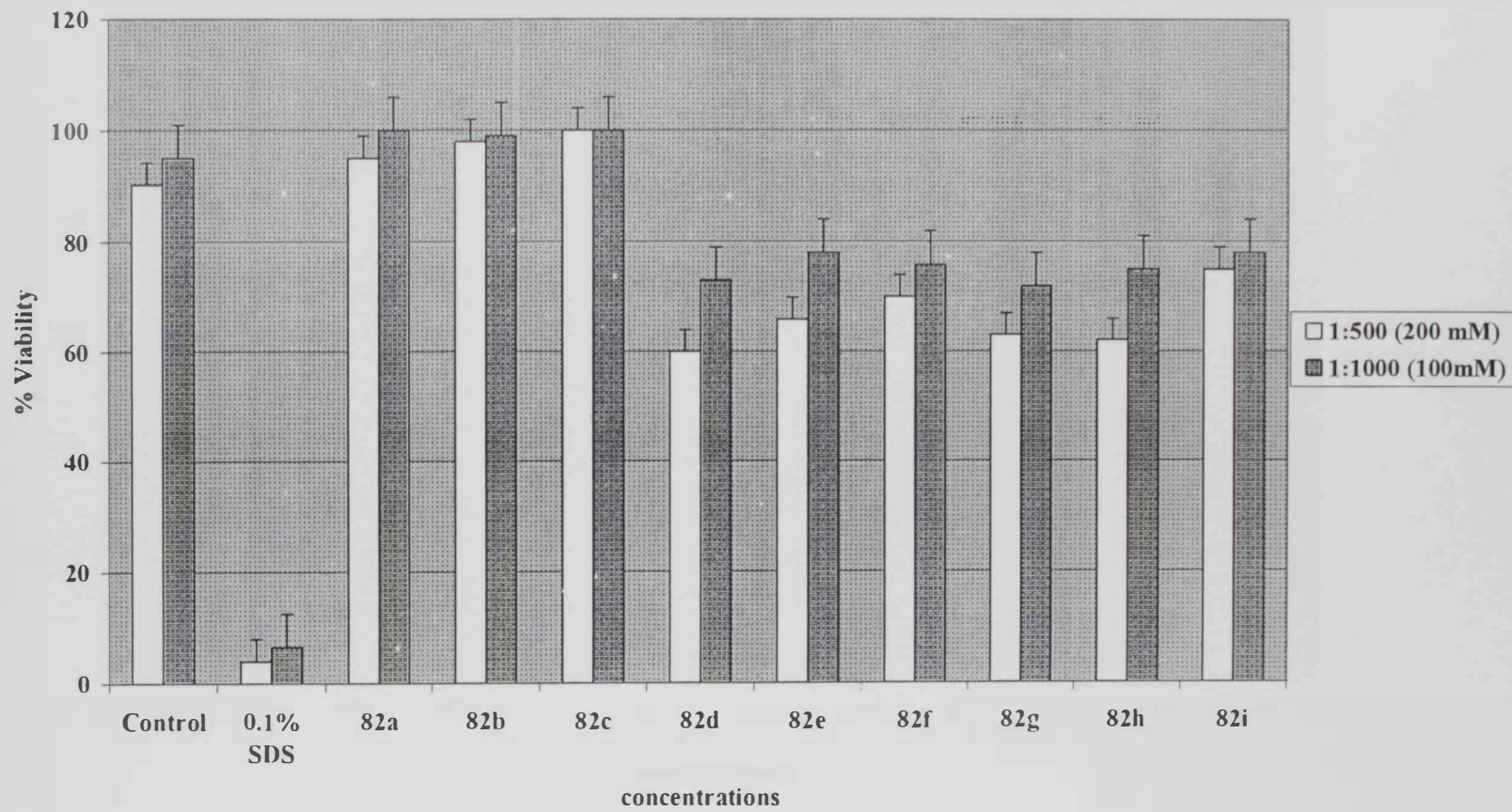


Figure 19: % Viability in HL-60 cell line treated with 3-deazapyrimidine derivative (82a-i) from MTT cell proliferation assay

% Viability in HL-60 Cell Line treated with Prydinone glucosides

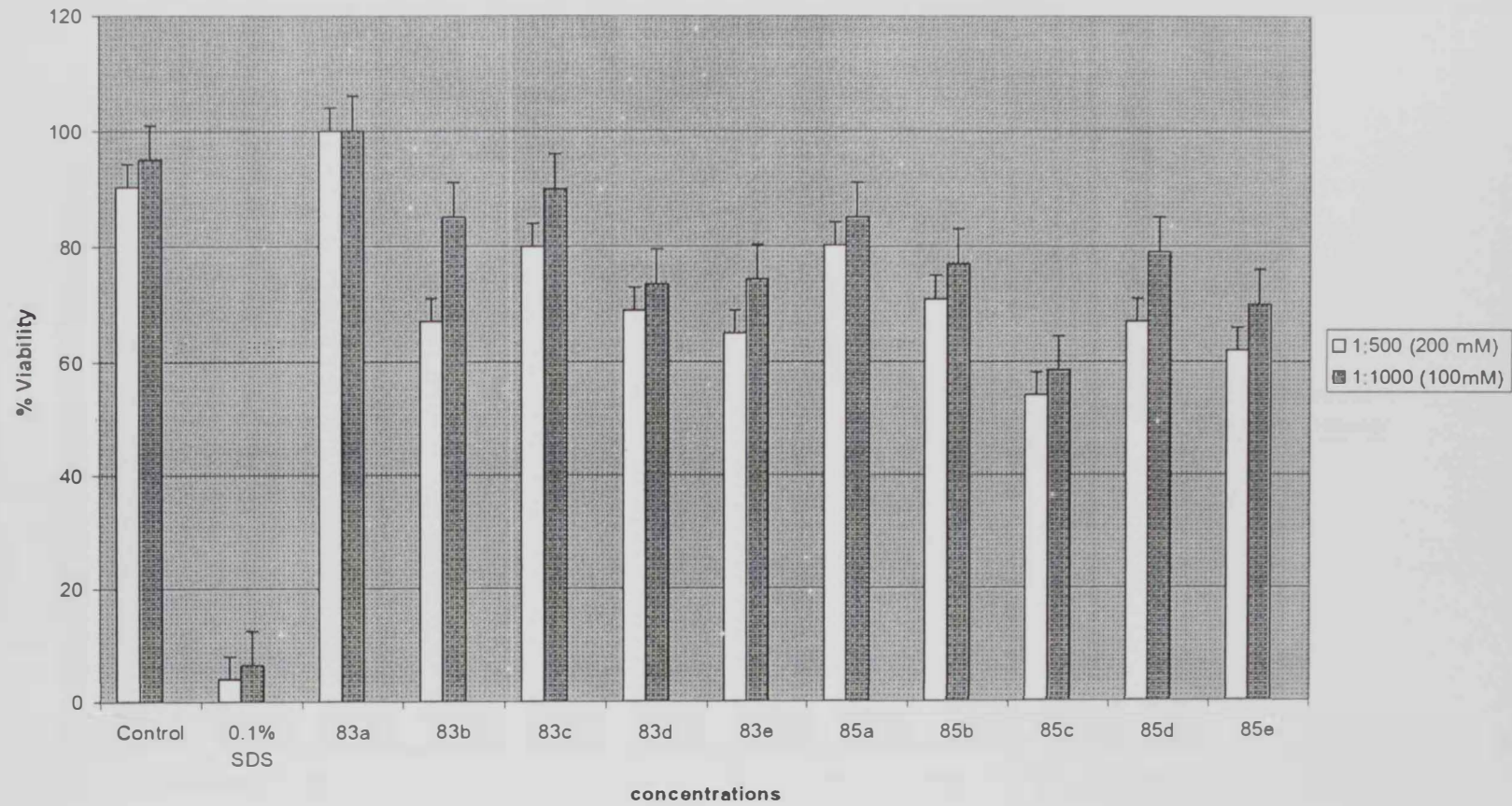


Figure 20: % Viability in HL-60 cell line treated with prydinone glucosides (83a-e) from MTT cell proliferation assay

% Viability in HL-60 Cell Line treated with 2 Pyridinone Galactosides

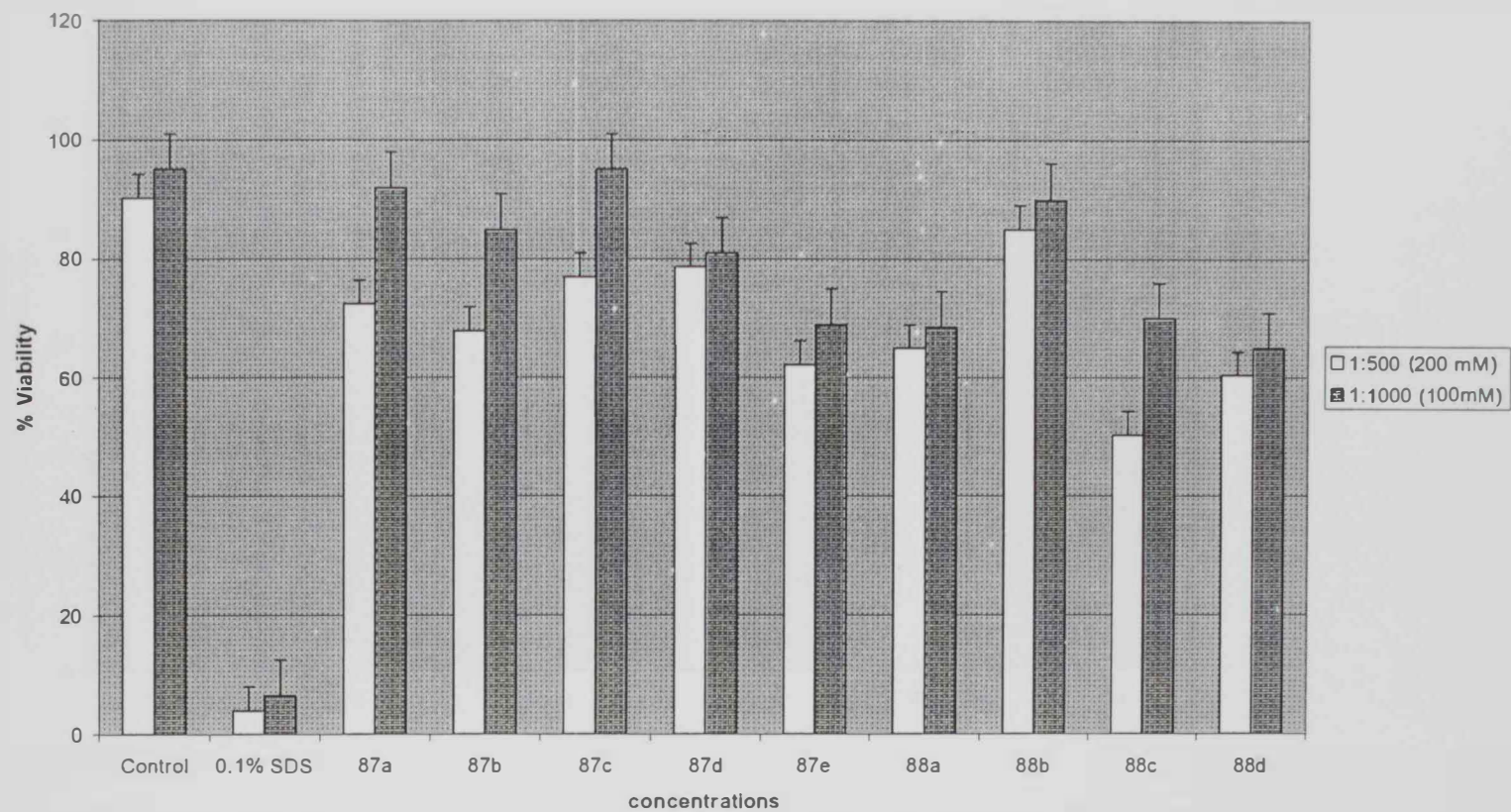


Figure 21: % Viability in HL-60 cell line treated with pyridinone galactosides (87a-d) from MTT cell proliferation assay

% Viability in HL-60 Cell Line treated with non-nucleoside derivatives

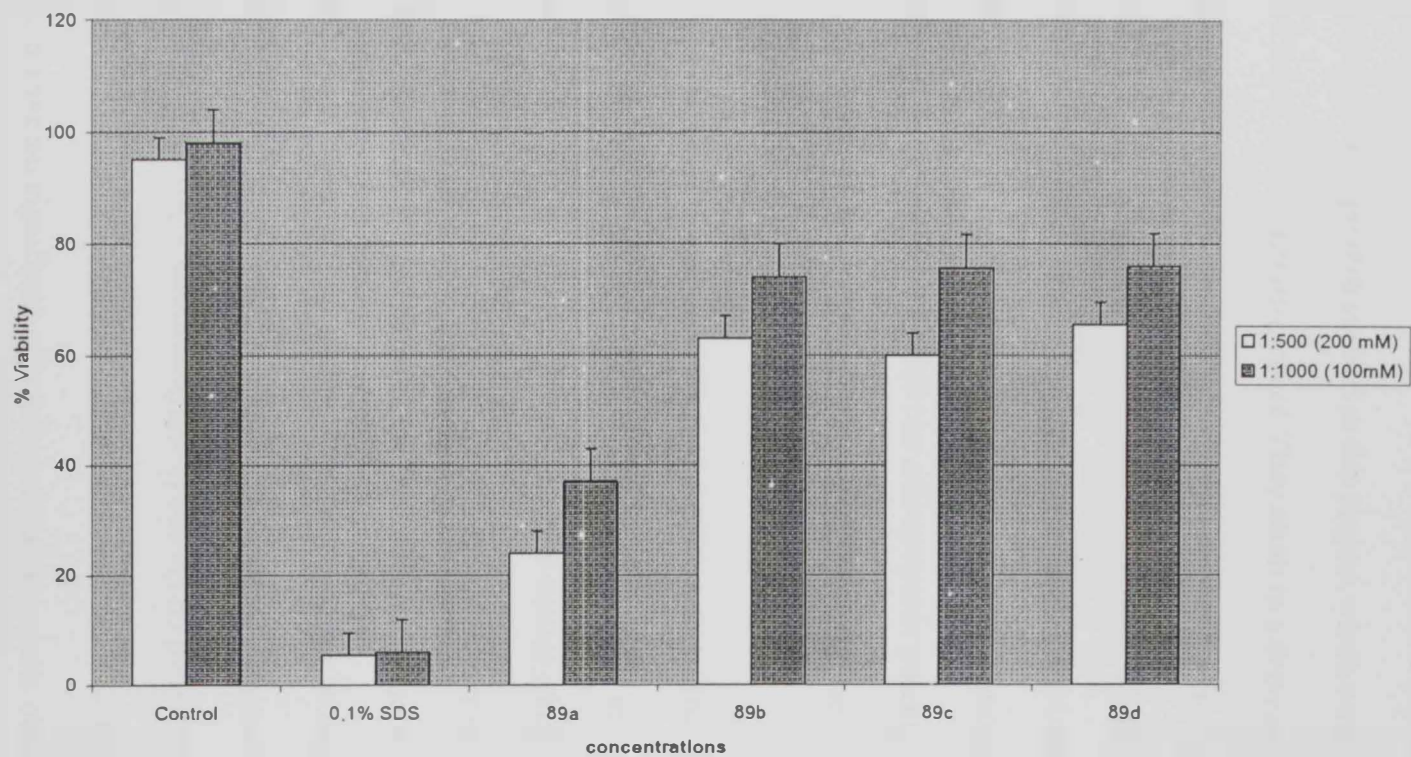


Figure 22: % Viability in HL-60 cell line treated non-nucleoside derivatives (89a-d) from MTT cell proliferation assay

4.3.2 Discussion

For a compound to act as an anti-cancer agent, it must be able to induce apoptosis. As such, in this study the ability of synthetic nucleosides analogues to induce cell death was examined. From the MTT cell proliferation assay. We showed that two of the twenty seven compounds studied in this project, which were (89a) and (85c), had the most powerful antiproliferative effect. They result in a decrease in the percentage of cell viability reaching 30% and 50% respectively. Interestingly, the rest were less effective, probably because of the difference in the structure, which affects the solubility and hence renders their uptake by the cells efficiently. Moreover, some of the nucleosides resulted in an decrease in the percentage of viability such as (85c) and (88a), which suggest that they may exert an anti-apoptotic potential, and therefore they might act as anti-neurodegenerative agents, since the key feature of these diseases is the excess in cell death.

Biological activity results established an interesting Structure-Activity Relationship (SAR). SAR of nucleosides (83a-e, 85a-e, 87a-e and 88a-d) and non-nucleosides (89a-d) showed interesting results. Different derivatives of 3-deazapyrimidine have shown different activities according to the nature of the substituents at either the 4- or 6-position of the pyridine ring. The results have shown that 2-thiophene at the 4-position has the highest activity among all analogues. In addition, the aryl groups at the 6-position have shown similar activities. For example, 4-(thiophen-2-yl)-6-phenyl-3-cyano-2(1*H*)-pyridinones (82d) and 4-(thiophen-2-yl)-6-(*p*-chlorophenyl)-3-cyano-2(1*H*)-pyridinones (82e) have shown similar activities at lower and higher concentrations. This result indicates that aryl groups at the 6-position have no significant effects based on the results obtained from the biological screening. Meanwhile, nucleosides containing the glucopyranosyl ring system showed

higher activity than the galactose isomer. For example, glucosides (83a-e) have shown better activities compared to the corresponding galactoside analogues (87a-e). Not all free nucleosides (83a-e) showed higher activity due to the solubility factor, other derivatives with low solubility showed better activity such as (89a).

Meanwhile, more interesting results were obtained from the non-nucleoside analogues (89a-d). SAR has explained these results as follows:

The solubility factor might not be the main factor because a low soluble non-nucleoside (89a) is continued to have the highest potential activity.

4.4 Conclusion

Nucleoside analogues are either purine analogues or pyrimidine analogues designed to inhibit DNA/RNA synthesis. In either case, the structures of the drugs closely resemble their natural counterparts. They are of special importance because they exhibit a wide range of biological properties, including anti-tumor potential. In order for a drug to be considered an anti-cancer agent it has to be able to destroy the cancerous cells and spare most normal cells, ideally through the mechanism of apoptosis. The synthetic nucleosides investigated (exclusively (89a) and (85c)) in this study result in a decrease in cell viability, and therefore might be considered as possible candidates to act as anti-tumor compounds. This inhibition occurs at 100 and 200 μM concentration and was detected after 24 hrs. In addition, the rest of the tested analogue showed no effect or preservation of the cells integrity, and as a result might be considered as an anti-neurodegenerative agent. These data indicate that compounds (89a) and (85c) could be considered as an effective anti-cancer. Whereas, the sugar could control the activity; the substituents at the 4-position and fluorinated benzoyl at pyridine-*N* have the most promising biological activity.

4.5 Recommendation and Future Work

In the field of nucleosides and their derivatives there has been increased focus on the design, synthesis and study of structure activity relationships (SAR). Data obtained from our work has shown that the activity has a direct relation to the substituents attached to the pyridinone ring at different positions. The procedure used to obtain these targeted products encourages us to give more attention for the synthesis of more derivatives to evaluate both of the biological activity and the undesired side effects. Interestingly, most of our studied products have shown high bioavailability and passive membrane diffusion. In fact, some of these novel synthesized nucleosides have high cytotoxic properties to most tumor cell lines *via* the enhanced apoptosis. Due to the results obtained from the structural activity relationships, the nucleoside and non-nucleoside analogues have increased our attention to further study more modified products to evaluate the biological properties.

The following will be emphasized in our future work:

- Synthesizing new derivatives with different pyridine substituents based on ribose and deoxyribose nucleosides.
- Studying QSAR, which may be ultimately be used to develop a new drug that has higher activity.
- Testing these agents on different cell lines.
- Tracking the toxic effect and elucidate the sequence of events involved in the mechanism of cell death caused by these agents.

REFERENCES

References:

- (1) Bilal A., *Medical Engineer*, 2005.
- (2) Voet D.; Voet J. G., *Fundamentals of Biochemistry*; 2nd edition; John Wiley & Sons, 2005.
- (3) Foye W. O.; Lemke T. L.; Williams D. A. Lippincott Williams & Wilkins: Media, 1995.
- (4) Chu C. K.; Baker D. C. Plenum Press: New York, 1993.
- (5) Montgomery J. A. *Medicinal Research Reviews*, 1982, 2, 271-308.
- (6) Mitsuya H.; Landes R., G. New York, 1997.
- (7) Horwitz J. P.; Chua J.; Noel M. *J. Org. Chem*, 1964, 29, 2076-2078.
- (8) Zhu X.-F. *Nucleosides, Nucleotides and Nucleic Acids*, 2000, 19, 651-690.
- (9) Simons C. Gordon and Breach: Amsterdam, 2001.
- (10) Carlos M.; Galmarini, M., D, 2002, 1, 22-32.
- (11) Ross S. R.; McTavish, D.; Faulds, D. F. *Drugs*, 1993, 45, 737-59.
- (12) Beutler E. C. *Lancet*, 1992, 340, 952-6.
- (13) McNamara D. H.; Cook, P. D. *J. Med. Chem*, 1987, 30, 340.
- (14) Ismai K.; Hosono A.; Honljo M. *Chem. Pharm. Bull*, 1966, 14, 1377.
- (15) Onodera K.; Hirano S. F. *Agr. Biol. Chem.*, 1964, 28, 173.
- (16) Nishimura T. S. *Chem. Pharm. Bull*, 1963, 11, 1470.
- (17) Onodera K.; Hirano S.; Fukumi H. *Agr. Biol. Chem.*, 1964, 28, 173.
- (18) Caorton B. S.; Ravel J. M.; Shive W. *J. Bio. Chem.*, 1957, 233, 331.
- (19) Montgonmery J. A.; Hewson K. *J. Med. Chem.*, 1966, 9, 105.
- (20) Khwaja T., A.; Kigwana L.; Meyer R., B.; Robins R., K. *Proc. Am. Assoc. Cancer Res*, 1975. 16, 162.

- (21) Simon L., N.; Sidwell R. W.; Robins R. K. *J. Am. Chem. Soc.*, **1975**, *97*, 2916.
- (22) Galmarini C. M.; Mackey J. R.; Dumontet C. *The Lancet Oncology*, **2002**, *3*, 415-424.
- (23) Galmarini C. M.; Mackey J. R.; Dumontet C. *Leukemia*, **2001**, *15*, 875-90.
- (24) Gluecksmann A. *Biological Reviews*, **1951**, *26*, 59-86.
- (25) Lockshin R. A.; Zakeri Z. *Nat. Rev. Mol. Cell Biol.*, **2001**, *2*(7), 545-50.
- (26) Lockshin R. A.; Williams C. M. *J Insect. Physiol.*, **1964**, *10*, 643-649.
- (27) Kerr J. F.; Wyllie, A. H.; Currie A. R. *Br. J. Cancer*, **1972** *26*(4), 239-57.
- (28) Saraste, A.; Pulkki, K. *Cardiovasc. Res.*, **2000**, *45*(3), 528-37.
- (29) Letai A.; Bassik M. C.; Walensky L. D.; Sorcinelli M. D.; Weiler S.; Korsmeyer S. J. *Cancer Cell*, **2002**, *2*(3), 183-92.
- (30) Beck W. T.; MO Y. Y.; Bhat U. G. *Biochem. Soc. Trans*, **2001**, *29*, 702-703.
- (31) Larsen A. K.; Escargueil A. E.; Skladanowski A. *Prog. Cell Cycle. Res.*, **2003**, *5*, 295-300.
- (32) Van Der Kolk D. M.; De Vries E. G.; Muller M. *Leuk. Lymphoma*, **2002**, *43*, 685-701.
- (33) Kluck R. M.; Bossy-Wetzel E.; Green D. R. *Science*, **1997**, *275*, 1132-1136.

APPENDIXES

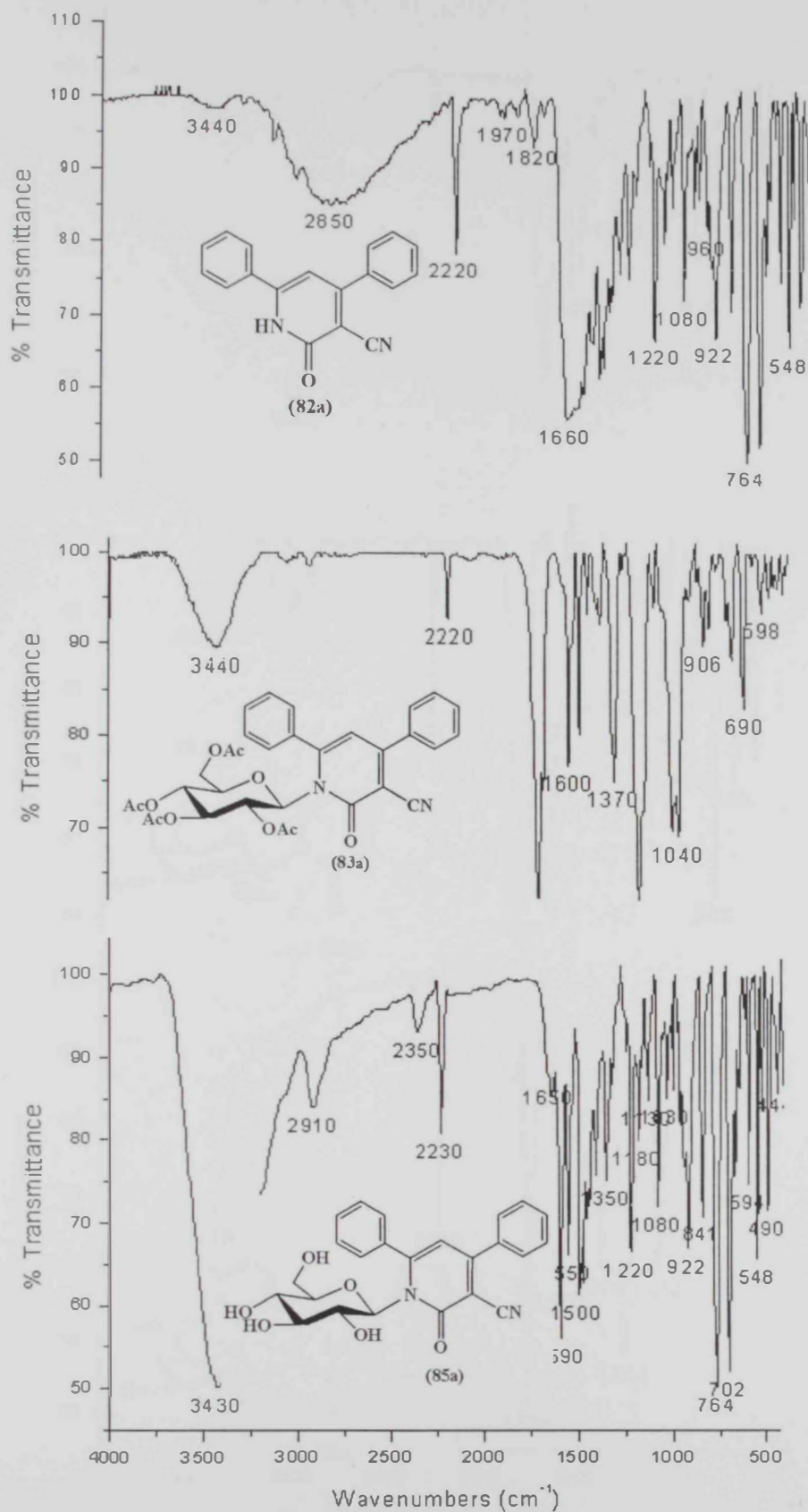


Figure 23: Infrared spectra for (82a), (83a) and (85a)

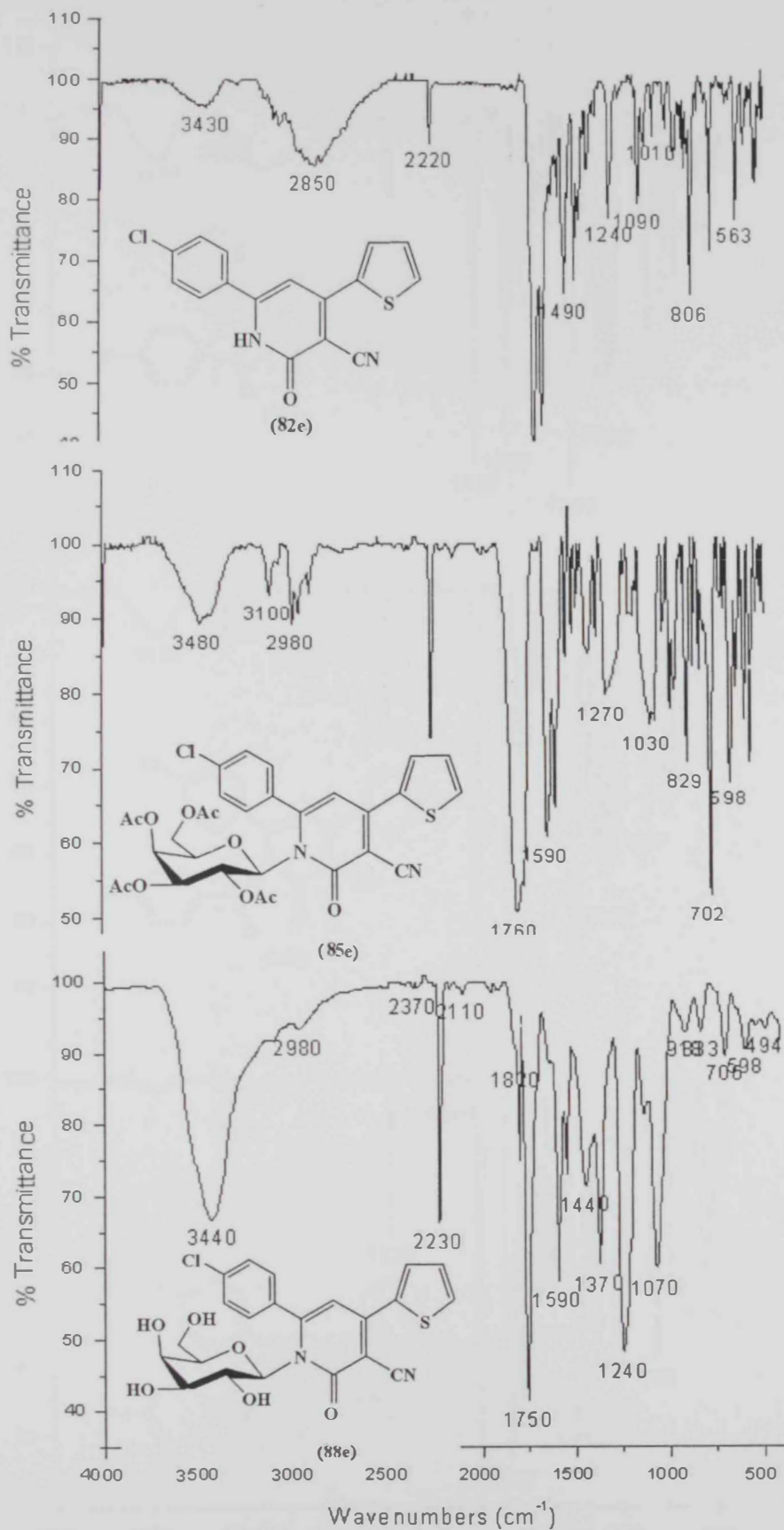


Figure 24: Infrared spectra for (82e), (87e) and (88e)

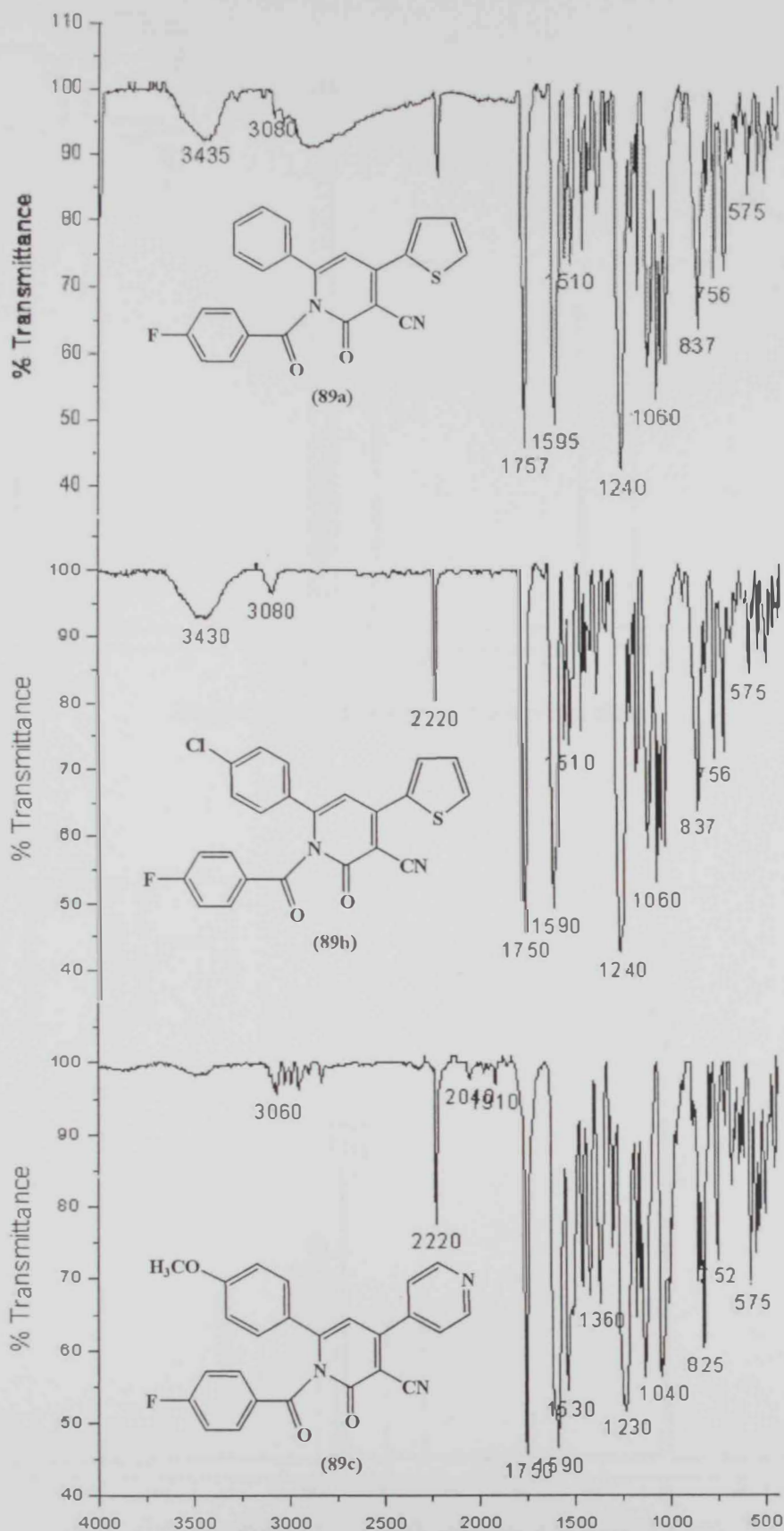


Figure 25: Infrared spectra for (89a), (89b) and (89c)

STANDARD IN ORNREP
 EXPI 02/01

```

SAMPLE
date Aug 10 2004 8:00 SPECIAL
solvent DMSO d6
file
ACQUISITION exp 001
sw 523.0 MHz
mf 12.500
fl 15.00
dl 1.000
ml 1.000
st 00
TRANSMITTE
sa 280.035
sf 250.0
sp 3201.0
sq 400.0
sv 6.820
DECOUPLER
ds 133
df 0
dm 100
dl 36
df 0.500
  
```

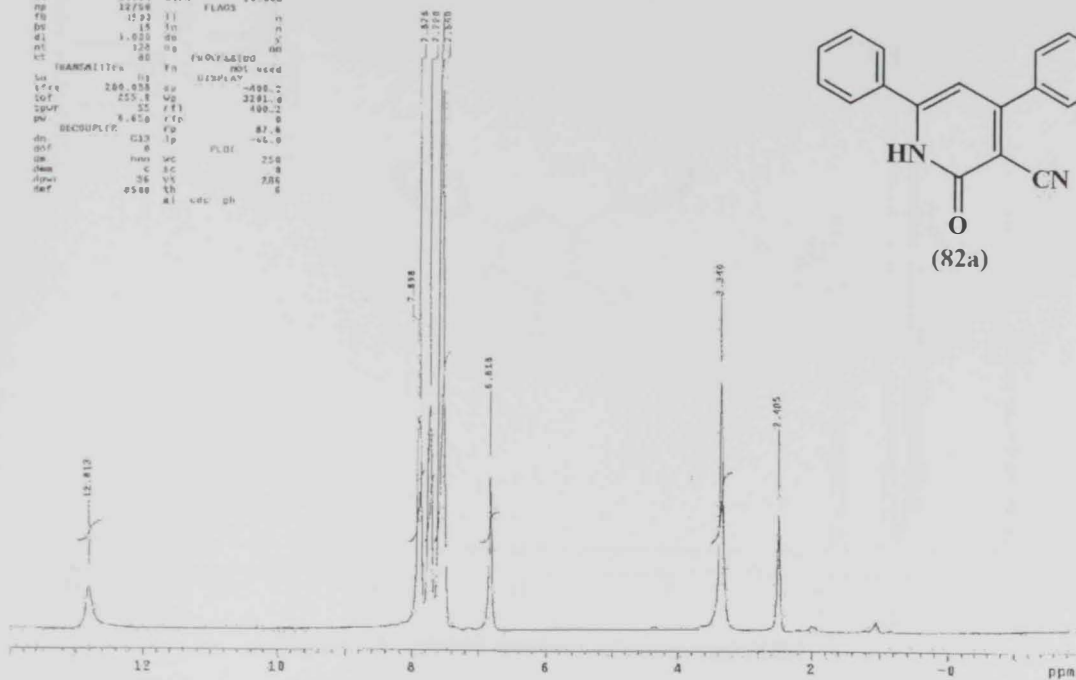


Figure 26: ¹H NMR spectrum of compound (82a)

13C OBSERVE

```

exp1 st413c
SAMPLE
date Aug 10 2004 8:00 DEC. 4 VT 200 05E
solvent DMSO d6
file
ACQUISITION exp 001
sw 125.760 MHz
mf 125.760
fl 15.00
dl 1.000
ml 1.000
st 00
PROCESSED
sa 125.760
sf 100.625
sp 15000.0
sq 100.0
sv 14.00
DECOUPLER
ds 133
df 0
dm 100
dl 36
df 0.500
  
```

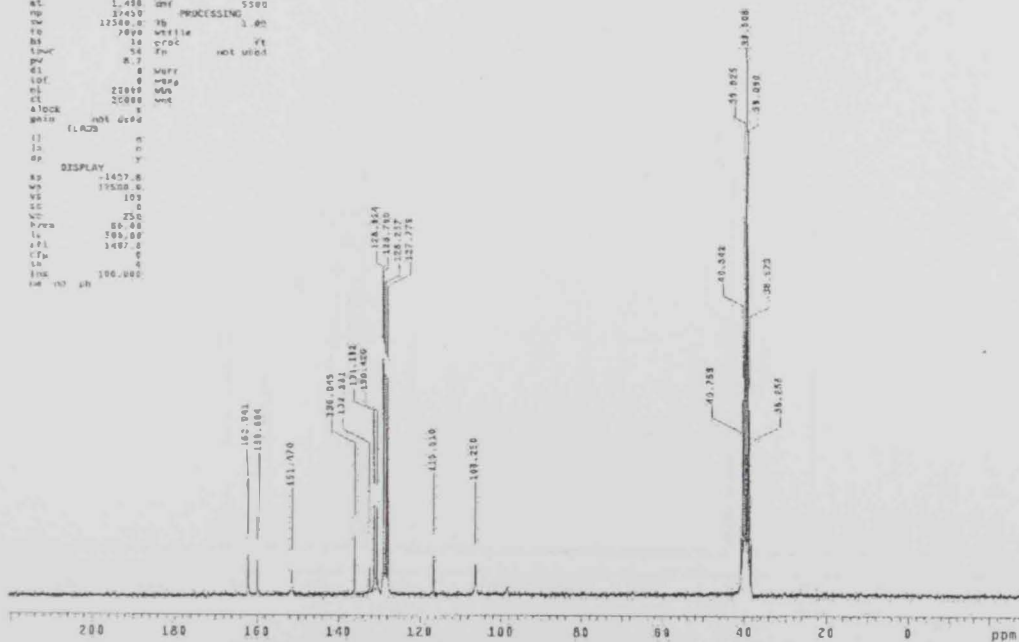
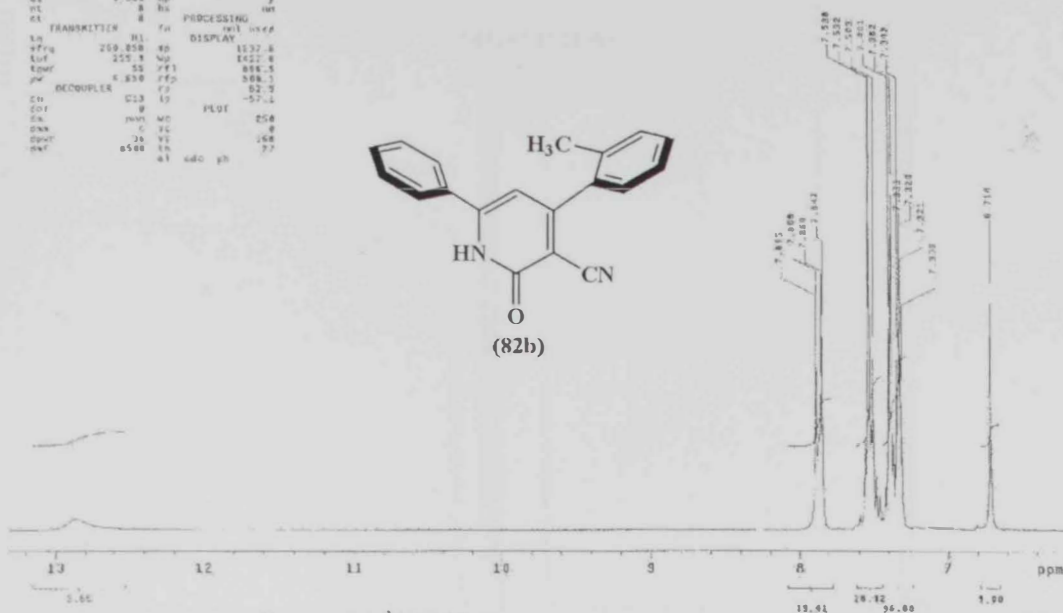
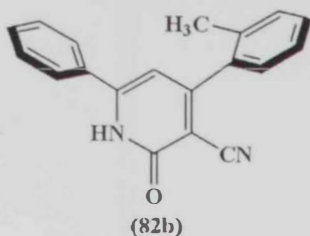


Figure 27: ¹³C NMR spectrum of compound (82a)

STANDARD IN OBSERVE

ANAL #2011

SAMPLE		SPECIAL	
DATE	MAY 14 2003	TEMP	301.500
COLLECT	0630	PH	7.7
TITLE		PROB	1H
ACQUISITION	649	SPIN	20
NUC1	13C	NUC2	13C
NUC2	13C	FLDS	20.000
TD	13768		
RG	1600		
GC	16		
HL	1.800		
HT	8		
KA	8		
TRANSMITTER		PROCESSING	
LO	125.760	FM	0.100
RF	250.130	DISP	0
NUC1	13C		
NUC2	13C		
PR	4.830		
DECOUPLER		PLOT	
LO	125.760		
RF	250.130		
NUC1	13C		
NUC2	13C		
PR	4.830		



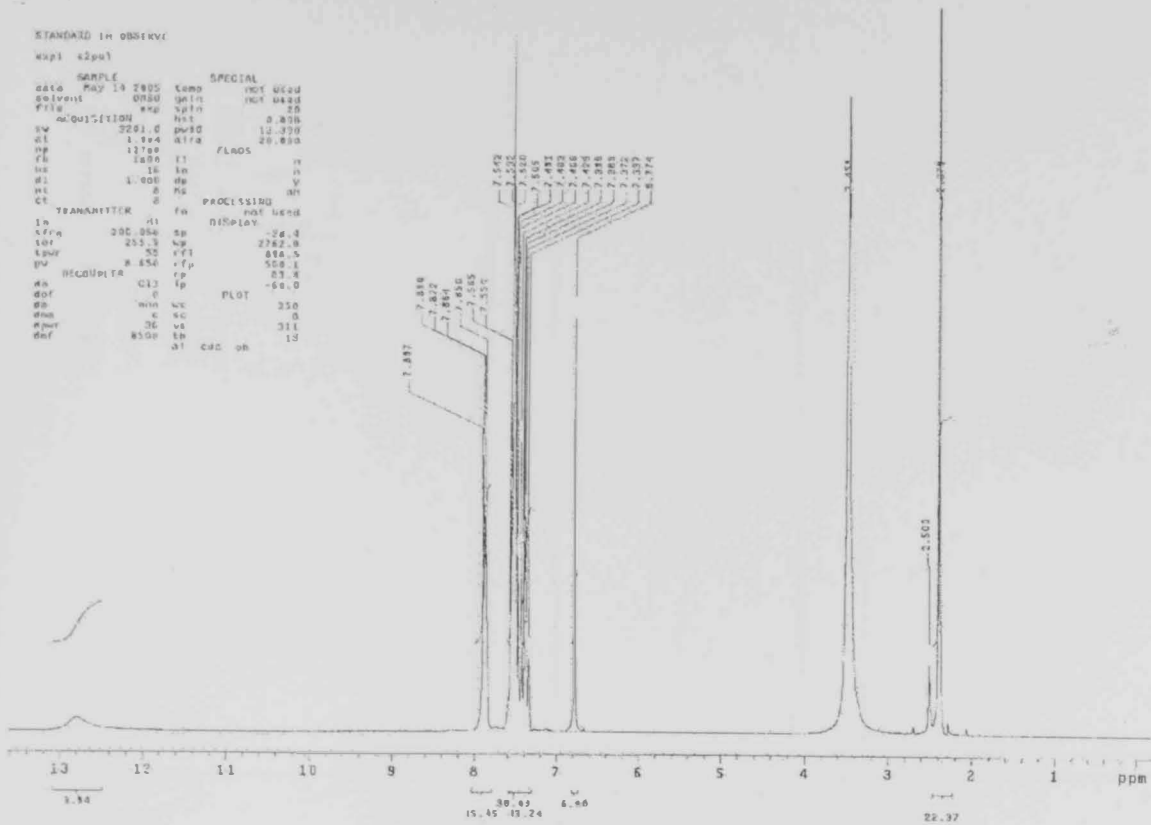


Figure 30: ¹H NMR spectrum of compound (82c)

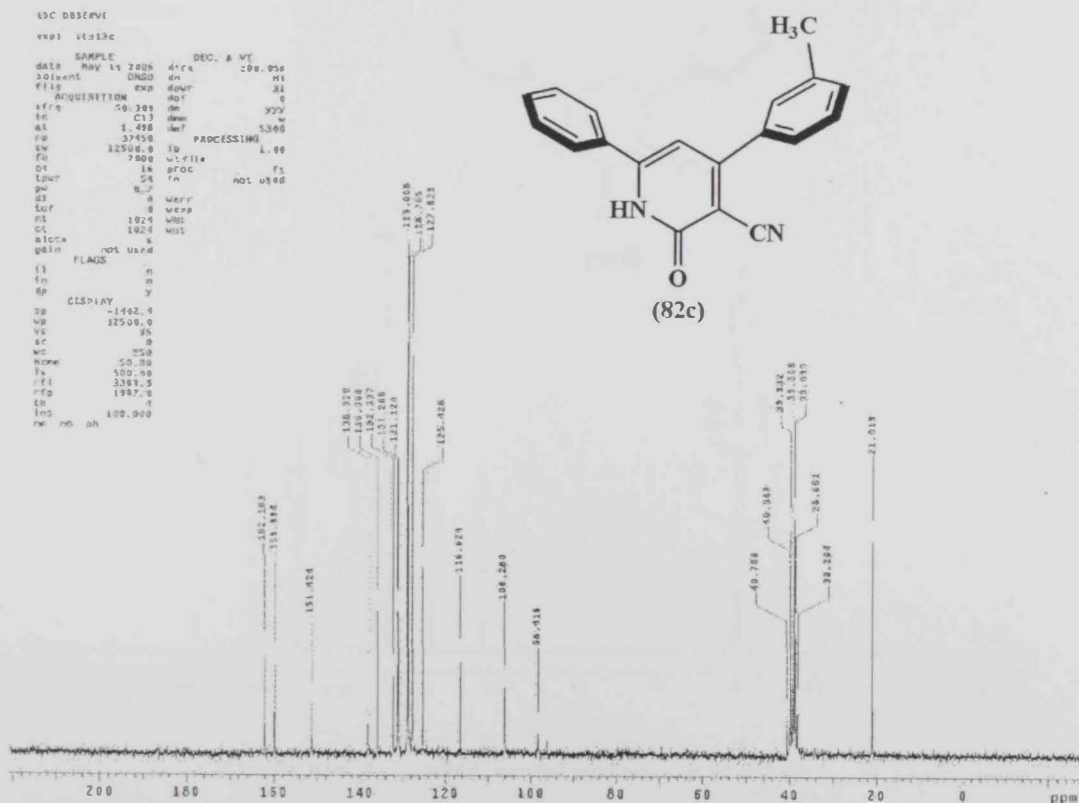


Figure 31: ¹³C NMR spectrum of compound (82c)

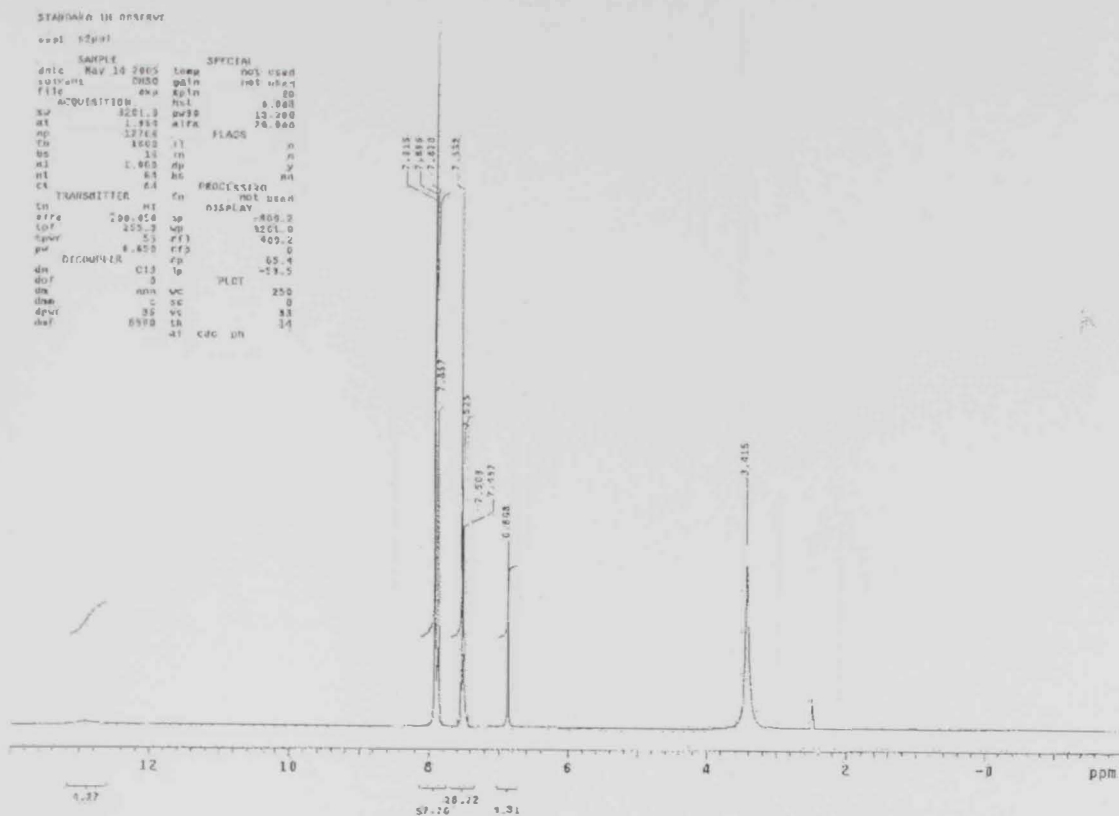


Figure 36: ^1H NMR spectrum of compound (82f)

390 OBSERVE

Pulse Sequence: g2p1

solvent: DMSO

Acquire: Lumberator

Mercury: 13 "mercury203"

Pulse 25.7 degrees

Acq. time 1.495 sec

width 12500 Hz

25790 resolutions

OBSERVE: c13, 51.5849200 MHz

BLUDDING: ht, 248.8974634 MHz

Power: 33 dB

Channel(s) on

VALF2: 16 calculated

LINE PROCESSING: 1.4 Hz

11 sine 0.5536

Total time 46 hr, 44 min, 15 sec

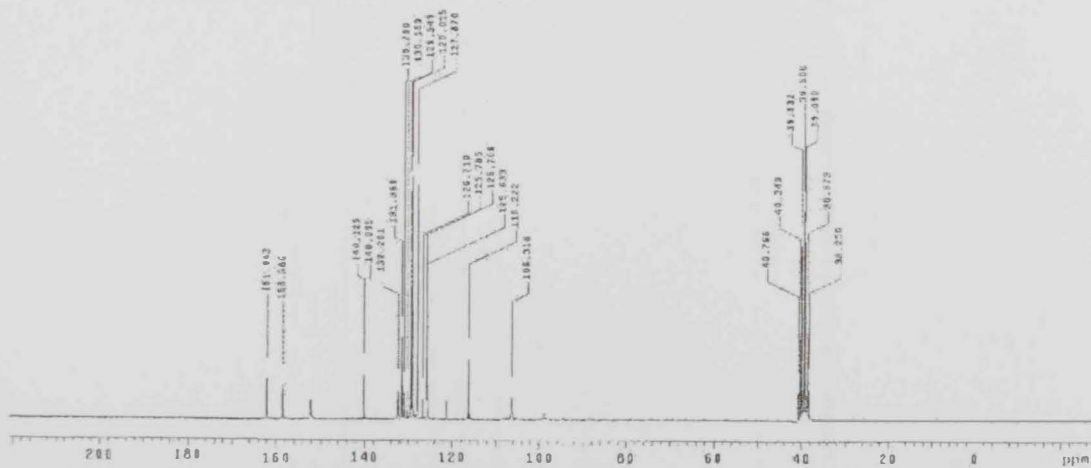
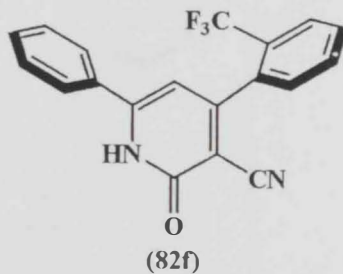


Figure 37: ^{13}C NMR spectrum of compound (82f)

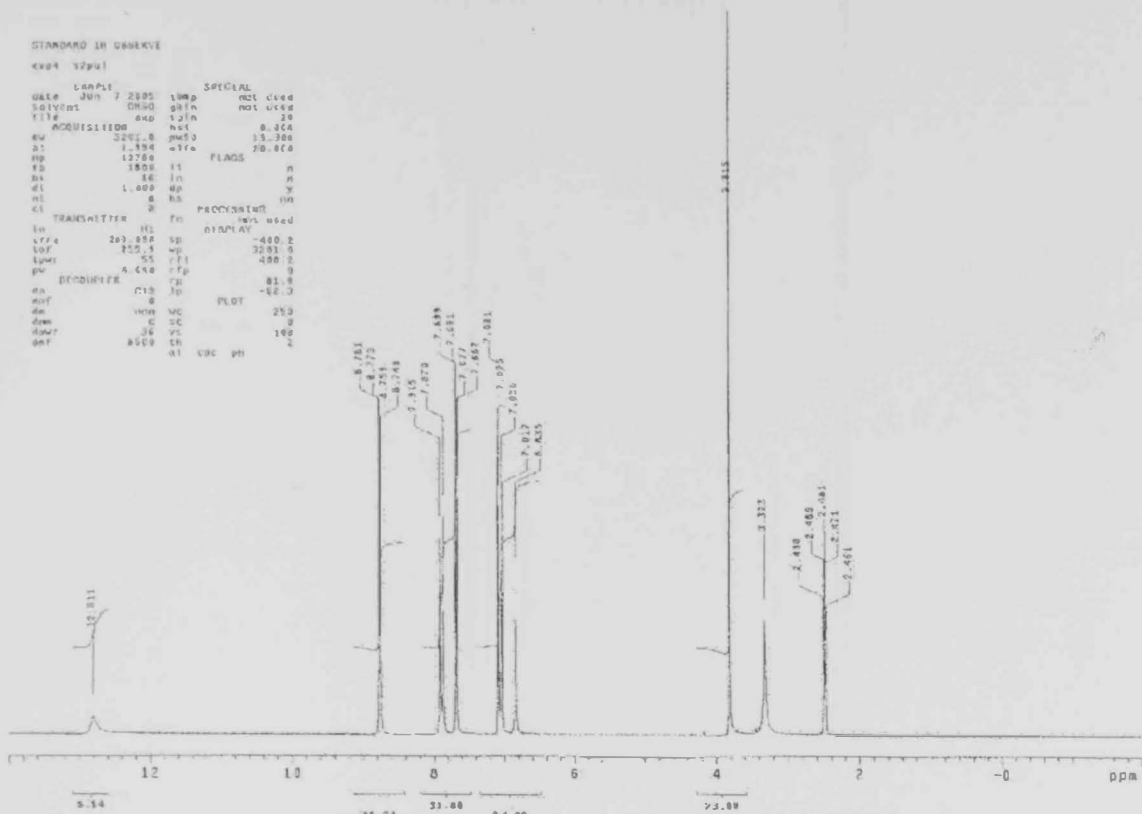


Figure 38: ¹H NMR spectrum of compound (82g)

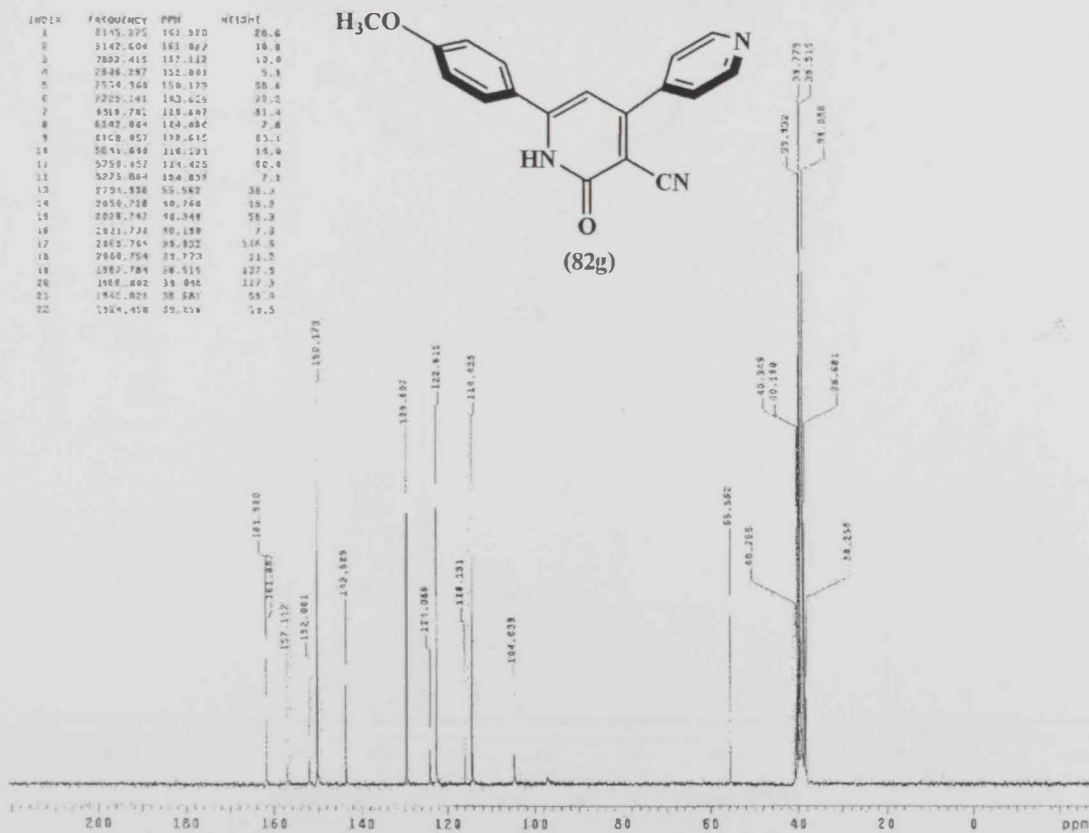


Figure 39: ¹³C NMR spectrum of compound (82g)

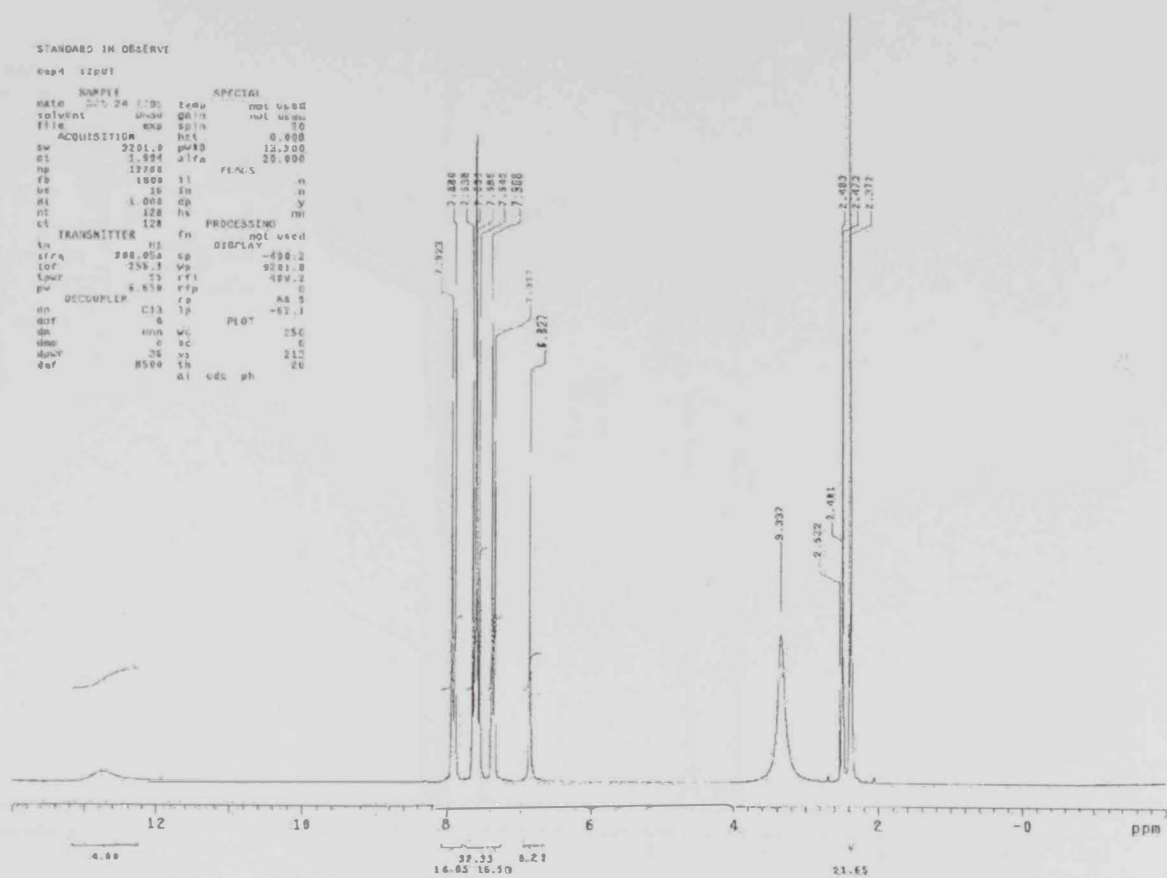


Figure 40: ¹H NMR spectrum of compound (82h)

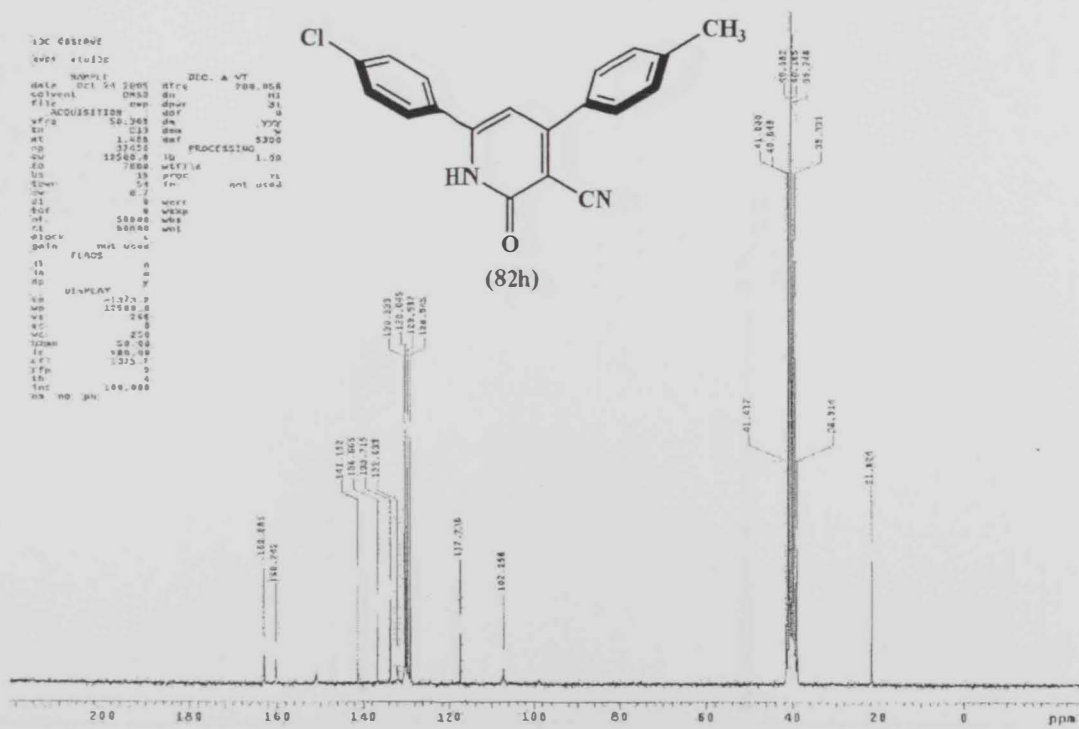


Figure 41: ¹³C NMR spectrum of compound (82h)

o-toluidinaldehyde nucleoside

expt 62pw1

```
SAMPLE SPECIAL
Date Oct 4 1984 10ap not used
Solvent CDCl3 galn not used
File ACQUISITION exp galn not used
sw 370.0 pps 9.480
af 1.334 alfa 20.800
rg 17.00
f2 1000 f1
ds 16 ln
af 1.025 dp
rt 32
ct 32
```

```
TRANSMITTER fn
ln HI not used
sf 700.057 sp
sf 251.0 sp
tpr 6.650 rfp
pv 8.013 rfp
de 8.402 rfp
dco 8.595 rfp
dco 8.727 rfp
dco 8.850 rfp
dco 8.983 rfp
```

```
DECOUPLER C13
ln HI
sf 8500 sp
sf 8500 sp
sf 8500 sp
sf 8500 sp
```

```
PLOT
ln HI
sf 250 sp
sf 140 sp
sf 6 cad ph
```

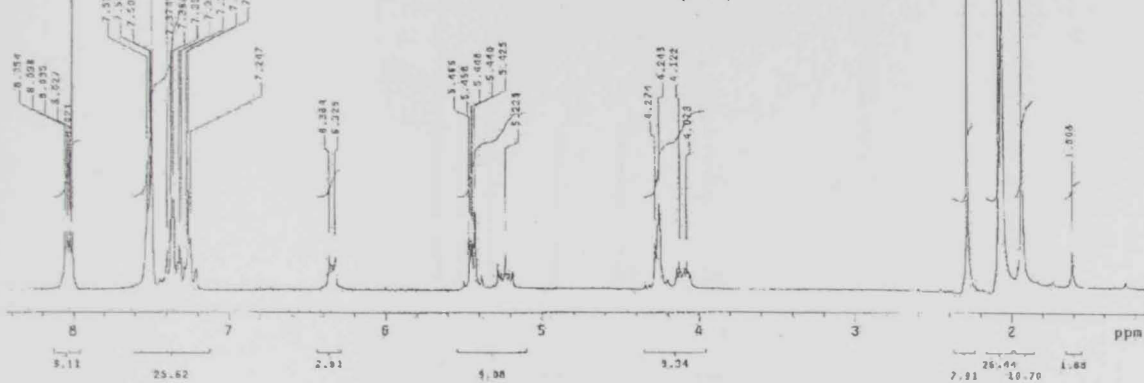
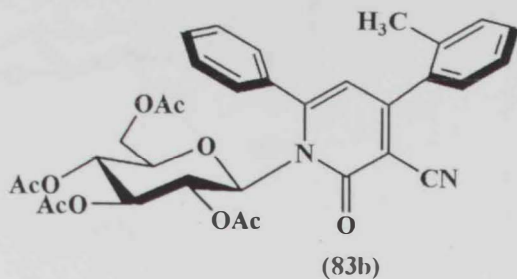


Figure 46: ¹H NMR spectrum of compound (83b)

o-toluidinaldehyde nucleoside 2

expt 37pm1

```
SAMPLE SPECIAL
Date Oct 6 1984 10ap not used
Solvent CDCl3 galn not used
File ACQUISITION exp galn not used
sw 12576.8 pps 14.682
af 1.188 alfa 22.680
rg 32000
f2 1000 f1
ds 60 ln
af 1.020 dp
rt 31800
ct 31800
```

```
TRANSMITTER ln
ln HI not used
sf 70.313 sp
sf 251.0 sp
tpr 7.880 rfp
pv 8.013 rfp
de 8.402 rfp
dco 8.595 rfp
dco 8.727 rfp
dco 8.850 rfp
dco 8.983 rfp
```

```
DECOUPLER C13
ln HI
sf 8500 sp
sf 8500 sp
sf 8500 sp
sf 8500 sp
```

```
PLOT
ln HI
sf 250 sp
sf 140 sp
sf 6 cad ph
```

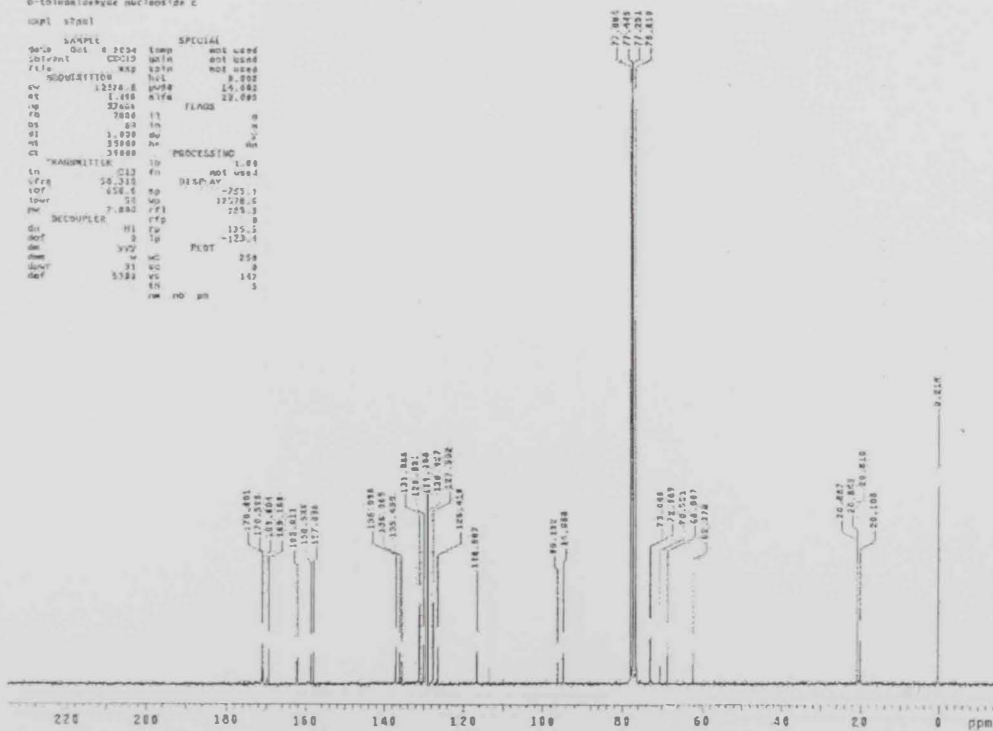


Figure 47: ¹³C NMR spectrum of compound (83b)

(4) on nucleoside
 exp1 02.u)

SAMPLE		SPECIAL	
date	Sep 15 2004	time	not used
solvent	CDCl3	gain	not used
file	exp	spin	20
PCOINTEGRATION	list	int	0.000
av	3201.0	gwnb	13.000
at	1.394	atfa	20.000
no	12761	flags	
fn	1800	fl	n
bu	10	in	n
dl	1.000	dp	y
nl	32	nt	n
cl	33	pr	n
TRANSMITTER	hi	fn	not used
in	MI	DISPLAY	
freq	250.057	sp	-400.0
tdf	255.0	vp	2201.0
tdw	55	rfl	400.0
pw	0.050	rff	0
DECOUPLER	fr	flp	52.0
dn	C13	lp	-14.2
dot	0	pl	
dm	nmn	WC	250
dmw	C	SC	C
dmw2	31	VS	30
dmw3	0500	LN	0
dmw4	at	cdc	ah

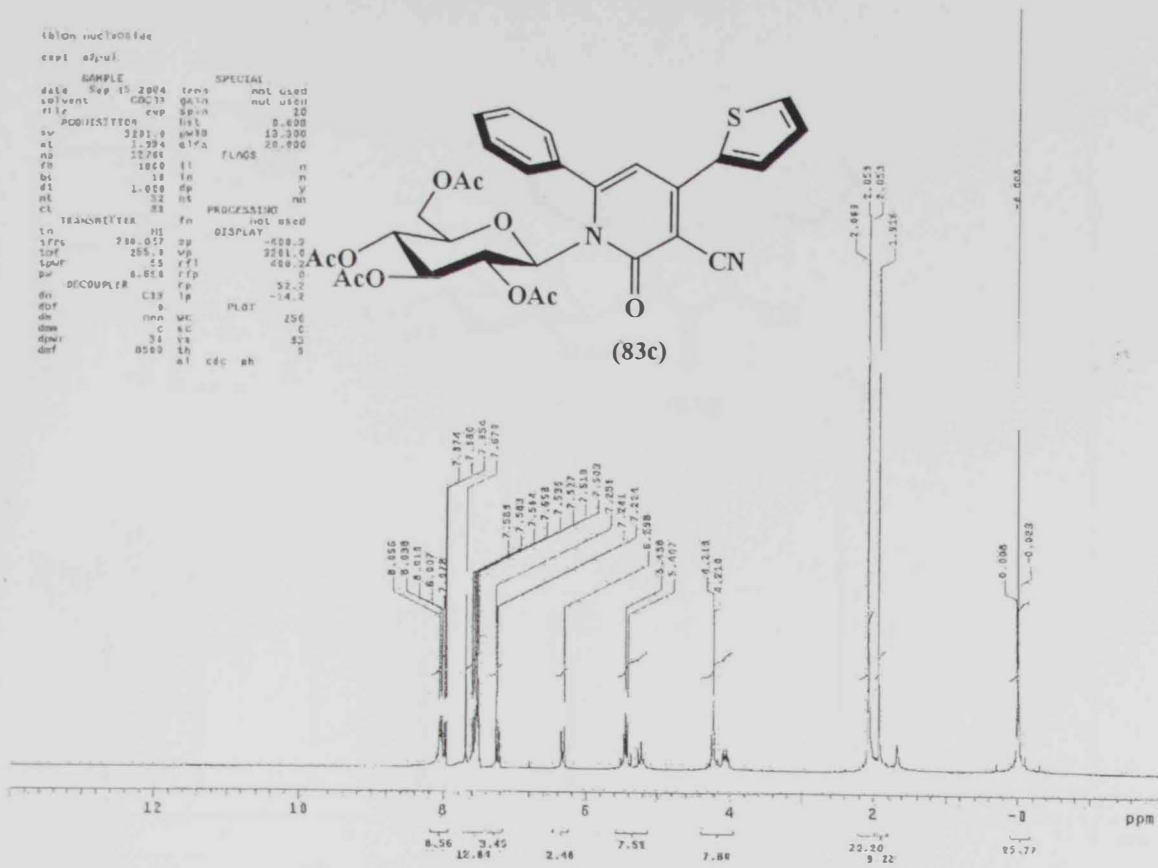
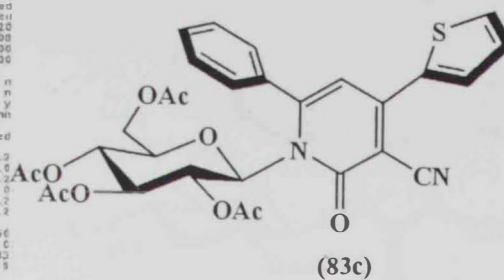


Figure 48: ¹H NMR spectrum of compound (83c)

C13 - thioinos

SAMPLE		SPECIAL	
date	Dec 14 2004	time	not used
solvent	CDCl3	gain	not used
file	exp	spin	not used
PCOINTEGRATION	list	int	0.000
av	11576.0	gwnb	64.000
at	1.498	atfa	70.000
no	37000	flags	
fn	7800	fl	n
bu	64	in	n
dl	1.000	dp	y
nl	30000	nt	n
cl	30000	pr	n
TRANSMITTER	hi	fn	not used
in	C13	DISPLAY	
freq	50.310	sp	-767.0
tdf	654.5	vp	11074.0
tdw	54	rfl	167.0
pw	7.000	rff	0
DECOUPLER	fr	flp	105.0
dn	8	lp	-100.4
dot	0	pl	
dm	970	WC	250
dmw	31	SC	C
dmw2	0300	VS	40
dmw3	1/4	LN	0
dmw4	at	cdc	ah

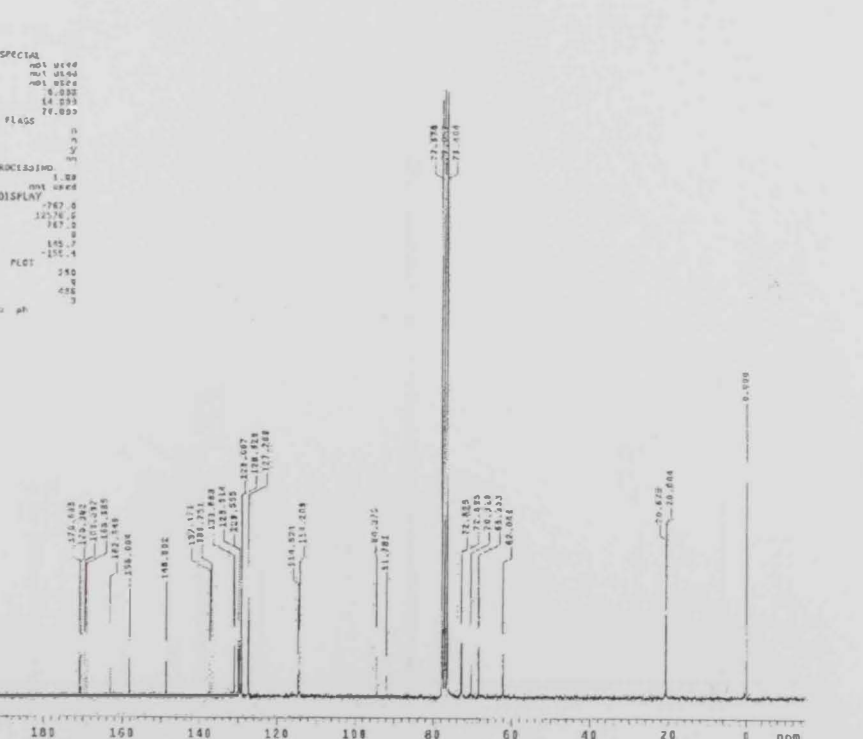


Figure 49: ¹³C NMR spectrum of compound (83c)

STANDARD IN OBSERVE

exp4 s7pat

NAME		SPECIAL	
DATE	SEP 27 2005	TEMP	NOT USED
SOLVENT	CDCl3	QAC	NOT USED
F1A	400	SPL	20
ACQUISITION			
EV	2201.0	NUC1	13.000
AS	1.194	ATYA	70.000
RF	10.746	FLABS	
LS	1820	TA	N
LS	10	IN	N
CL	1.000	DP	V
CL	120	HS	NH
CL	120	PROCS	NH
TRANSMITTER			
IN	H1	FN	NOT USED
DISPLAY			
OFF	100.000	SP	-57.7
LOF	255.0	HP	1854.7
LPW	55	FF1	400.2
PO	0.650	RF	0
DECODER			
DN	D15	RP	65.7
DR	0	TP	-68.0
DA	NON	WC	250
DB	C	CC	0
DPW	30	SS	50
DEF	8500	TH	0
	AL	CFC	PH

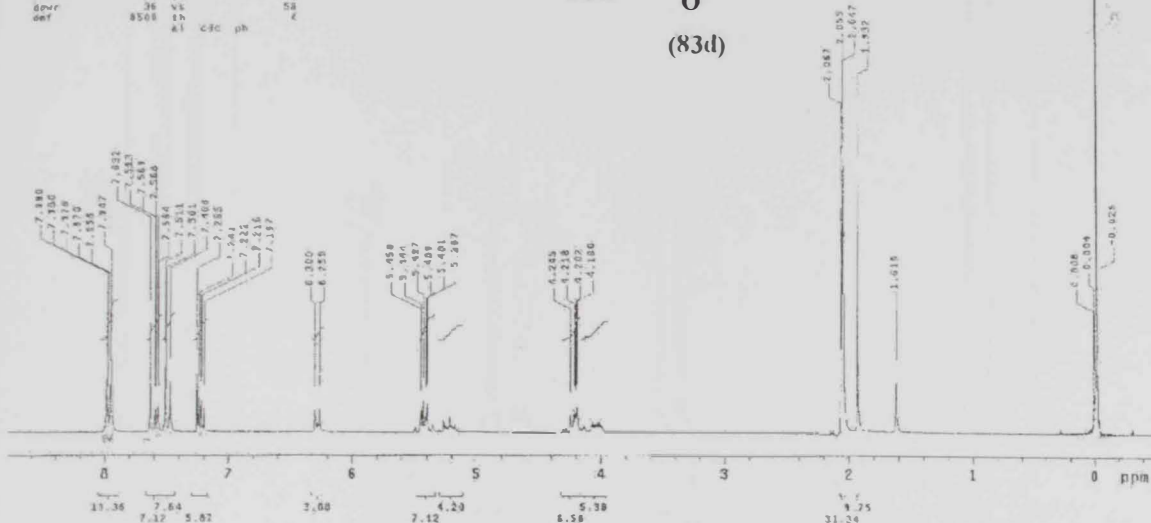
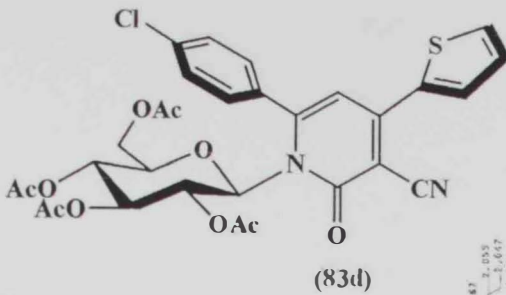
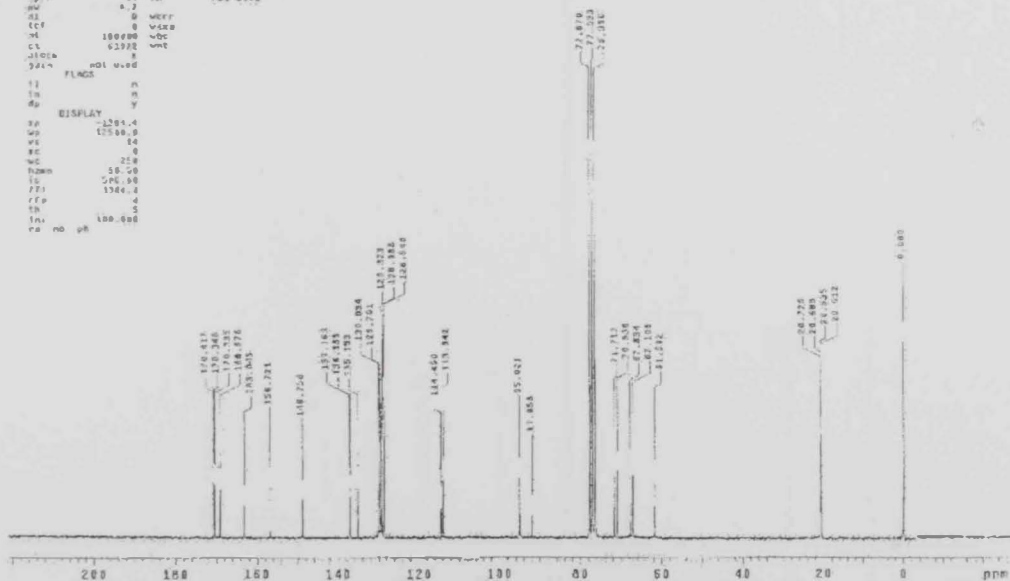


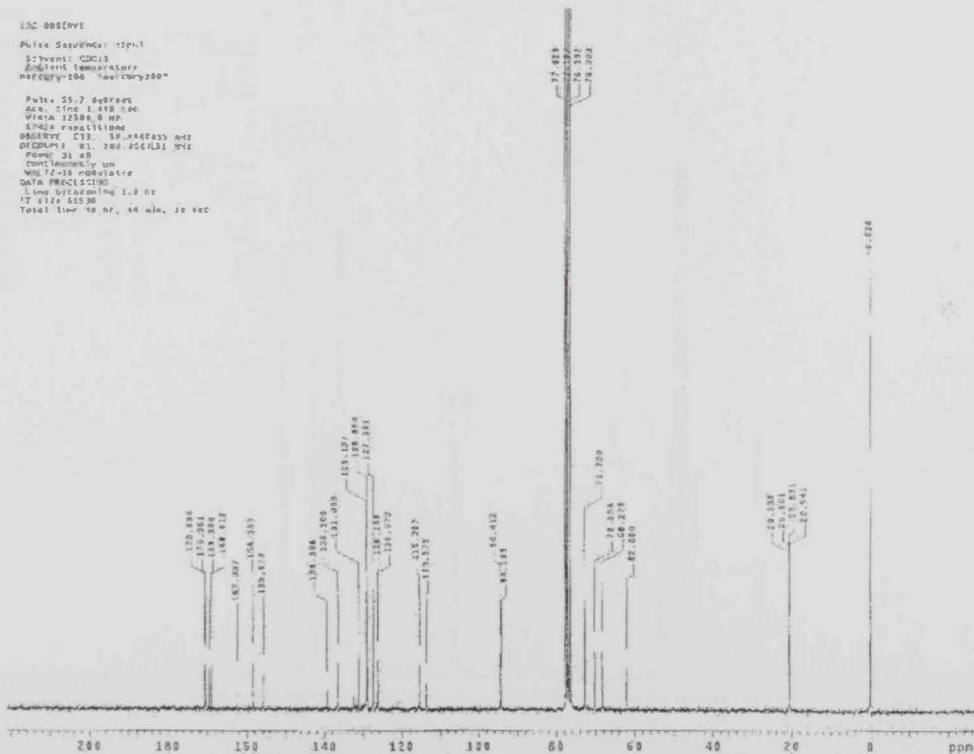
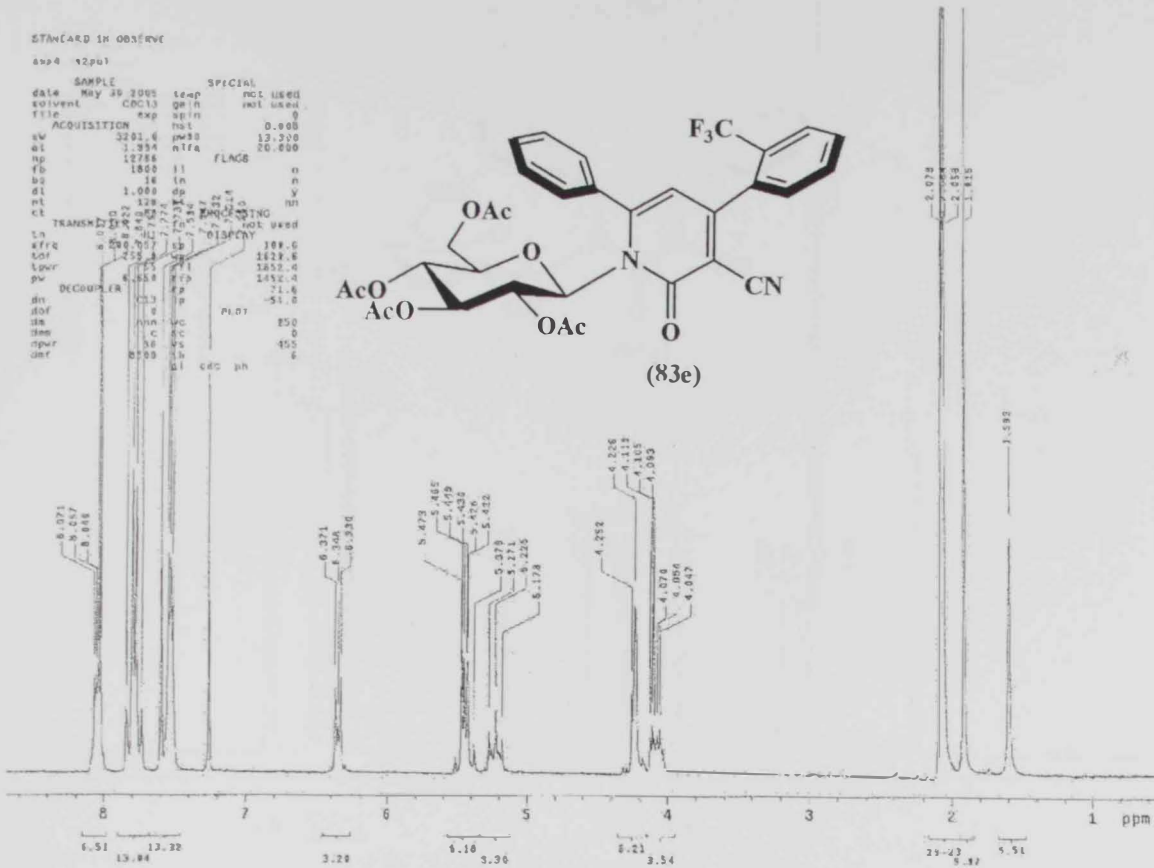
Figure 50: ¹H NMR spectrum of compound (83d)

13C OBSERVE

exp4 s7pat

SAMPLE		DEC. 4 V1	
DATE	SEP 26 2005	OFF	200.000
SOLVENT	CDCl3	ON	11
F1A	400	OFF	0
ACQUISITION			
EV	10.100	DN	3300
AS	1.194	ATYA	70.000
RF	10.746	FLABS	
LS	1820	TA	N
LS	10	IN	N
CL	1.000	DP	V
CL	120	HS	NH
CL	120	PROCS	NH
TRANSMITTER			
IN	H1	FN	NOT USED
DISPLAY			
OFF	100.000	SP	-57.7
LOF	255.0	HP	1854.7
LPW	55	FF1	400.2
PO	0.650	RF	0
DECODER			
DN	D15	RP	65.7
DR	0	TP	-68.0
DA	NON	WC	250
DB	C	CC	0
DPW	30	SS	50
DEF	8500	TH	0
	AL	CFC	PH





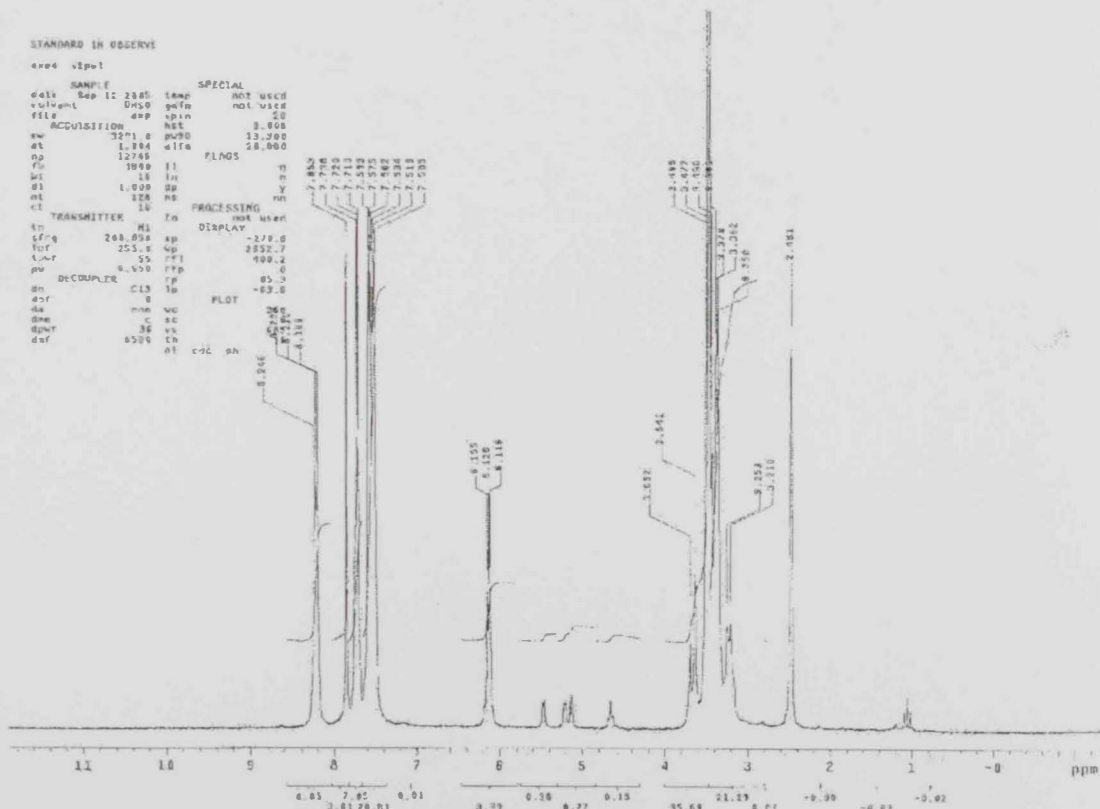
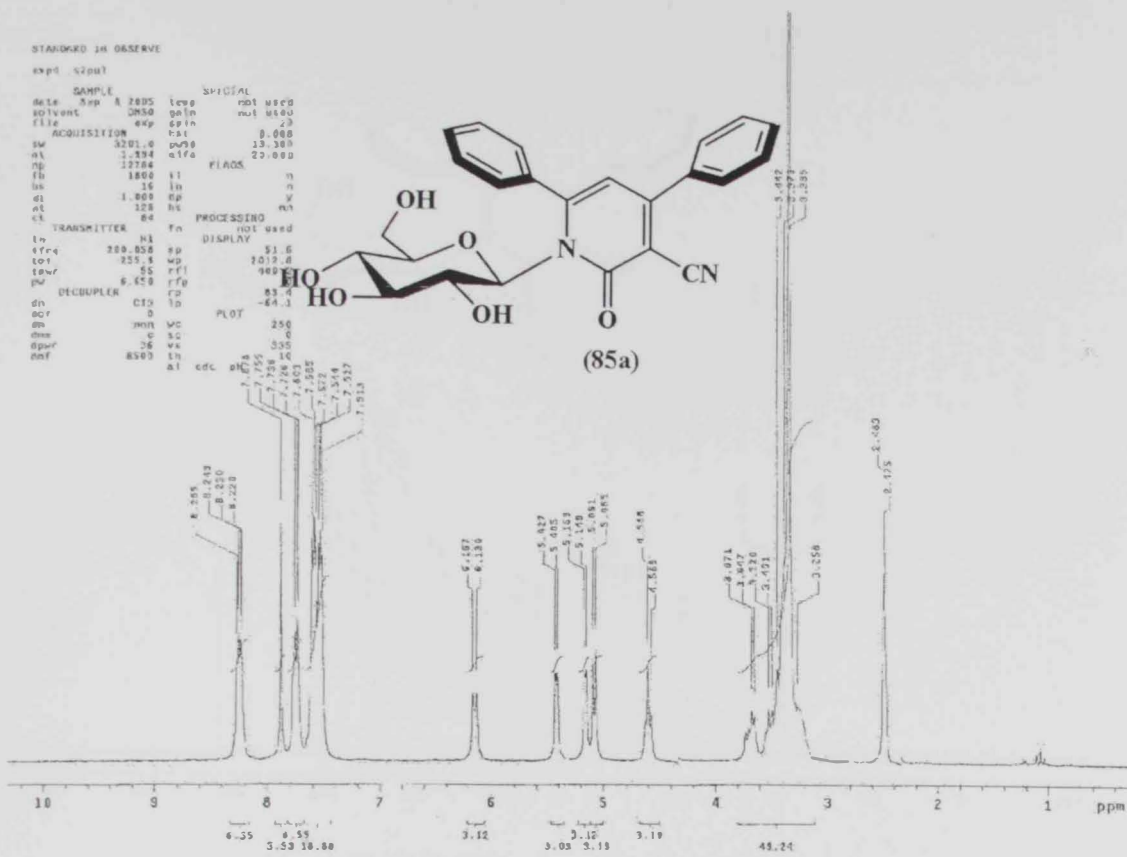


Figure S4: ^1H NMR spectrum of compound (85a) $\text{DMSO-}d_6$ & D_2O

13C NMR
 Pulse Sequence: zgpg30
 Solvent: DMSO
 Shift: 400.136 MHz
 Frequency: 125.762 MHz
 Power: 21.83
 Continuity on
 WALTZ-16 modulated
 DATA PROCESSING
 Line broadening 1.8 Hz
 FT size 65536
 Total time 23 hr, 22 min, 8 sec

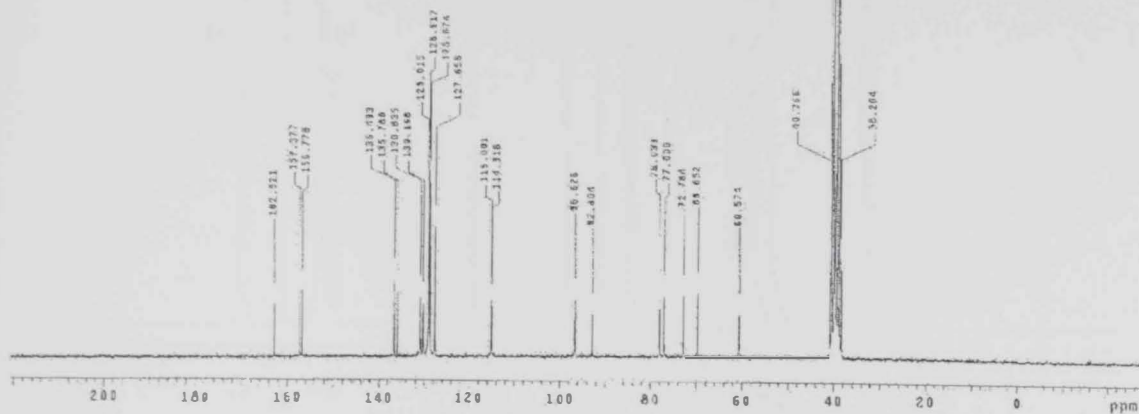
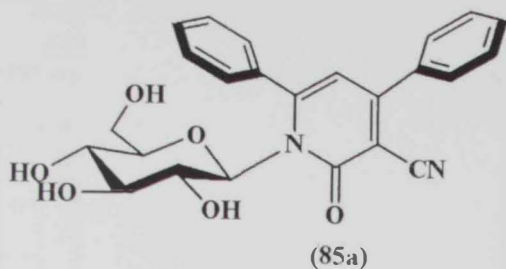


Figure 55: ¹³C NMR spectrum of compound (85a)

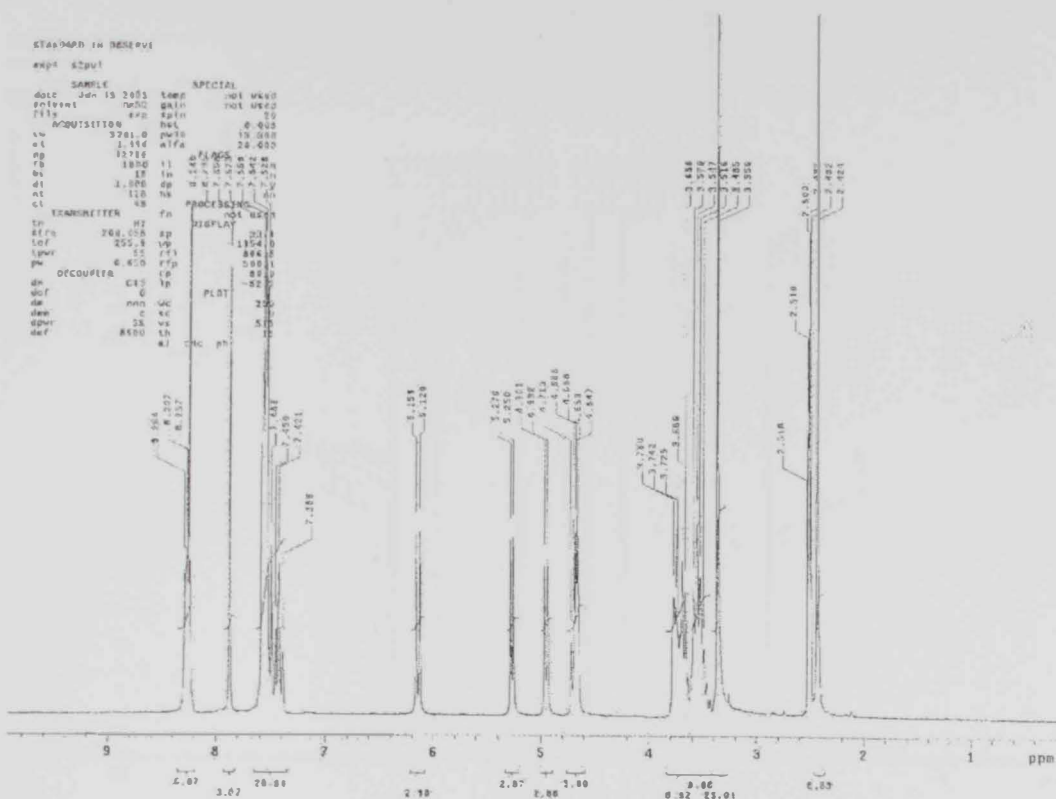


Figure 56: ^1H NMR spectrum of compound (85b)

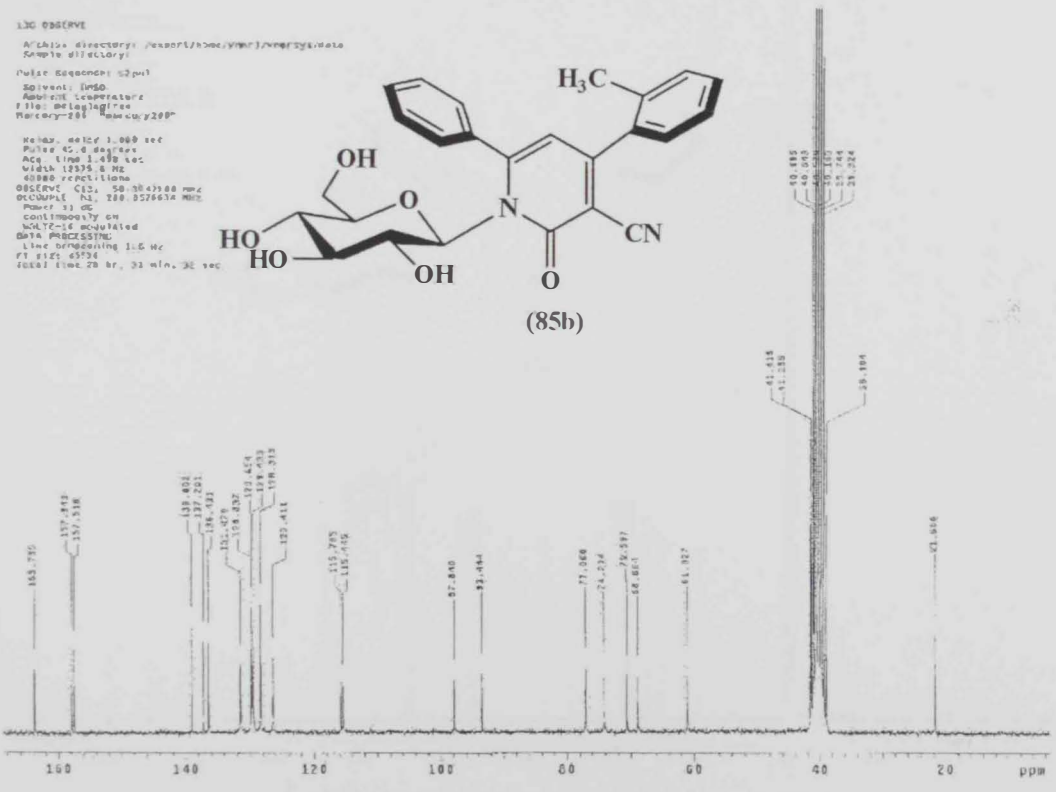


Figure 57: ^{13}C NMR spectrum of compound (85b)

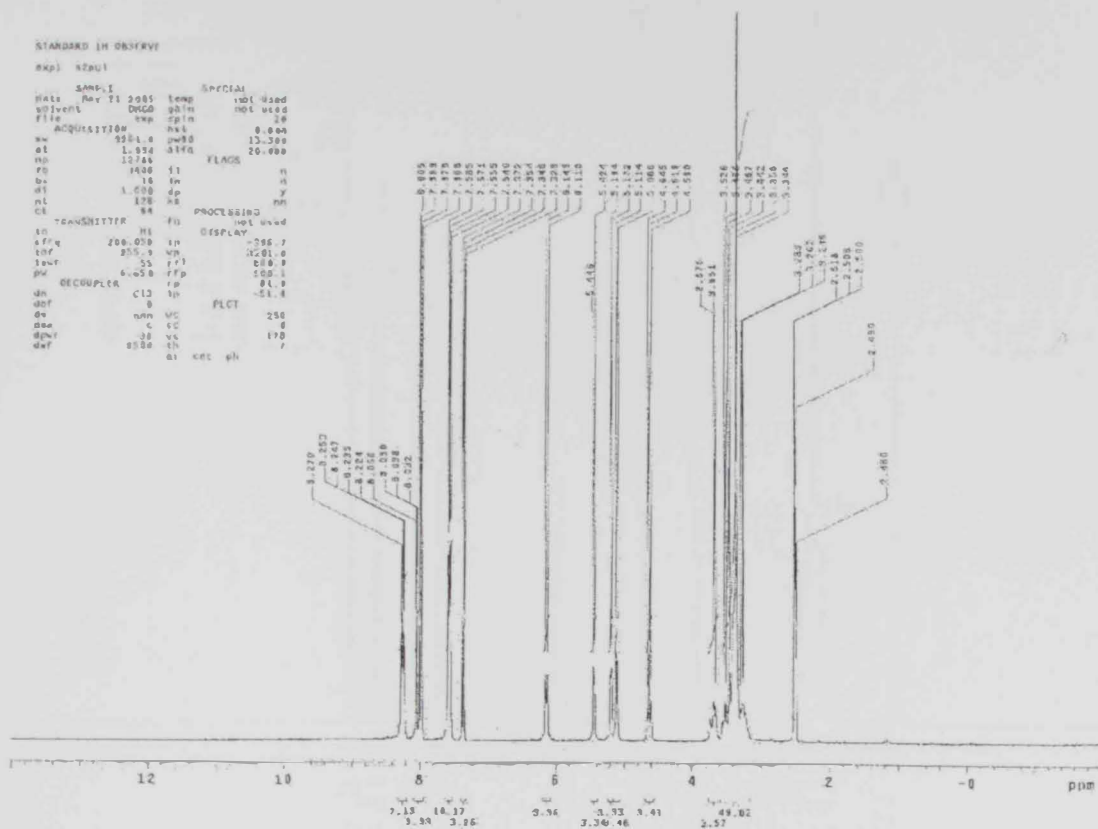


Figure 58: ¹H NMR spectrum of compound (85c)

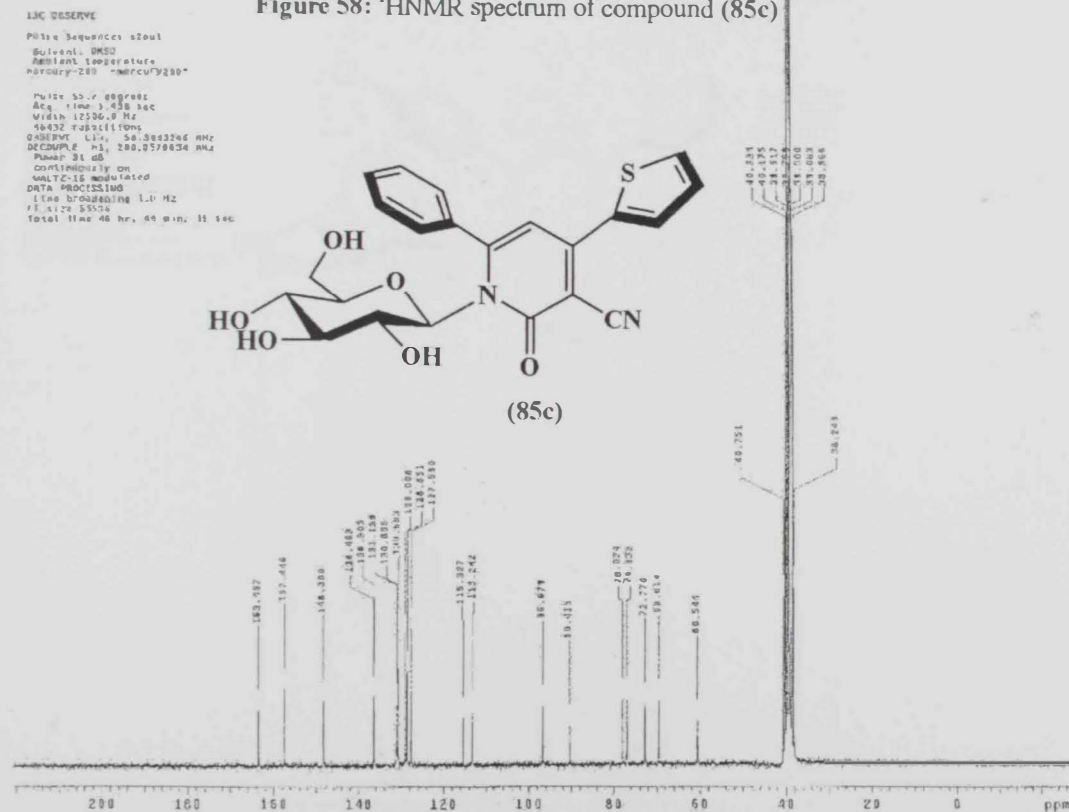


Figure 59: ¹³C NMR spectrum of compound (85c)

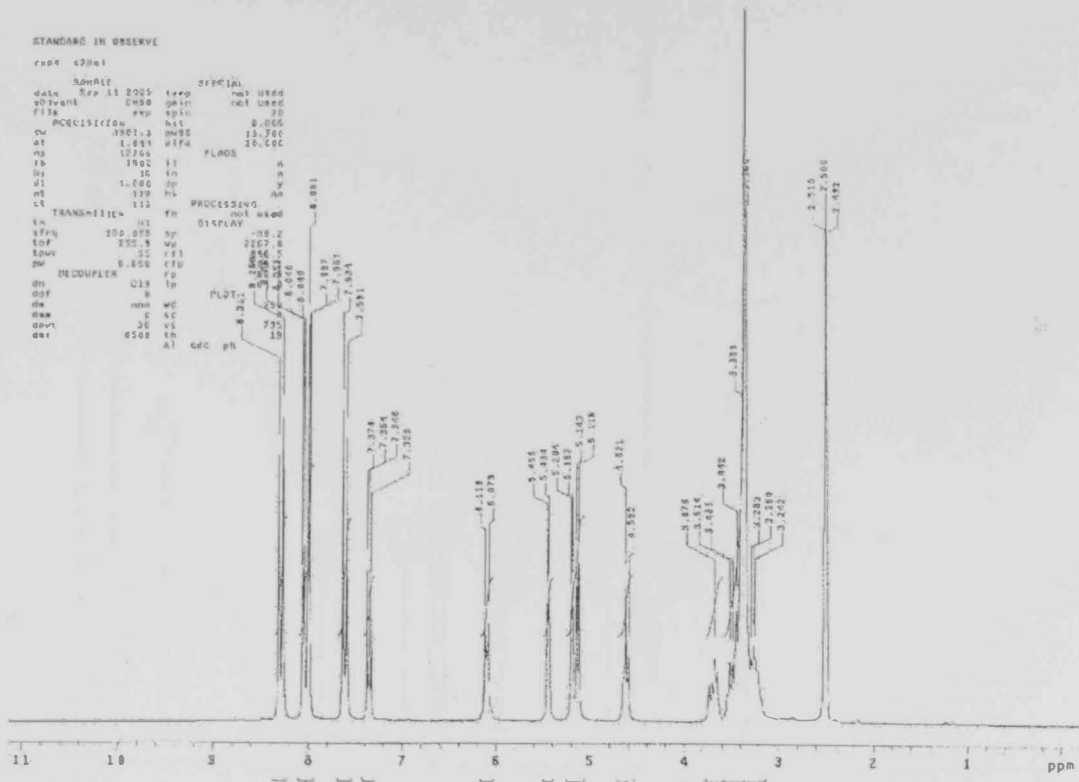


Figure 60: ¹H NMR spectrum of compound (85d)

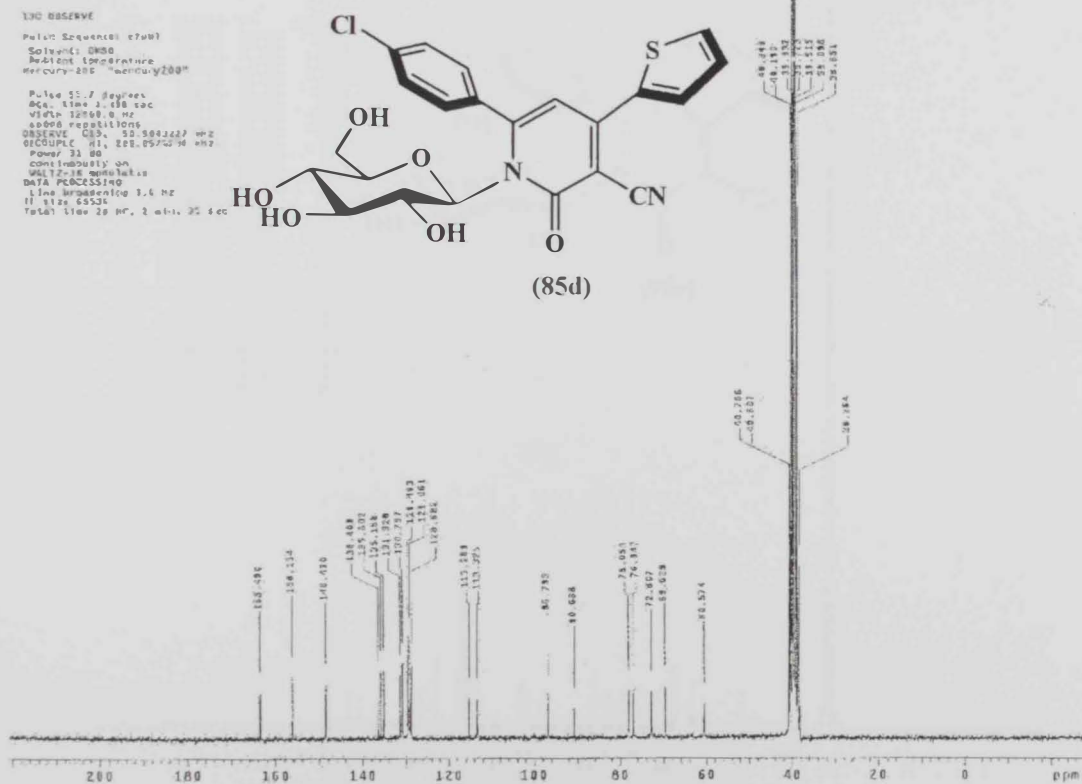
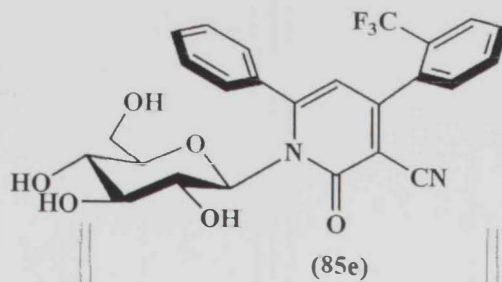


Figure 61: ¹³C NMR spectrum of compound (85d)



STANDARD IN OBSERVE

exp# COSY

SAMPLE		SPECTAL	
date	8ep 1 2005	temp	not used
solvent	DMSO	gate	3c
sample		split	1
ACQUISITION			
sv	3281.0	PF/ig	h
at	0.163	hgate	2000
ns	1024	hsgl	0.00500
fs	1000	f2	PROCESSION
ss	32	stt	-0.000
dl	1.000	svs	not used
hl	2	fn	1024
2D ACQUISITION			
sv1	3031.0	chl	-0.040
sv2	328	scal	not used
TRANSMITTER			
tn	hl	fnl	1024
svta	200.000	sp	DISP
lof	255.3	wp	200.0
tpwr	55	wp	1024.2
pw	10.000	sp1	0.02.2
PULPROGATION			
satmode	n	rfl	310.0
caspar	0	rfp	0
satidy	0	rfl1	034.1
satfrs	0	rfl2	300.1
COUPLER			
dn	013	wd	324.0
do	vim	fc	6.2
flags	ms	wsp	174.0
hl	ms	sc2	0
vcpl	n	vl	504
		th	2
		cd	AV

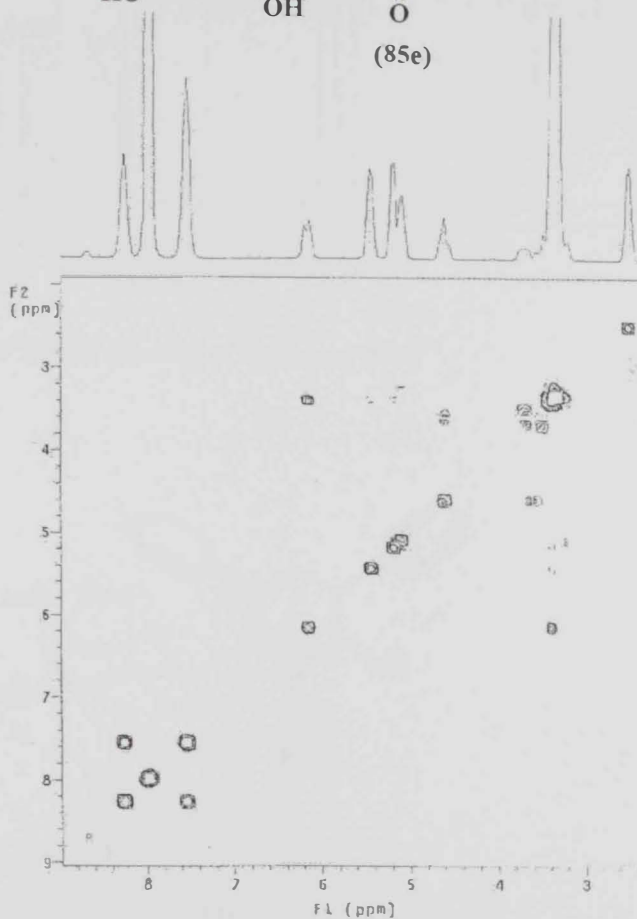


Figure 64: COSY spectrum of compound (85e)

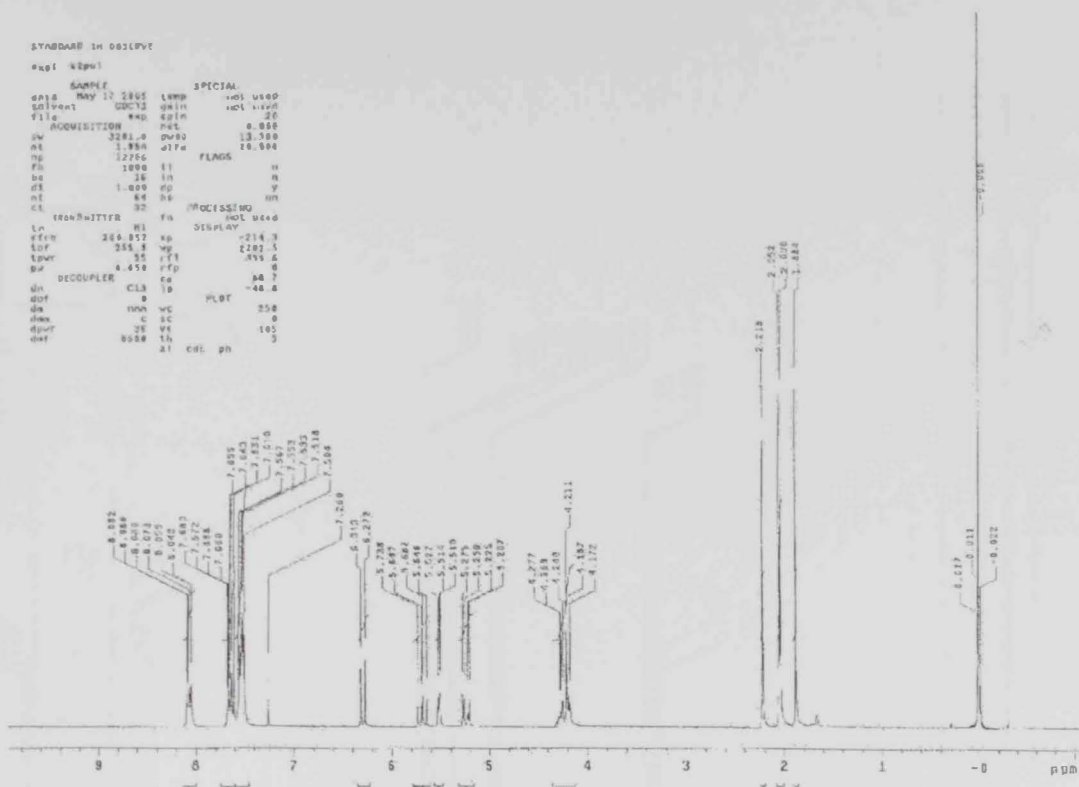


Figure 65: ¹H NMR spectrum of compound (87a)

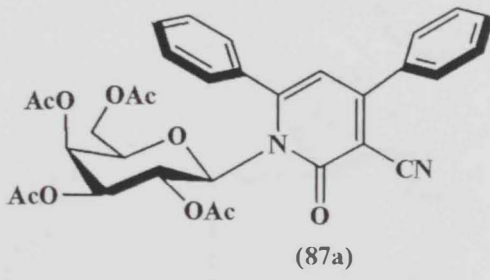
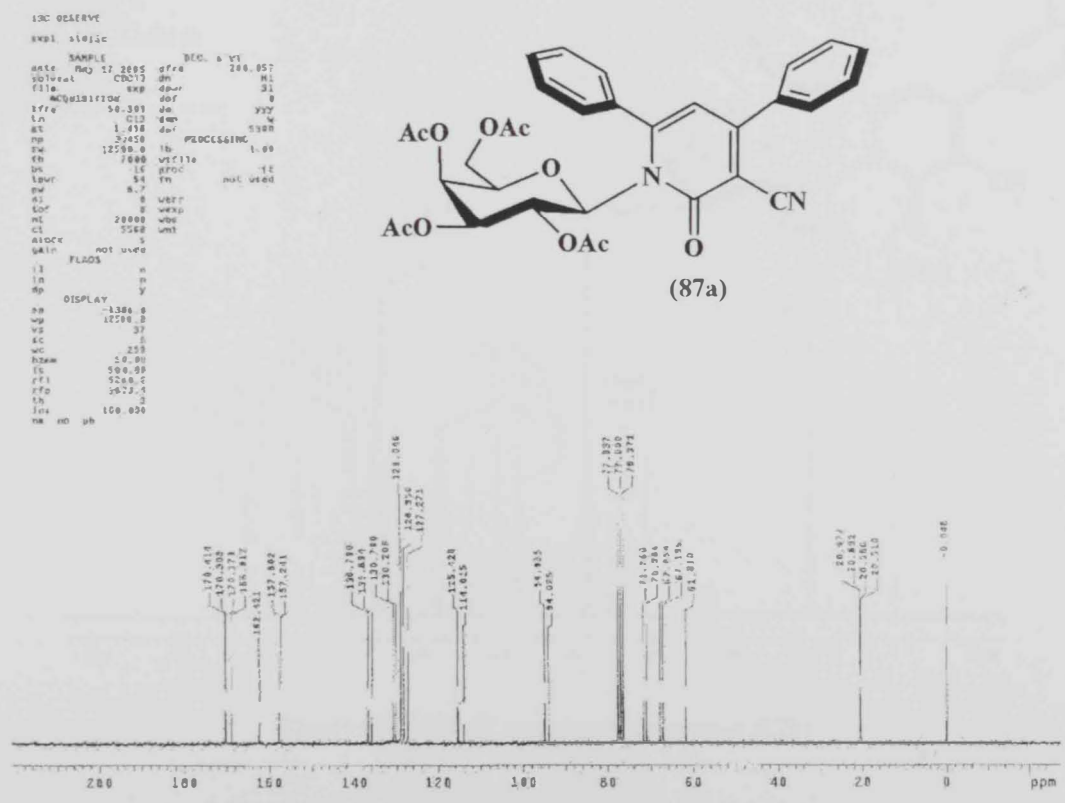


Figure 66: ¹³C NMR spectrum of compound (87a)

STANDARD IN OBSERVE

#001 12pu1

```

SAMPLE
date May 17 2005 temp nml used
solvent CDCl3 gain not used
rt 0 exp spin 20
ACQUISITION hz 6.883
sc 0.201.0 pu1d 13.300
at 1.000 m1va 20.000
TD 17364
FO 1000 f1
DI 18 f2
SI 1-000 dp Y
CL 64 hz
TRANSMITTER 64
PROCESSING
IN 701 v1ed
SFRS 900.057 Ep DISPLAY 32.8
TDF 15.5.4 EP 1043.7
LPUT 2.5 FFI 400.2
PUL 0.050 rfd 0
DECOUPLER C13 f2 PLOT -34.6
dnt 0
DB 0
SW 5.0
DWD 30 v3
DET 0.0000 th 7
C4C ph
  
```

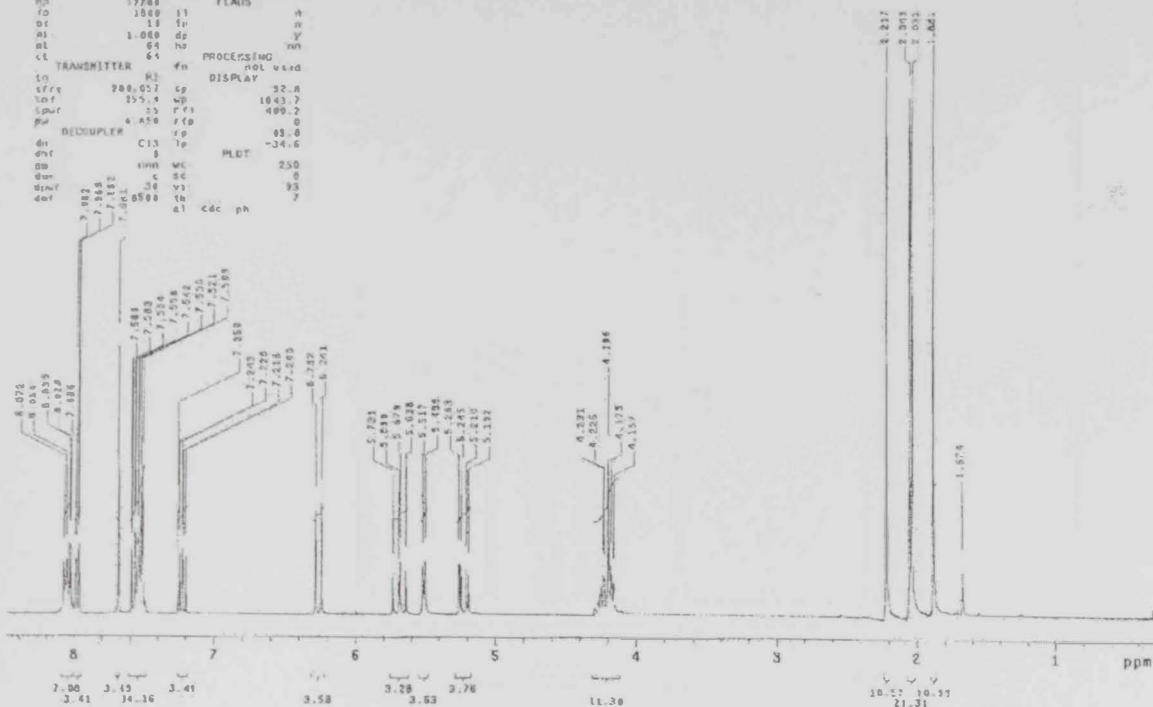


Figure 69: ¹H NMR spectrum of compound (87c)

13C OBSERVE

Pulse Sequence: 12pu1

Solvent: CDCl3

Reference Temperature: 298.15 K

Reference: 125.763 MHz

Pulse: 55.7 degrees

Acq. Time: 1.488 sec

Width: 12500.0 Hz

30000 P20011000

OBSERVE: C13, 50.3046507 MHz

DECOUPLER: H1, 200.626131 MHz

Power: 21 dB

continuously on

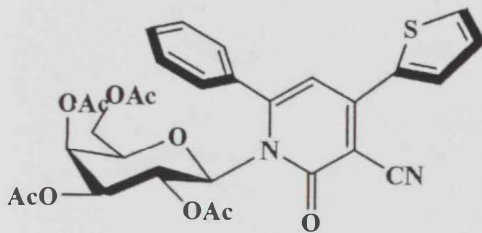
WALTZ-16 modulated

DATA PROCESSING

Line broadening: 1.0 Hz

SI size: 55526

Total Time: 46 hr, 44 min, 38 sec



(87c)

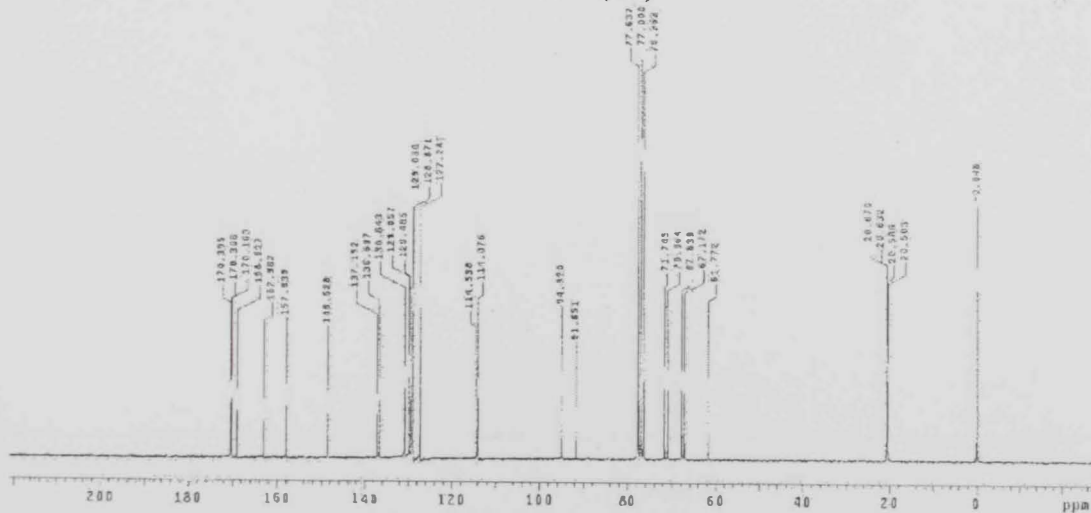


Figure 70: ¹³C NMR spectrum of compound (87c)

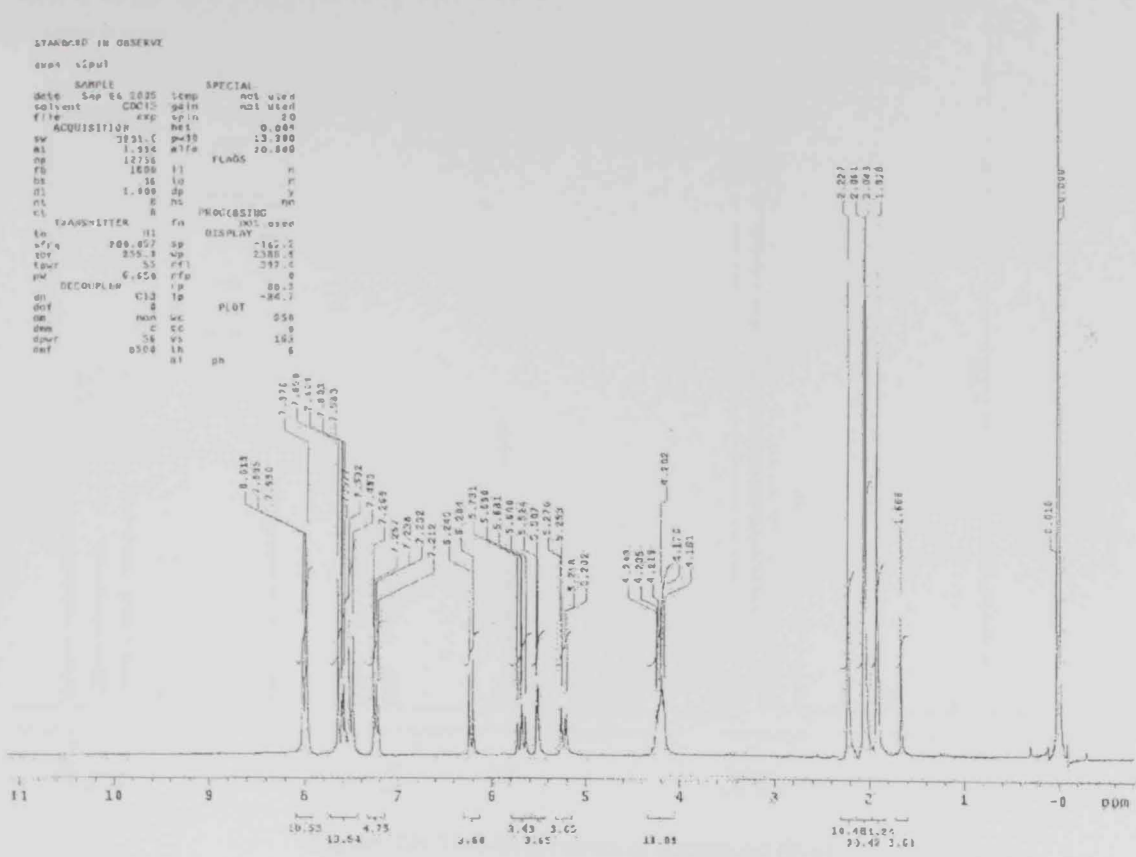


Figure 71: ¹H NMR spectrum of compound (87d)

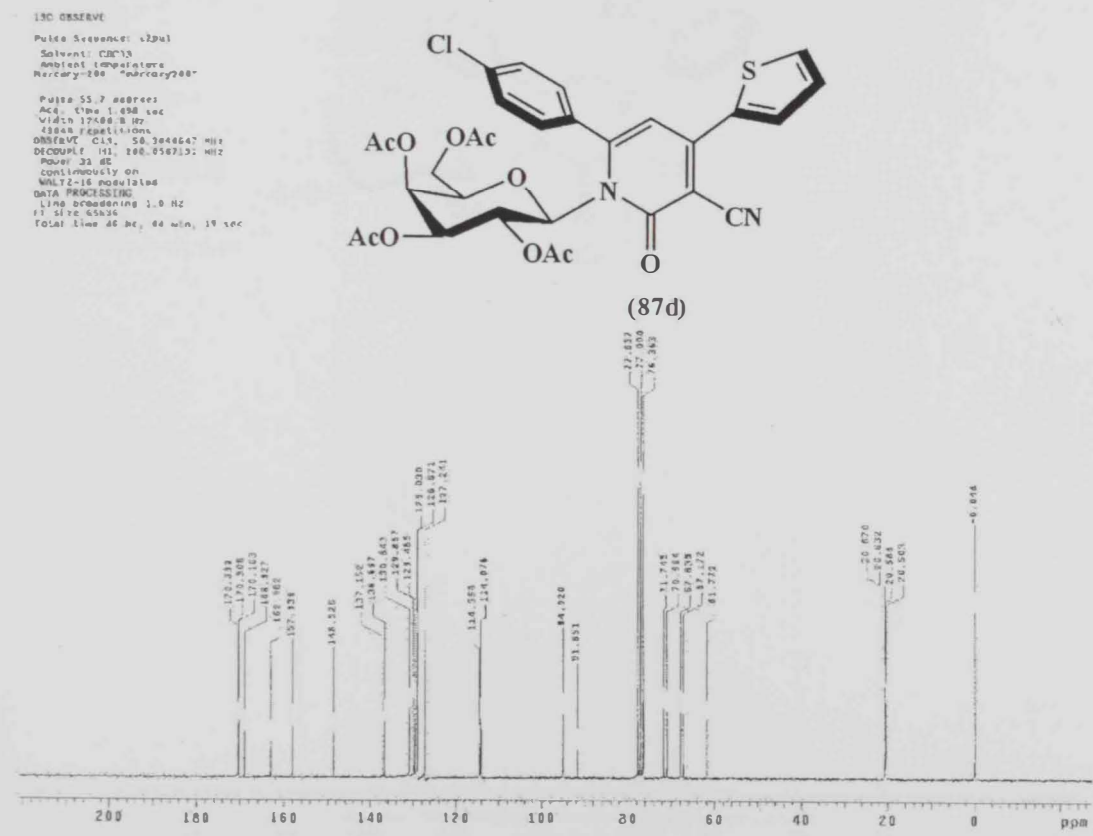


Figure 72: ¹³C NMR spectrum of compound (87d)

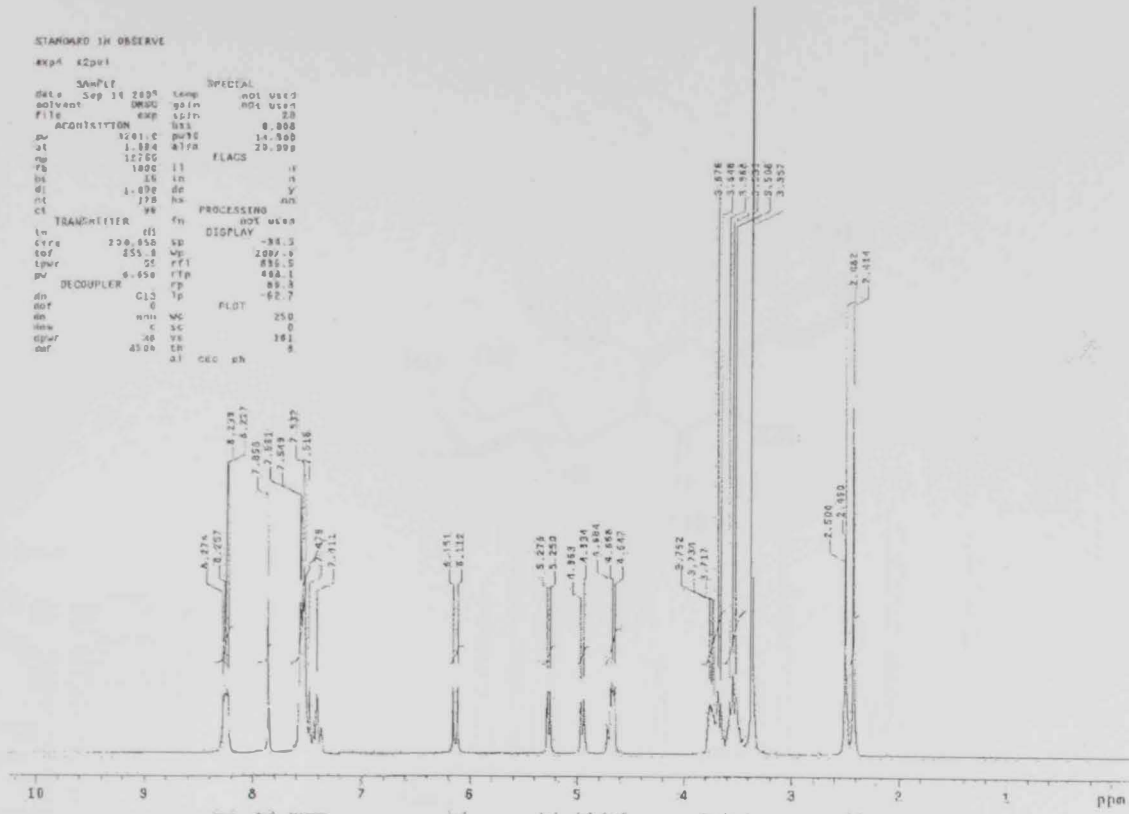


Figure 77: ¹H NMR spectrum of compound (88b)

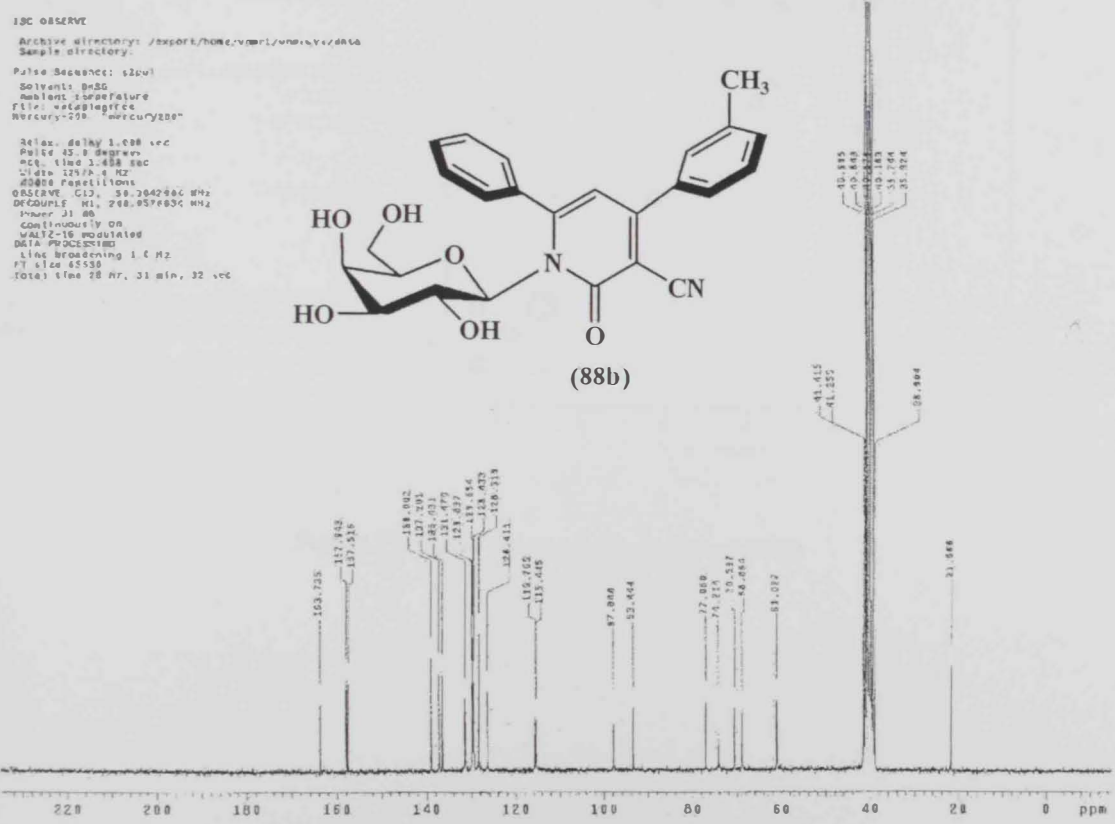
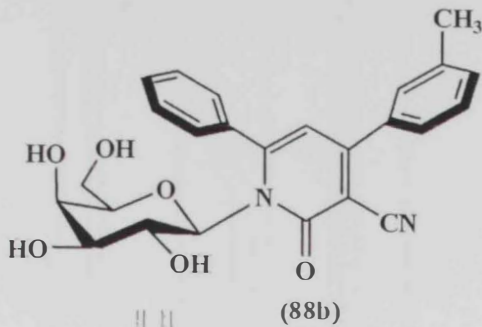


Figure 78: ¹³C NMR spectrum of compound (88b)



STANDARD IN OBSERVE
 EXP# COSY

PARAMETER	VALUE	SPECIAL
date	Sep 14 1988	1000
solvent	DMSO	gain
temp	30	spin
freq	400	cpd
acqptc		
ACQUISITION		
sw	3261.0	PGPFI
at	0.100	hvc1v1
mp	1024	hvc1
fs	1000	F2 PITCHING
ca	32	sb
sl	1.000	sdu
nl	2	fn
2D ACQUISITION		
sw1	3261.0	hvc1
at1	0.100	hvc1
mp1	1024	hvc1
fs1	1000	hvc1
ca1	32	hvc1
sl1	1.000	hvc1
nl1	2	hvc1
TRANSMITTER		
ch	13	prout
fl	1000	prout
fn1	1000	prout
RECEIVER		
ch	13	prout
fl	1000	prout
fn1	1000	prout
PULSES		
pr	1	prout
pr1	1	prout
pr2	1	prout
pr3	1	prout
pr4	1	prout
pr5	1	prout
pr6	1	prout
pr7	1	prout
pr8	1	prout
pr9	1	prout
pr10	1	prout
pr11	1	prout
pr12	1	prout
pr13	1	prout
pr14	1	prout
pr15	1	prout
pr16	1	prout
pr17	1	prout
pr18	1	prout
pr19	1	prout
pr20	1	prout
pr21	1	prout
pr22	1	prout
pr23	1	prout
pr24	1	prout
pr25	1	prout
pr26	1	prout
pr27	1	prout
pr28	1	prout
pr29	1	prout
pr30	1	prout
pr31	1	prout
pr32	1	prout
pr33	1	prout
pr34	1	prout
pr35	1	prout
pr36	1	prout
pr37	1	prout
pr38	1	prout
pr39	1	prout
pr40	1	prout
pr41	1	prout
pr42	1	prout
pr43	1	prout
pr44	1	prout
pr45	1	prout
pr46	1	prout
pr47	1	prout
pr48	1	prout
pr49	1	prout
pr50	1	prout
pr51	1	prout
pr52	1	prout
pr53	1	prout
pr54	1	prout
pr55	1	prout
pr56	1	prout
pr57	1	prout
pr58	1	prout
pr59	1	prout
pr60	1	prout
pr61	1	prout
pr62	1	prout
pr63	1	prout
pr64	1	prout
pr65	1	prout
pr66	1	prout
pr67	1	prout
pr68	1	prout
pr69	1	prout
pr70	1	prout
pr71	1	prout
pr72	1	prout
pr73	1	prout
pr74	1	prout
pr75	1	prout
pr76	1	prout
pr77	1	prout
pr78	1	prout
pr79	1	prout
pr80	1	prout
pr81	1	prout
pr82	1	prout
pr83	1	prout
pr84	1	prout
pr85	1	prout
pr86	1	prout
pr87	1	prout
pr88	1	prout
pr89	1	prout
pr90	1	prout
pr91	1	prout
pr92	1	prout
pr93	1	prout
pr94	1	prout
pr95	1	prout
pr96	1	prout
pr97	1	prout
pr98	1	prout
pr99	1	prout
pr100	1	prout

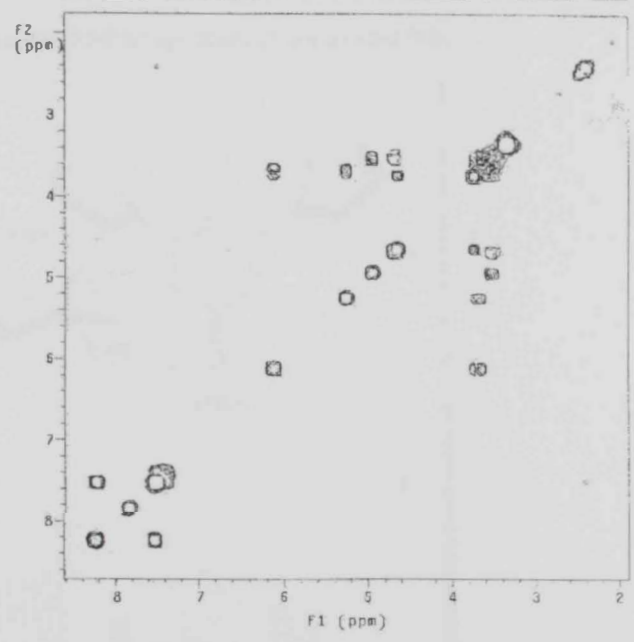
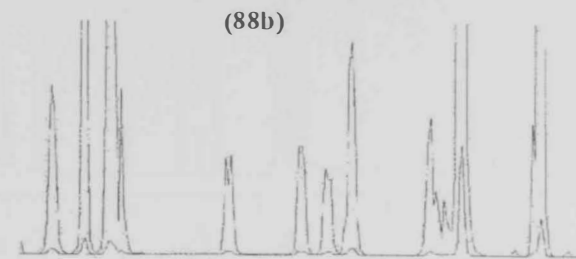


Figure 79: COSY spectrum of compound (88b)

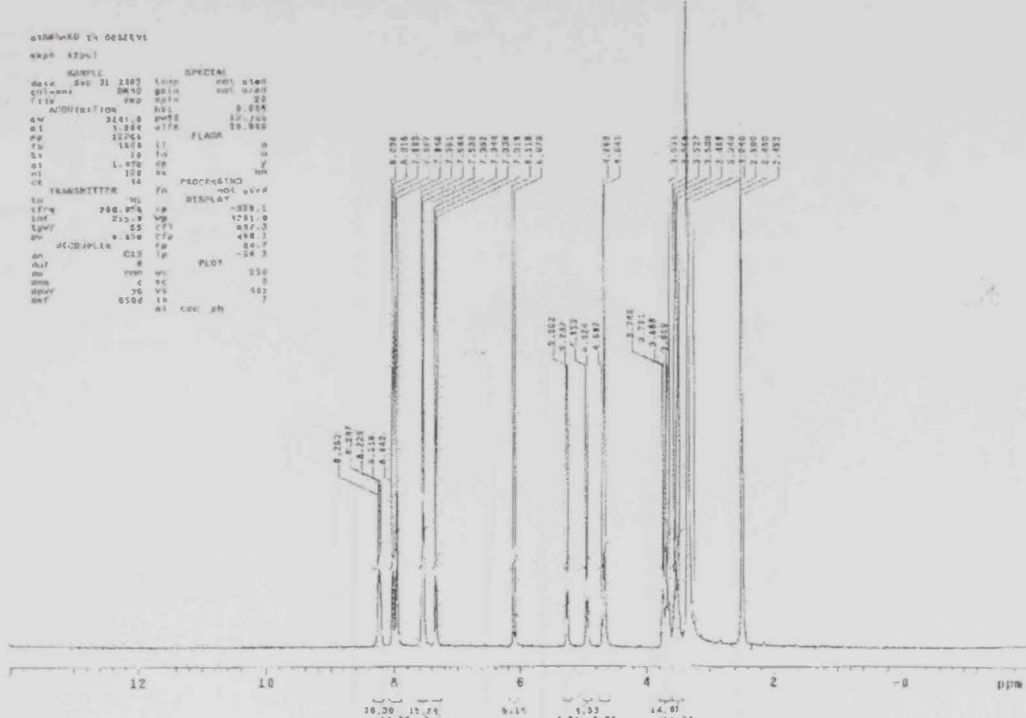


Figure 80: ¹H-NMR spectrum of compound (88c)

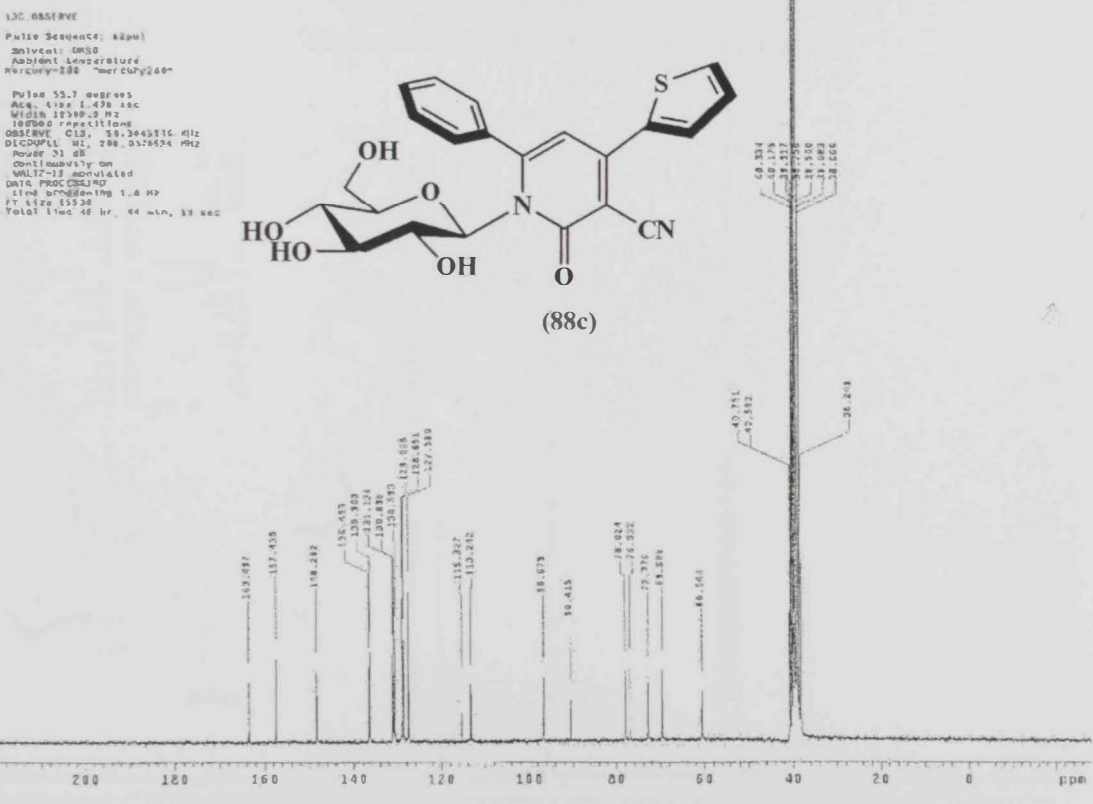


Figure 81: ¹³C-NMR spectrum of compound (88c)

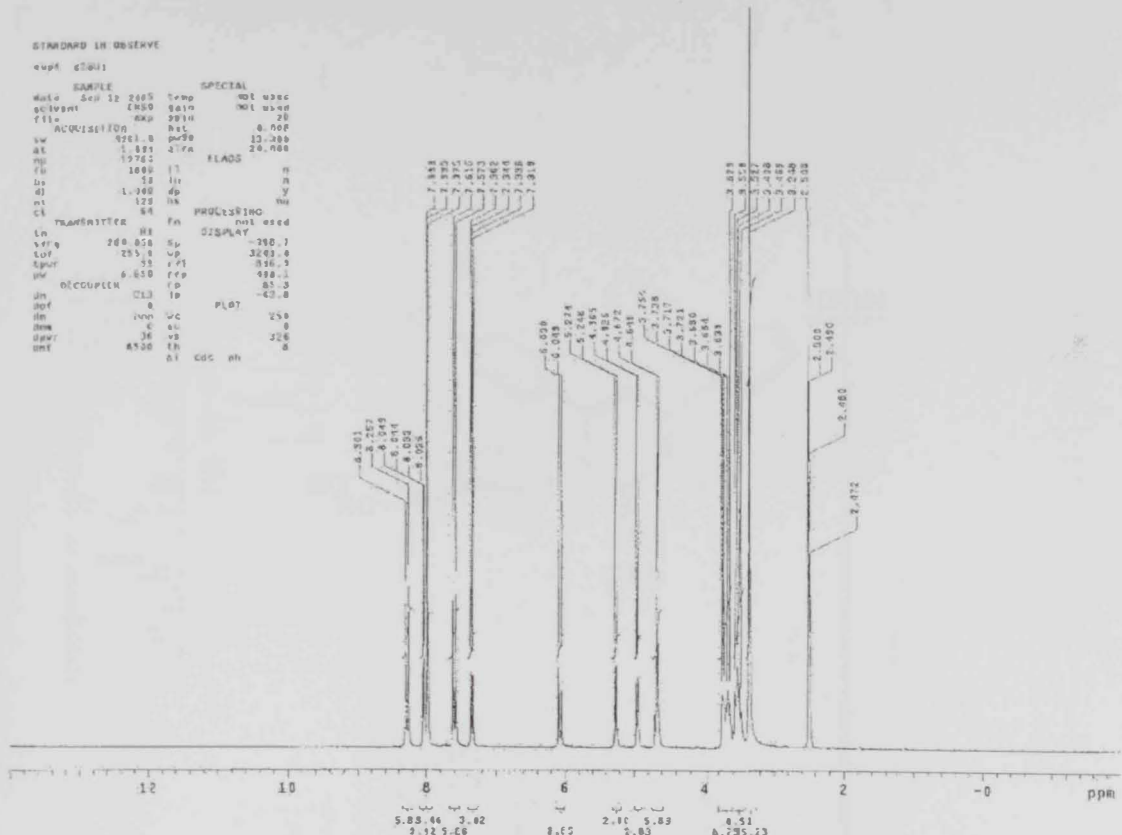


Figure 82: ¹H NMR spectrum of compound (88d)

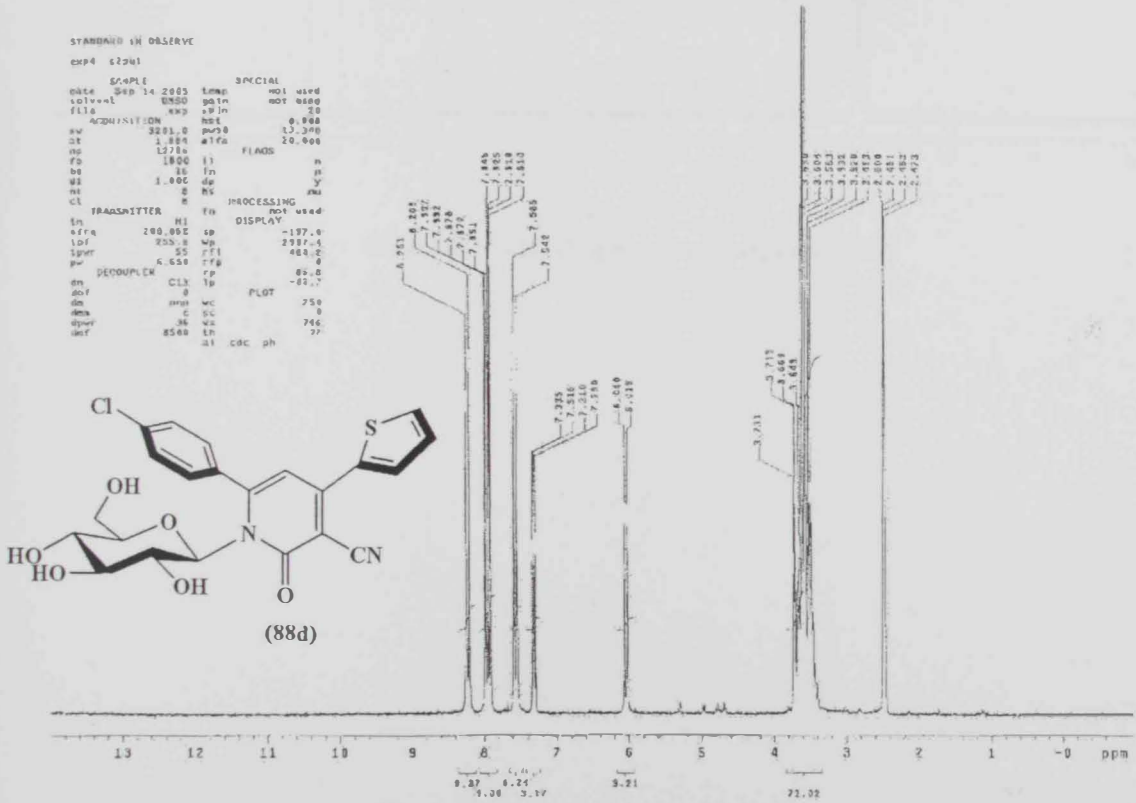


Figure 83: ¹H NMR spectrum of compound (88d) in D₂O

13C OBSERVE

exp# 156106

```
data Sep 12 1983 07:14 DEC. & VI 100.050  
solvent 0000 on RI  
file 0000 exp 0000 3) C  
ACQUISITION 0000 def C  
F1 F2 50.303 00 VVV  
AT 1.490 00 520F  
AD 2740 00  
SR 12200.0 1b PROCESSING 1.00  
VS 2800 wfile  
RZ 25 pFQC  
IPVR 34 Fw not used  
PR 4.7  
SI 0  
LOF 0  
NS 40000 wde  
CS 40000 wot  
BLOCK %  
DATA not used  
F1A03  
I1 n  
I2 n  
I3 Y  
DISPLAY  
PP 1405 8  
WP 10500 0  
VF 350  
VC 0  
WC 250  
NORM 50.00  
IS 500.00  
F1L 1300 3  
F1P 1302 9  
F1M 100.000  
END NO P3
```

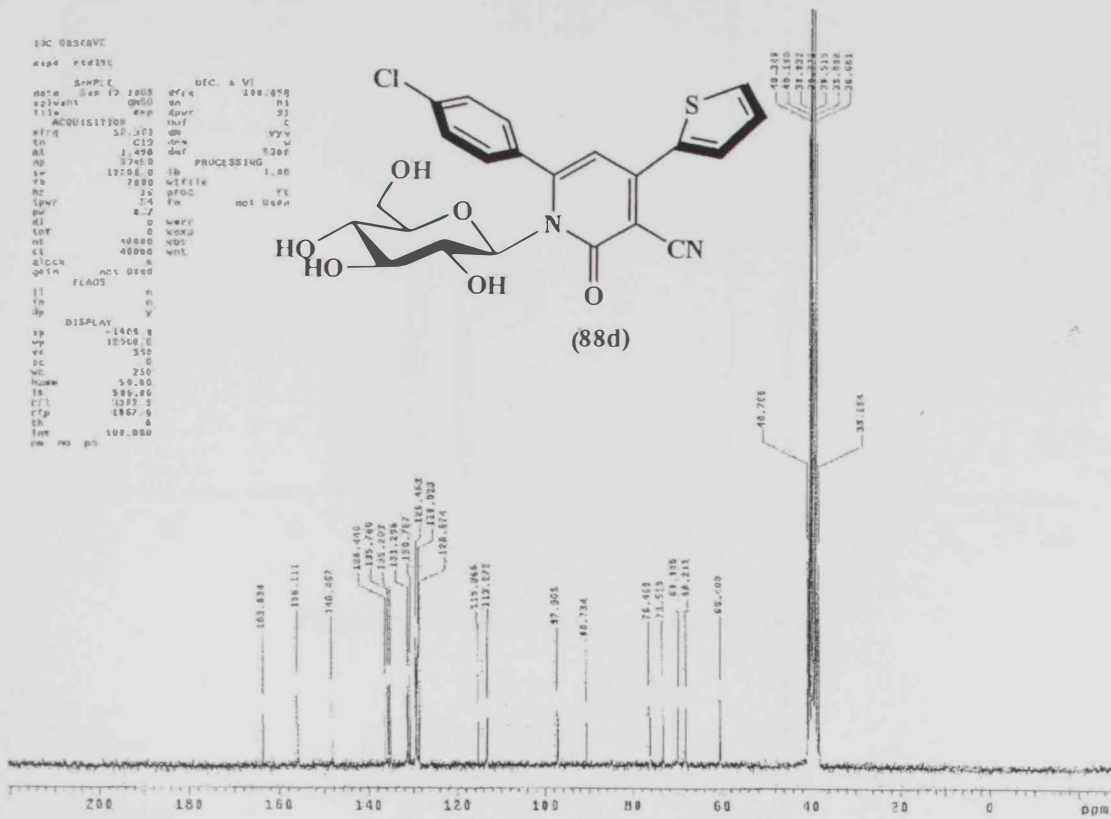
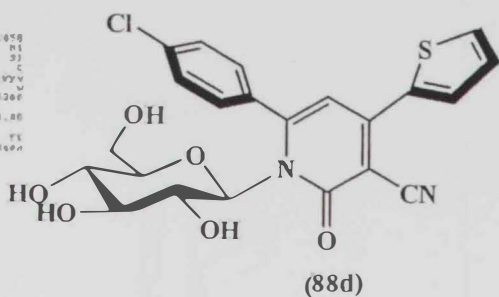


Figure 84: ¹³CNMR spectrum of compound (88d)

STANDARD IN OBSERVE

exp# 88pu1

date	MAY 31 2005	loop	not used
solvent	DMSO	gain	not used
fla	exp	spin	70
ACQUISITION			
sw	1201.6	psf	0.000
at	1.334	atfa	20.000
ng	12766	FLACS	
fs	1800	fl	n
li	18	lq	n
dl	1.000	dp	y
rl	128	rs	mn
ct	84	PROCESsing	
TRANSMITTER			
la	W1	hdL	used
lfr	200.350	sd	-400.2
lof	250.1	wp	3201.0
lwr	55	rfl	-400.2
pw	6.850	rpf	0
DEMODULATOR			
di	CLX	fp	01.4
shf	0	lp	-51.4
dm	nm	wd	250
slam	C	sc	0
hour	36	va	120
def	8500	lh	6
	at	kdc	ph

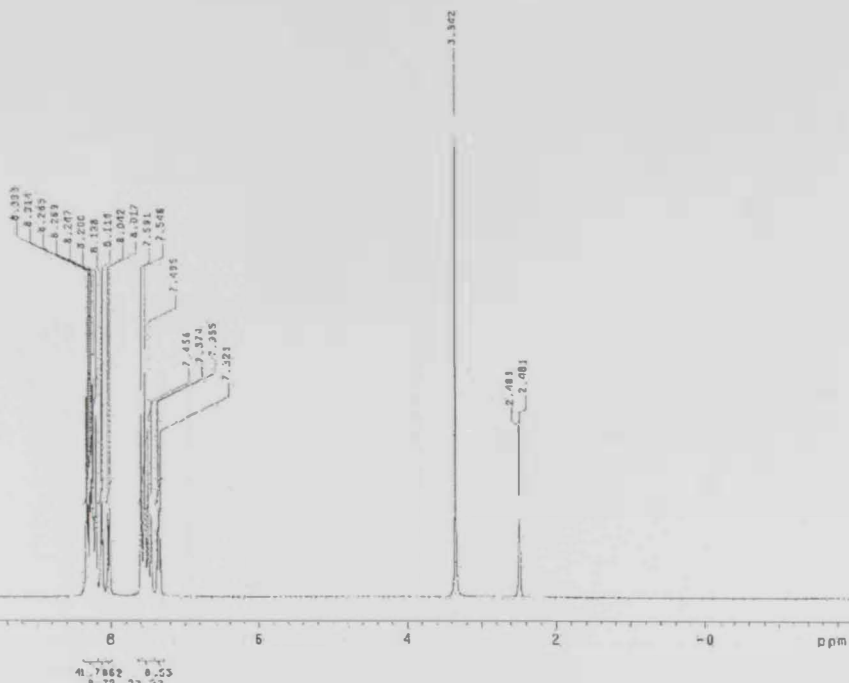


Figure 87: ¹H NMR spectrum of compound (89b)

13C OBSERVE

File: 88pu1

Balance: 88pu1

Temperature: 200

Probe: 13C

Pulse: 15.7 degrees

Acq. Time: 1.500

Width: 12.500

54500 resolution

OBSERVE: C13, 20.000000 MHz

PROBHD: 51, 20.000000 MHz

Power: 11.00

Control: 13C

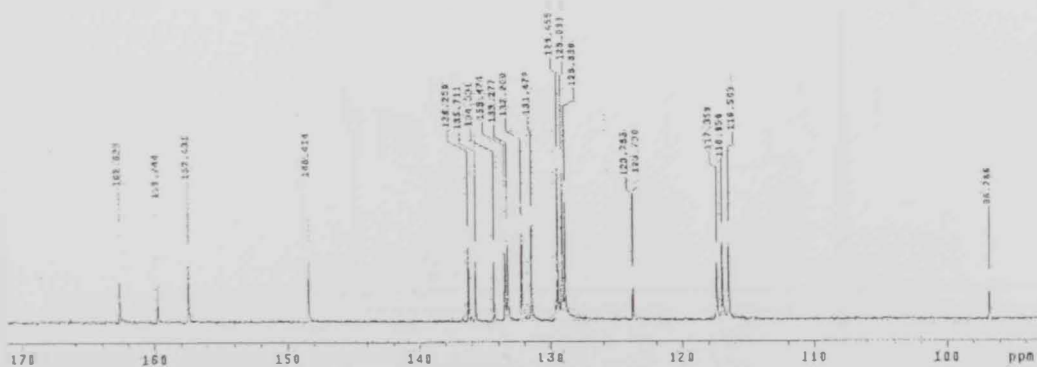
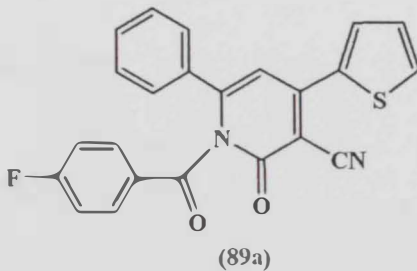
WALTZ-16 modulation

DATA PROCESSING

Time: 0.000000

SI: 13C

Total time: 0.00, 0.00, 0.00



STANDARD IN U68697

exp# 12101

SAMPLE		SPECIAL	
date	Dec 12 2005	temp	not used
solvent	DMSO	sol'n	not used
file	482	spin	28
ACQUISITION	851	RES	6.089
sc	3281.0	pc90	13.305
at	1.884	ctf	26.089
sp	17743	PLAOS	
fu	1800	ix	n
ub	16	in	n
st	1.040	sp	y
nt	120	ns	m
ct	48		
TRANSMITTER		PROCESSING	
ch	48	fm	not used
lch	48	OTAP	47
freq	200.354	fb	-385.6
tor	255.3	wb	3201.0
lpr	75	rf	415.7
pw	6.850	rfp	180.1
dc	0	fb	80.2
dd	0	sp	-82.4
dd	0	sp	0
de	0	mc	250
dm	0	sc	0
dm	30	vs	141
dm	8500	in	13
dm	41	gdc	ph

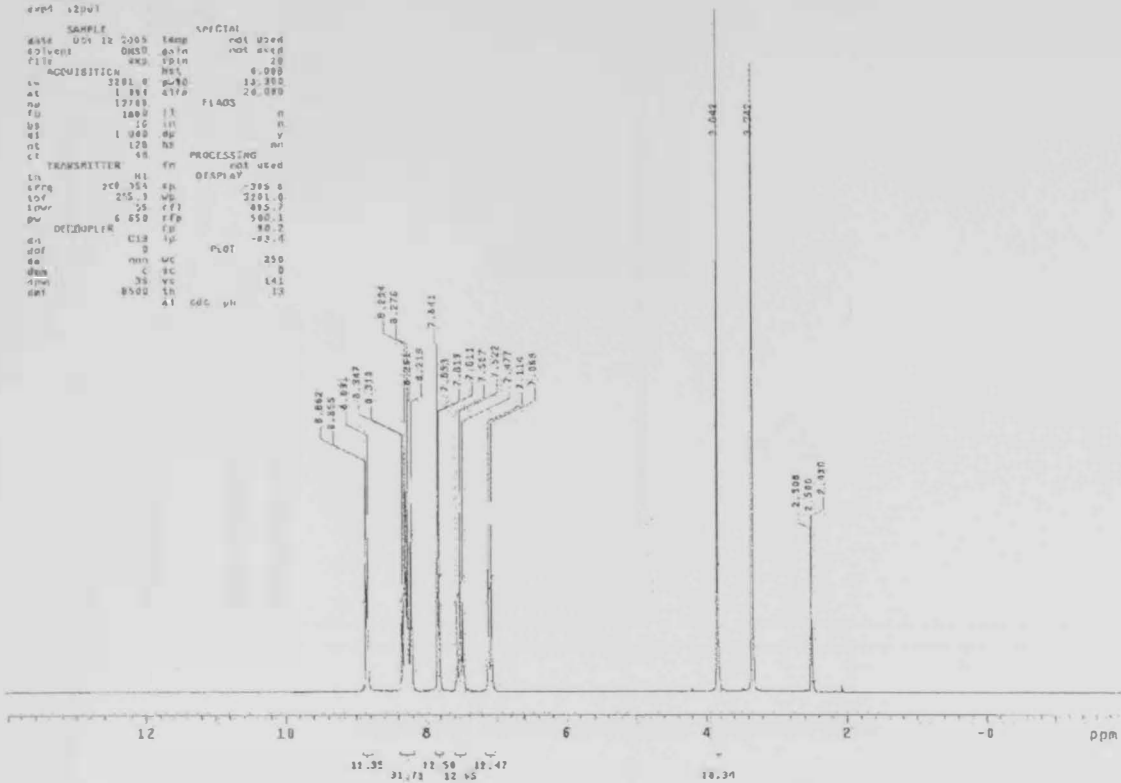
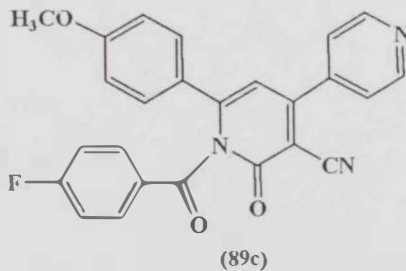


Figure 89: ¹H NMR spectrum of compound (89c)

13C OBSERVE

Pulse Sequence: zgpg30
 Solvent: DMSO
 Subsol: vaporature
 PC: 40.7-708 "accuracy706"
 Relax: 20.7 seconds
 Acq. time: 1.000 sec
 Width: 19500.0 Hz
 13C75: 90/180/90
 DRPGM: F10, 50 samples per
 DDCP: 101, 200.000000 Hz
 Power: 21 db
 Continuously on
 WALTZ: 16 minutes
 DATA ACQUISITION
 Line Broadening: 1.4 Hz
 F1: 40.000000
 Total time: 46 hr 48 min, 19 sec



(89c)

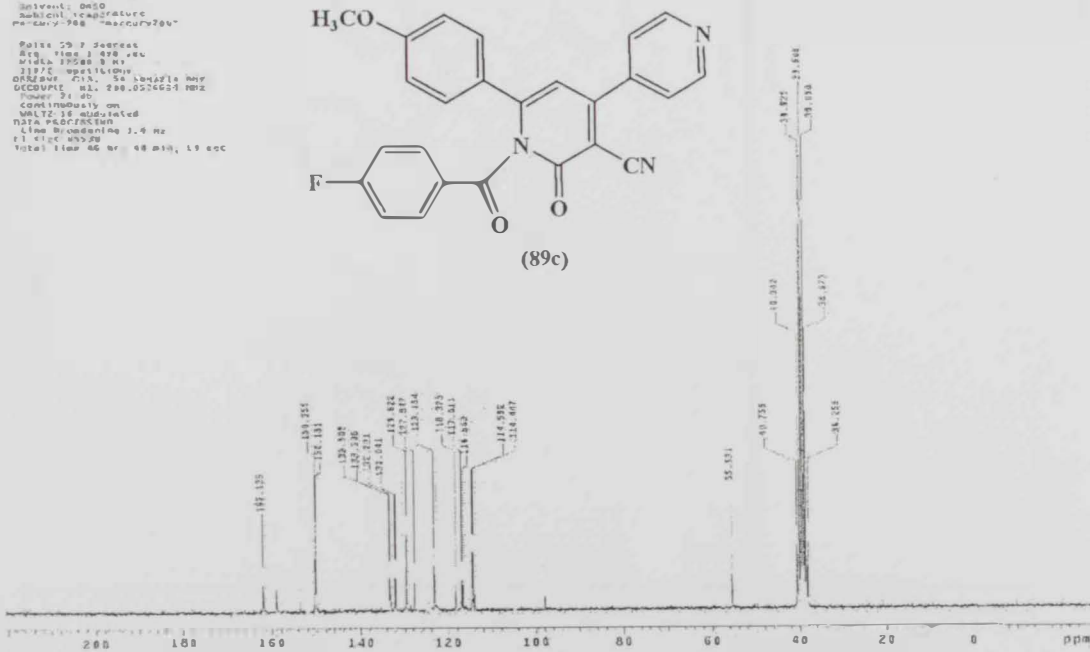


Figure 90: ¹³C NMR spectrum of compound (89c)

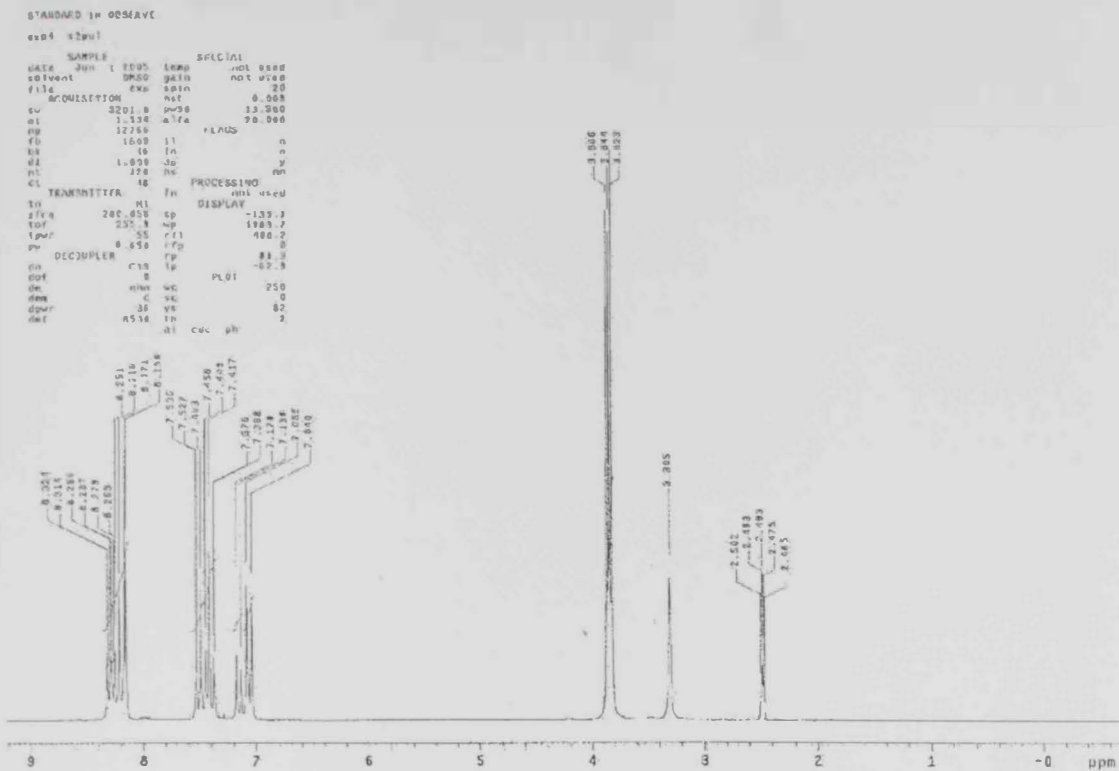


Figure 91: ¹H NMR spectrum of compound (89d)

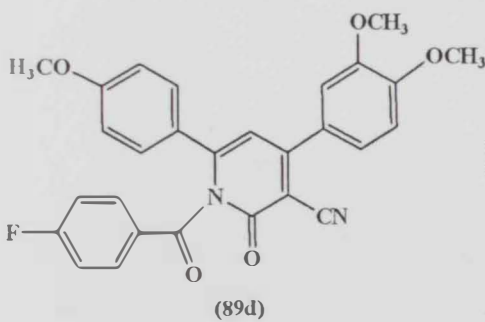
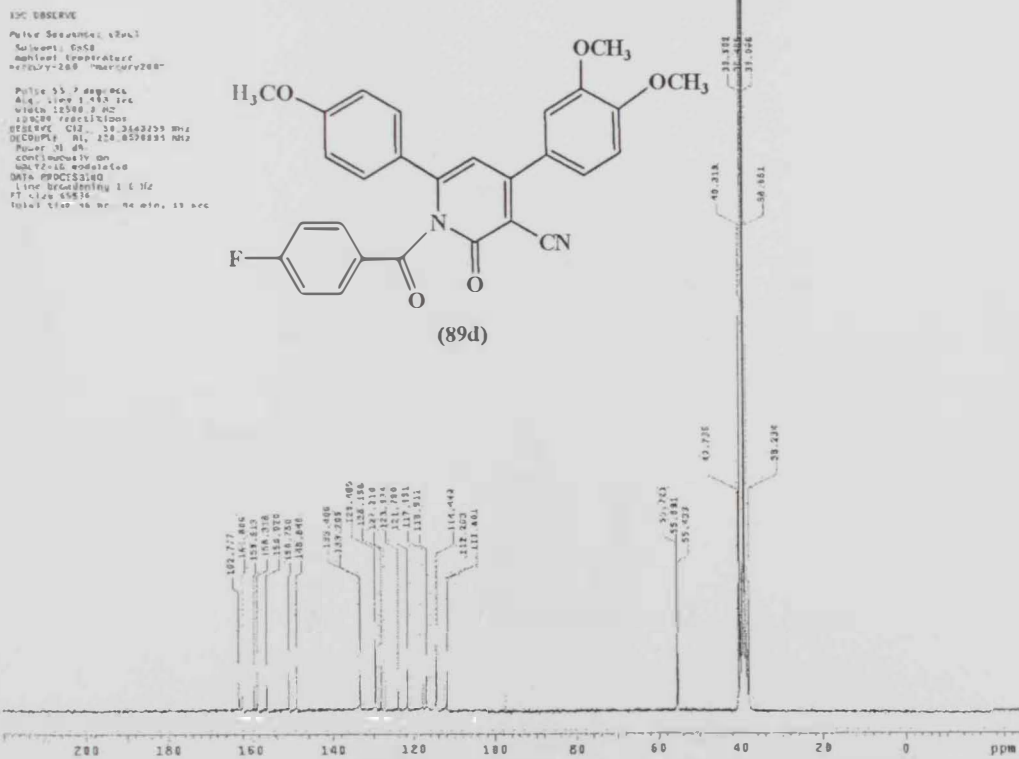


Figure 92: ¹³C NMR spectrum of compound (89d)



الخلاصة

لقد أظهرت مركبات 3-ديازا بريميدين نوكلوزيد فعالية كبيرة عندما تم استخدامها في شتى المجالات الطبية خاصة عقار كمضاد للأورام السرطانية وفيروس الإيدز. ولقد ركزت الأبحاث الأخيرة على تصميم و تخليق و دراسة خواص المركبات نوكلوزيدات مشابهة لتلك الموجودة في الحمض النووي ، ولذا تم اختيار فلوروبريدينون و نوكلوزيداتها المشتقة وتم تخليقها ومعرفة خواصها لتعطي خواص مضادة للأورام ، حيث تم تحضير 6-4-ثنائي أريل 3-ميانو 2-(1H) بريدنون (82a-i) و نوكلوزيداتها المشتقة بطرق قياسية حتى تتشابه الحمض النووي. أما بالنسبة لمجموعة ثلاثي فلوروميثيل، فقد تم إدخالها لنظام حلقة بريدنون لدراسة تأثيرها على خلايا الأورام المختلفة. وأيضاً تم إنتاج و تخليق كميات جيدة من الجلايكوسايد عن طريق التفاعل بين مشتقات 3-ديازا بريميدين و سكر سداسي البيرانوسيل المنشط ليعطي N-نيوكليوسايد (83a-e, 85a-e, 87a-e 88a-d) كنتائج أساسية. ومن خلال المسح الحيوي وجد أن مشتقات الفلورو و ثلاثي فلوروميثيل لحلقة البريدنون يعزز من النشاط الحيوي، وعلاوة على ذلك فإن المشتقات اللانيوكليوسايد وجد أنها أكثر نشاطاً من مشتقات N-نيوكليوسايد العادية المقابلة. و يرجع التحسن في الخواص البيولوجية بسبب وجود مجموعة الفلوريد في حلقة البريدن . ولقد ساعدت حسابات ميكانيكا الكم باستخدام نظرية الكثافة النسبية والتي استخدمت في دراسة تفاعلية 3-ديازا بريدن مع جزيئات السكر المنشطة حيث استخدم برنامج جوسيان 98 و قد تم توظيفه لحساب الاتجاهات الفراغية والطاقة وكثافة الشحنة في حسابات الحالة الغازية. البيانات الناتجة من ميكانيكا الكم وحساباتها دعمت النتائج العملية بأن أظهرت أن الكثافة الإلكترونية على ذرة النيتروجين في حلقة البريدن أعلى و أكثر منها على ذرة الأكسجين في الموقع (C-2).

كما دعمت دراسات الأطياف دراسة الكثافة الإلكترونية لكل من (HOMO) و (LUMO). وأظهرت دراسة العلاقة بين الشكل و النشاط إن للنيوكليوسايدات (83a-e, 85a-e, 87a-e, 88a-d) و مركبات اللانيوكليوسايدات (89a-d) أظهرت نتائج مهمة و مثيرة بيولوجياً .

حيث أظهرت المشتقات المختلفة ل3-ديازا بريميدين نشاطاً مختلف حسب نوع الجزء المستبدل على الموقع 4 أو 6 لحلقة البريدن، والنتائج أظهرت أن 2-ثيوفين عند الموقع 4 له النشاط الأكبر من بين كل المركبات المشابهة وكذلك إدخال مجموعة الأريل عند الموقع 6 ليس له تأثير ملحوظ على النشاط الحيوي . فعلى سبيل المثال مركبا (82d) و (82e) أظهرت نفس النشاط عند التركيزات الأعلى و الأقل وهذه النتائج تظهر إن مجموعة الأريل عند الموقع 6 ليس لها تأثير ، و في نفس الوقت فإن النيوكليوسايد المحتوي على حلقة جليكوز أظهر نشاط أعلى من حلقة جلاكتوز المشابهة .

وأظهرت كل النيوكليوسايدات الحرة نشاط أعلى بسبب معامل الإذابة و لكن بعض المشتقات الاستيلايد الأقل ذوبانية أظهرت نشاطية ملحوظة. النيوكليوسايد الذي يحتوي على مجموعة ثيوفين عند الموقع 4 أظهر نشاط حيوي. و كذلك نتائج أكثر إثارة تم الحصول عليها من اللانيوكليوسايدات المشابهة (89a-d). حيث أوضحت دراسة العلاقة بين الشكل و النشاط النتائج كما يلي : إن عامل الذوبان ربما ليس العامل الأساسي في النشاط الحيوي لان اللانيوكليوسايد الأقل ذوباناً مثل (89a) كان الأكثر نشاطاً من بين المركبات .



جامعة الإمارات العربية المتحدة
عمادة الدراسات العليا
برنامج ماجستير علوم بيئة

تخليق لبعض مركبات بيريدينون النيكلوزيدات كمضادات للأورام

رسالة مقدمة من الطالبة /

شيخة سيف سعيد النيادي

إلى

جامعة الإمارات العربية المتحدة
استكمالاً لمتطلبات الحصول على درجة الماجستير في علوم بيئة

